ANL/OTEC-BCM-023

ANL/OTEC-BCM-023

OTEC BIOFOULING, CORROSION, AND MATERIALS STUDY FROM A MOORED PLATFORM AT PUNTA TUNA, PUERTO RICO

D. S. Sasscer, T. R. Tosteson,
and T. O. Morgan

Argonne National Laboratory
9700 South Cass Avenue
Argonne, Illinois 60439

Prepared for the
U. S. Department of Energy
Division of Ocean Energy Systems
under Contract W-31-109-Eng-38

SOLAR ENERGY

Printed in the United States of America
Available from
National Technical Information Service
U. S. Department of Commerce
5285 Port Royal Road
Springfield, VA 22161

NTIS price codes
Printed copy: A07
Microfiche copy: A01

Distribution Category:
Ocean Energy Systems
(UC-64)

ANL/OTEC-BCM-023

ANL/OTEC-BCM--023

DE82 007037

ARGONNE NATIONAL LABORATORY
9700 South Cass Avenue
Argonne, Illinois 60439

OTEC BIOFOULING, CORROSION, AND MATERIALS STUDY FROM A MOORED PLATFORM AT PUNTA TUNA, PUERTO RICO

D. S. Sasscer, T. R. Tosteson,
and T. O. Morgan

OTEC Division
Center for Energy and Environment Research
University of Puerto Rico
College Station
Mayaguez, Puerto Rico 00708

August 1981

Prepared for
Argonne National Laboratory
under Subcontract 31-109-38-5205

TABLE OF CONTENTS

LIST OF FIGURES

LIST OF TABLES

ABSTRACT

During the 404 days between 29 January 1980 and 10 March 1981 the Center conducted an uninterrupted biofouling test at Punta Tuna, Puerto Rico, of periodically cleaned, OTEC evaporator tubes. The fouling resistance (R_f), total surface carbon and nitrogen content, ATP, and the wet film thickness (WFT) were determined throughout the test. Visual observations of the fouling film were made by light sectioning and scanning microscopy, and at the end of the test, a study was made of the macrofouling of the flow system.

The results of these tests indicate that a base layer of bacteria and exudated polysaccharides enhance microbial adhesion and thereby create an environment conducive to rapid film growth. Fouling rates (dR_f/dt) for aluminum were generally higher than for titanium but they were linear for both materials and did not exceed $0.3(10^{-4})ft^2$-hr-°F/Btu-day for either material during the 13-month study. Excellent correlation was found to exist between R_f and WFT which supports the hypothesis that it is the stagnant film of water entrapped by bacteria which is largely responsible for the insulating properties of the biofilm. The macrofouling study identified 61 species of benthic invertebrates representing ten phyla growing in those parts of the flow system, where flow was less than 3 fps but no macrofouling where the flow velocity significantly exceeded 3 fps.

EXECUTIVE SUMMARY

In order to better understand the biofouling phenomenon of OTEC evaporators, the Center has undertaken an intensive, heat exchanger biofouling study at a potential OTEC site near the coast of Puerto Rico.

During the 404 days between 29 January 1980 and 10 March 1981 a continuous flow of ocean surface water was passed through simulated OTEC evaporator tubes in order to determine, in situ, effects of microbiofouling on heat exchanger efficiency.

This study was conducted by determining and correlating fouling resistance, R_f, and fouling rate, dR_f/dt, with the bioanalysis of the fouling film which occurred in tubes which were periodically cleaned each time R_f equaled $5(10^{-4})ft^2$-hr-°F/Btu.

When the 13-month study ended, the flow system was disassembled and the macrofouling which had occurred in the system was studied.

Heat transfer was measured using modified Carnegie-Mellon University (CMU) Heat Transfer Monitors (HTM's). The HTM time constants along with physical parameters (flow rate, water temperature, tube dimensions, thermal conductivity, etc.) were determined at three- to four-day intervals and were used to calculate R_f. The presence of microfouling was assessed by determining the total organic carbon, nitrogen, wet film thickness (WFT) and adenosine triphosphate (ATP) associated with these surfaces. Visual analysis of the exposed surfaces both before and after cleaning was made with light sectioning and scanning electron microscopy.

During the induction period, approximately one month or less, the biofilm was only loosely attached to the metal surface. Some spontaneous sloughing occurred which left only a "patchy" film on the tubes. The base layer of what appears to be exudated polysaccharides was found on the surfaces after brush cleaning. This layer evidently enhances the microbial adhesion and probably is necessary for rapid biofilm growth. This hard base layer has a maximum thermal resistance, however, of less than $1 \times 10^{-4} ft^2$-°F/Btu and thus does not constitute the major portion of the thermal resistance of the film.

The time rate of increase of the fouling, dR_f/dt, was found to be best described by linear equations, aluminum and titanium generally having different rates but both experience maxima of approximately $0.3(10^{-4})ft^2$-hr°F/Btu-day.

Excellent correlation was found between R_f and wet film thickness, WFT, which enabled the calculation of the coefficient of thermal conductivity of the film. This was found to be 0.34 Btu/ft^2-hr-°F and approximates the thermal conductivity of seawater, which supports the hypothesis that stagnant water, entrapped by microorganisms, is largely responsible for the insulating properties of the biofilm of OTEC evaporator surfaces.

The test surfaces of titanium and aluminum appear to be different with respect to the relative proportions of biomass (ATP) and organic carbon associated with them both before and after cleaning. On the titanium surfaces prior to cleaning, an average of 51% of the organic carbon is microbial. This value falls to 5.2% on the clean titanium surface. These values are to be contrasted to those found on the aluminum surfaces which are 8.4% before and 0.8% after cleaning. Twelve strains of bacteria have been isolated from the test surfaces during the course of this study with those isolated from the titanium appearing to be distinct from those obtained from the aluminum surfaces.

The post-test macrofouling study found a total of 61 species of benthic invertebrates representing ten phyla growing in those portions of the system where flow was maintained at less than 3 fps. No macrofouling was observed when flow significantly exceeded 3 fps.

1. INTRODUCTION

One of the major obstacles which closed cycle Ocean Thermal Energy Conversion (OTEC) technology faces is the reduction of heat exchanger efficiency due to the development of microbial communities on heat exchanger surfaces exposed to sea water. In order to better understand this phenomenon, the Center for Energy and Environment Research of the University of Puerto Rico has undertaken an intensive, DOE funded, biofouling study at a potential OTEC site near the coast of Puerto Rico.

Between 29 January 1980 and 10 March 1981, a continuous flow of ocean surface water was passed through simulated OTEC evaporator tubes in order to determine, *in situ,* effects of microbiofouling on heat exchanger efficiency.

This study was conducted in two phases. The first phase study, the initiation of microfouling, consisted of relating the fouling resistance (R_f) to the biological analysis of aluminum and titanium sacrificial tube samples on eleven occasions during the first 143 days. The second phase consisted of the long-term determination of microfouling. This was accomplished by correlating fouling resistance, (R_f), and fouling rate, (dR_f/dt), with the bioanalysis of the microbiofouling which occurred in tubes which were periodically cleaned.

2. SITE

The experiment was conducted at a potential OTEC site off Punta Tuna on the southeast coast of Puerto Rico (Figure 1). The site (17° 57.6' N, 65° 51.9' W) lay approximately 2.1 miles (3.4 Km) off the Puerto Rico coast where the water depth was 500 fathoms (1100 m) deep. Site characterization studies have been conducted by Atwood *et al* (1) and Goldman (2). Additional studies by the Center for Energy and Environment Research of Puerto Rico were still in progress when this report was prepared. Figure (1) shows a plot of temperature vs depth at the site.

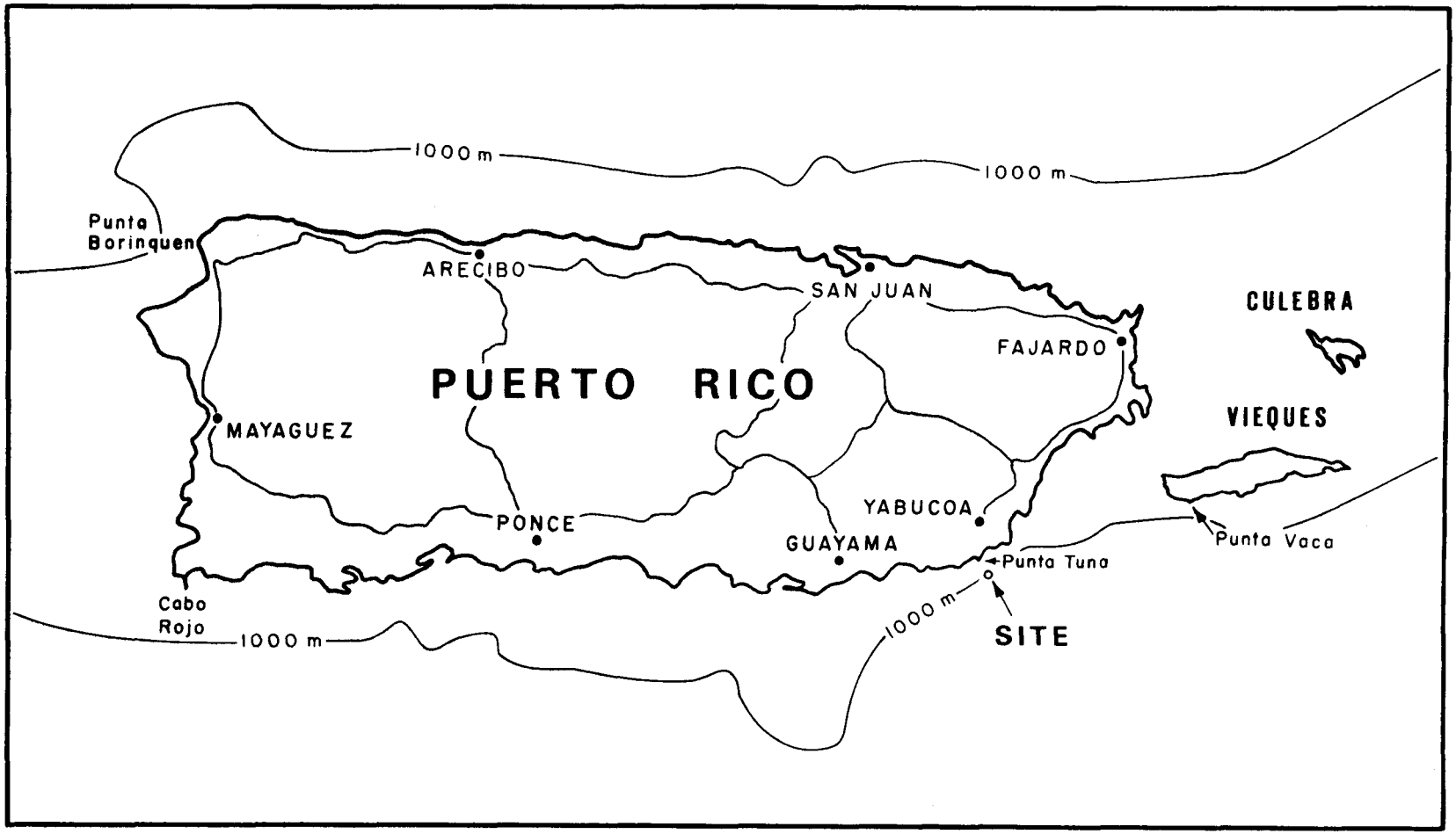

FIGURE 1 MAP OF PUERTO RICO SHOWING LOCATION OF TEST SITE

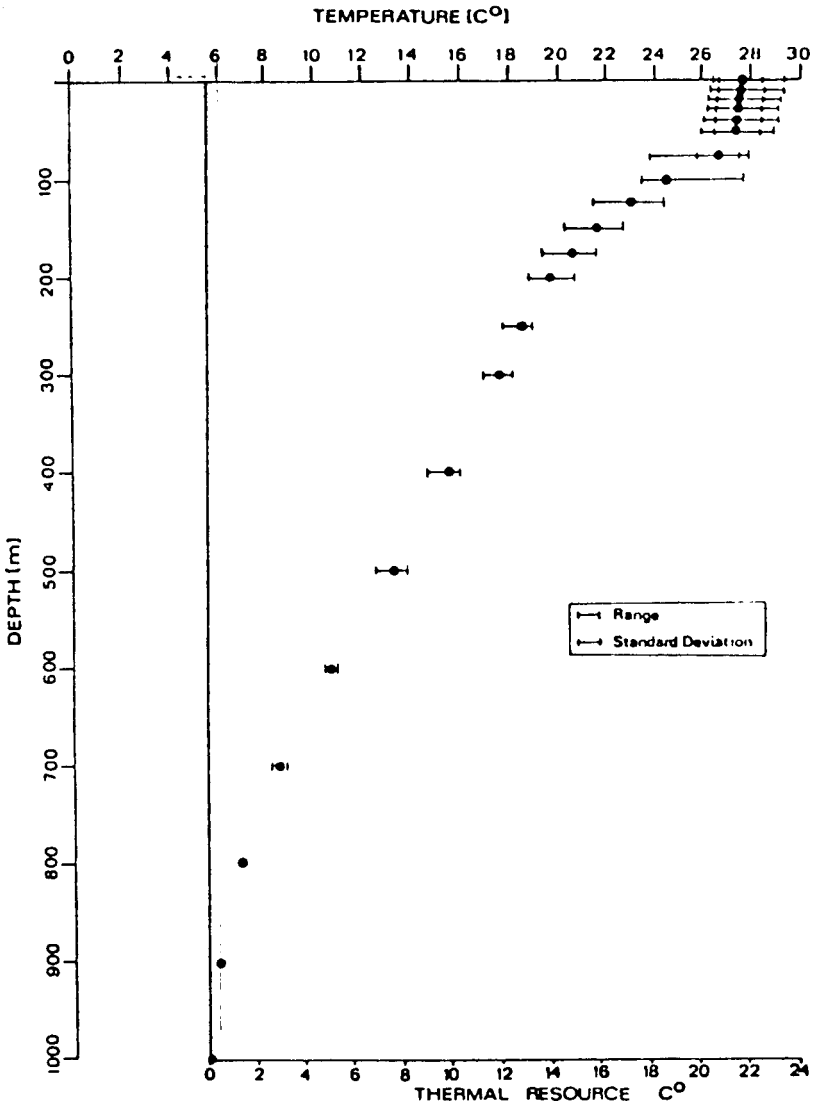

FIGURE 2 TEMPERATURE PROFILE OF THE AVERAGE TEMPERATURE DATA TAKEN AT PUNTA TUNA, FROM AUGUST, 1978 TO JUNE, 1979

3. MOORING

A tension-moored buoy was placed at the site. The mooring system was designed by Mr. Daniel C. Probert of the Naval Air Development Center in Key West, Florida. A light buoy 12 ft in diameter and 12 ft high was used. Attached to the buoy were 30 ft of 2 inch stud link chain. A type 3 Miller Swivel connected the bottom of the chain with 50 ft of 1 1/2 in steel wire rope. The other end of the wire rope was shackled to 3,000 ft of 2 in Kevlar line.

The mooring system was anchored by a 3,000 lb Danforth anchor attached to 1,100 ft of 1 in.stud link chain. The chain was joined to the bottom of the Kevlar line by a second, type 3 Miller swivel.

The research platform was attached to the mooring by a 400 ft section of 2 in nylon line shackled to the lower portion of the top swivel.

4. TEST FACILITIES

4.1 RESEARCH PLATFORM. The vessel used as a research platform was a Landing Craft, Utility (LCU) which had been an active vessel of the U.S. Army Heavy Boat Company of Moorehead City, North Carolina until the summer of 1978 when it was transferred to the DOE for OTEC experimental use (Figure 3). The LCU was a 350 ton vessel, 115 ft (35 m) long with a 34 ft (10.4 m) beam and was powered by three 165 hp diesel engines. Electrical power for housekeeping purposes was provided by two 20 kW DC diesel-electric generators. The LCU proved to be ideal for use as a research platform because it had approximately 1600 ft^2 (150 m^2) of open, usable deck area, boat motion was minimal during normal weather due to its wide, flat bottom, and because it could accomodate up to 14 people.

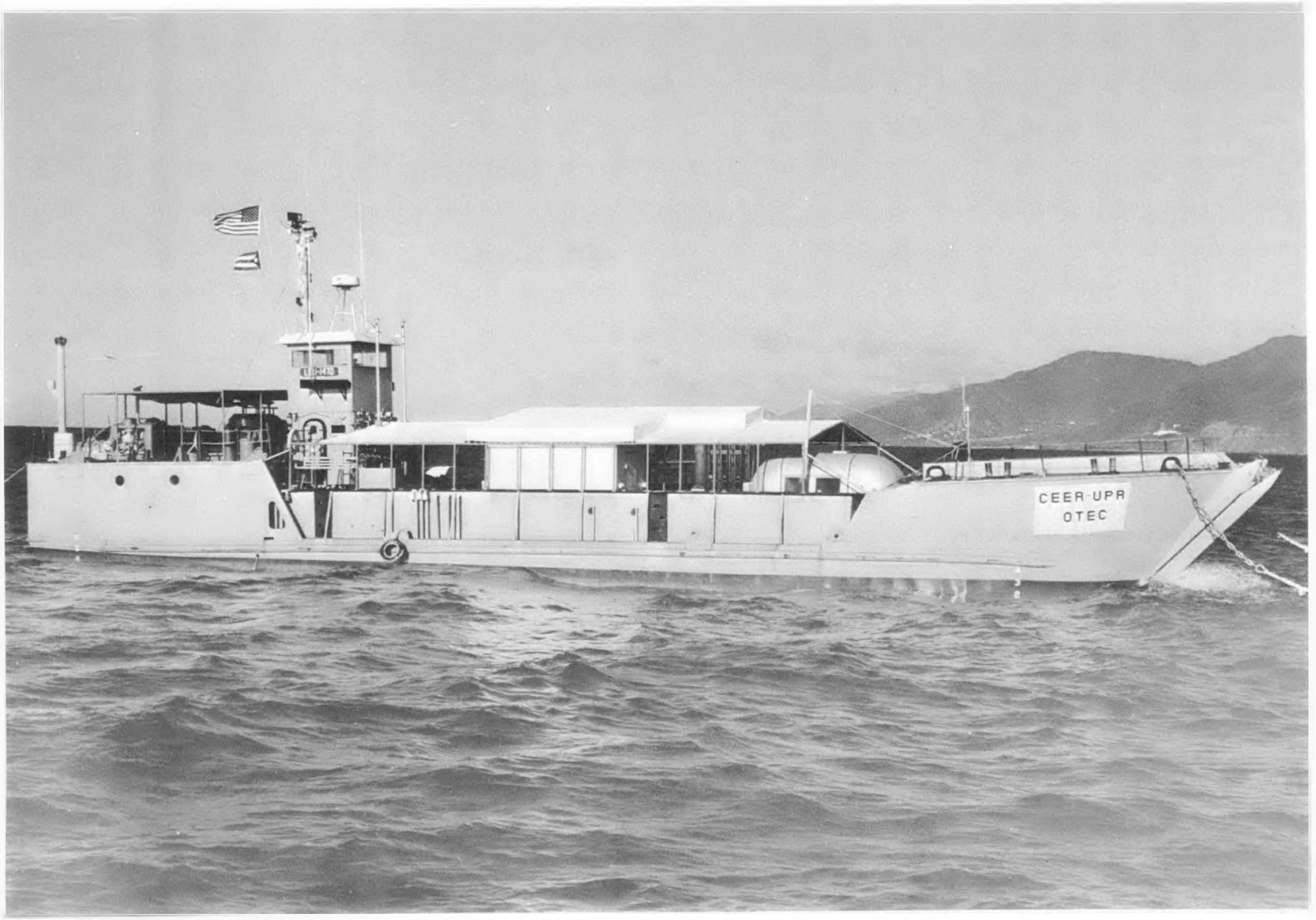

FIGURE 3. THE LANDING CRAFT, UTILITY (LCU) RESEARCH PLATFORM MOORED ON SITE AT PUNTA, PUERTO RICO

4.2 MODIFICATIONS TO VESSEL. The following modifications were made to the LCU for use as an OTEC biofouling research platform.

1. A 0.46 m (18 in) diameter well was made through the deck near the center of the vessel. The seawater intake and exhaust hoses passed through this well.

2. An "A" frame was placed over the well (Figure 4) to support a weighted cable to which the intake and exhaust hoses were attached.

3. Two support frames (Figure 5) were situated fore and aft of the well. Each frame held three pumps and two experimental modules, one testing 5052 aluminum and the other testing ASTM 3-338 grade 2 titanium. Each module had its own pump, intake hose and exhaust hose.

4. An air-conditioned, fiberglass house was placed beside the well to house the data acquisition system and other electronics.

5. Two 50 kVA, diesel-electric, AC generators were added on deck to supply power for the experiment. The generators were rotated daily.

6. Two of the ballast tanks were converted to fuel tanks to increase the fuel capacity.

7. The deck was covered by a canopy to provide partial protection from the sun and the rain.

4.3. FLOW SYSTEM. The flow system (Figure 6) was designed by Southwest Research Laboratory of San Antonio, Texas according to specifications provided by the Center. To minimize fluctuations of flow rate due to boat motion, the intake and exhaust hoses passed through a well near the center of mass of the platform. The intake hoses drew water from a depth of 17 m (55 ft), and the exhaust hoses discharged water 1 m below the vessel.

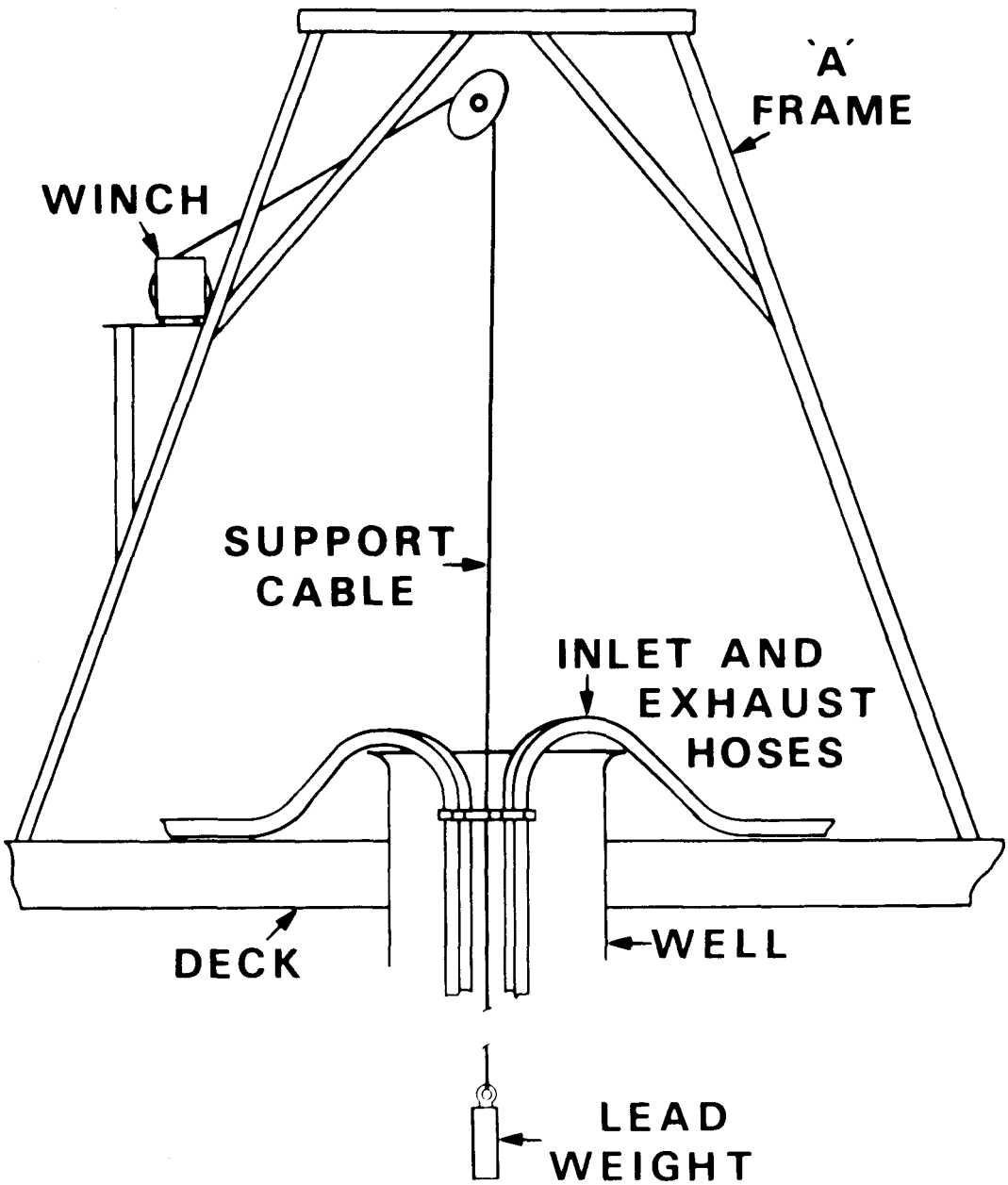

FIGURE 4 THROUGH DECK WELL AND "A" FRAME FOR DEPLOYMENT OF INTAKE AND EXHAUST HOSES

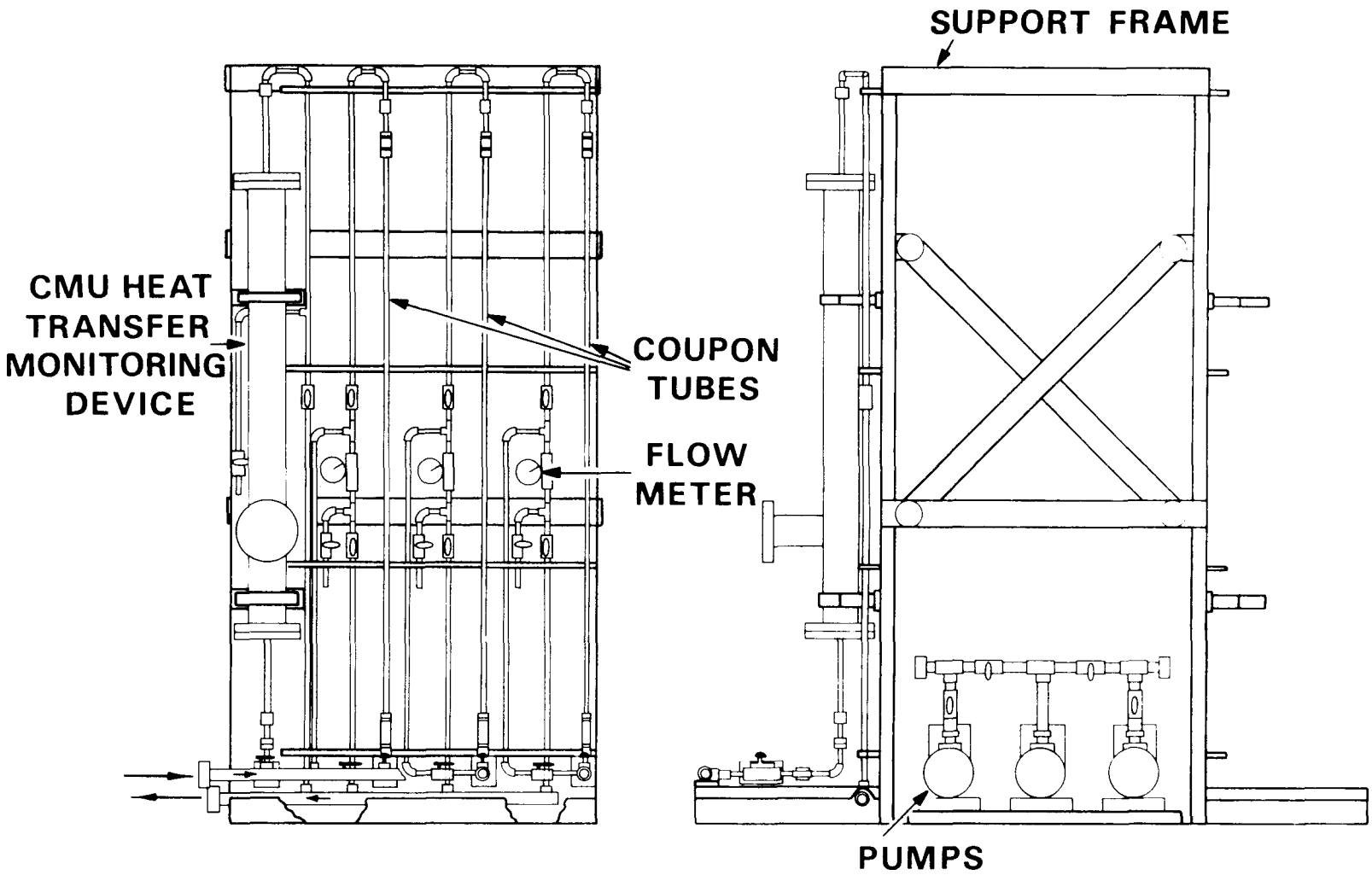

FIGURE 5 DRAWING OF ONE MODULAR FLOW LOOP SHOWING THE ARRANGEMENT OF THE CMU HEAT TRANSFER DEVICE AND THE SACRIFICIAL TUBES (LEFT) AND THE MOUNTING OF THE MODULE ON DECK (RIGHT).

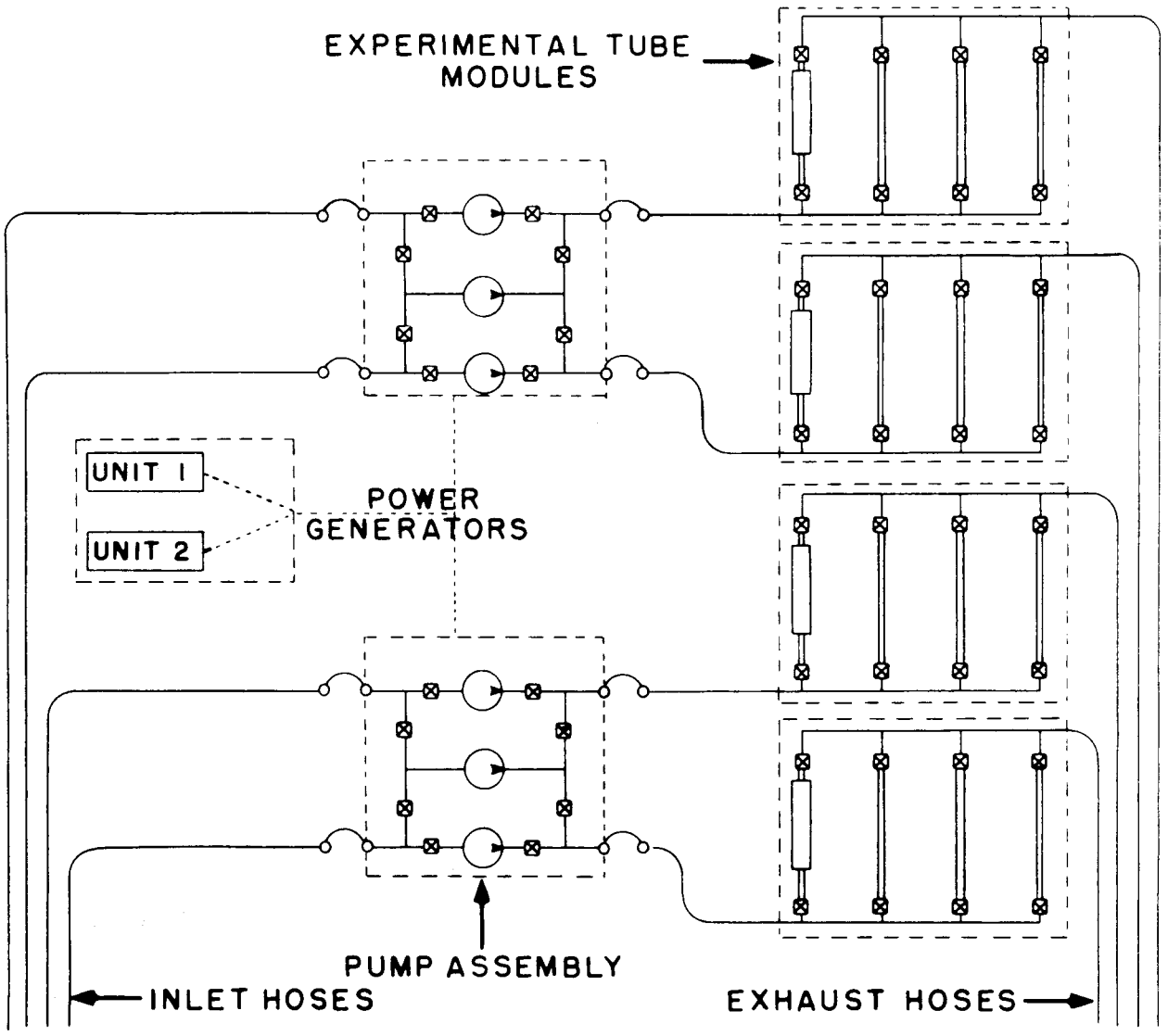

FIGURE 6 SCHEMATIC DIAGRAM OF THE FOUR MODULAR FLOW LOOPS OF THE HYDRAULIC SYSTEM

To avoid chafing of these hoses against the well wall, they were suspended from the aforementioned "A" frame, and a toroidal bumper system was attached to the suspending cable just above the bottom of the well. To prevent the intake hoses from flexing sharply below the vessel and thereby causing them to fatigue, they were reinforced with 1.2 m (4 ft) sections of 7.6 cm (3 in), T22 discharge hose; and to prevent them from swinging beneath the platform, the cable to which they were attached was weighted with 227 kg (500 lb) of lead. The lead was hung 4.6 m below the intake hoses by a 1.2 cm nylon line which had been substituted for the last 9 m of cable so that there was no metal near the water intake which might affect the results of the experiment.

The intake hoses were fitted with PVC strainers 0.9 m long with a slit width of 0.47 cm (3/16 in). Biogrowth was removed from the strainers by cleaning them underwater with a brush at least once a month.

Each experimental module (Figure 6) consisted of four parallel flow loops which insured that each flow path had the same potential for biofouling. One loop contained a modified Carnegie Mellon University heat-transfer monitoring (HTM) device mounted on a 2.54 cm (1 in) o.d. tube, and the remaining three loops had sacrificial tubes (also 2.54 cm.o.d.) from which samples for biofouling analysis were removed. The aluminum tubes were alloy 5052 with 0.165 cm wall thickness, and the titanium tubes were commercial grade 2 with 0.089 cm wall thickness. Water flow through the sacrificial tubes was upward so that when flow is stopped, they remain full of water. A pair of modules was vertically mounted back-to-back on a frame, and each pair had a third, auxiliary pump to guarantee continuous operation.

The pumps were rotated at one to two week intervals. Marlow, 1.5 hp chemical service pumps with NORYL pump housings were used. Seawater velocity was controlled manually by a ball valve and was kept at approximately 1.8 m/s (6 ft/s). All tube fittings and fixtures were made of polyvinyl chloride to prevent contamination of the water.

4.4 SHIPBOARD PROCEDURES. On board at all times were four crewmen (one engineer, two seamen, and one cook) who maintained a 24 hour watch and at least one member of the scientific staff. In addition to normal shipboard responsibilities, the crewman on watch was also expected to check the experiment hourly to assure that everything was functioning properly.

5. FOULING RESISTANCE

5.1 TEST PROCEDURES. Heat transfer was measured using modified Carnegie-Mellon University (CMU) HTM's (Figure 7) acquired from the National Data Buoy Office which had made two minor modifications to them: the pipe was moved lower in the housing and the flow meter was attached to the bottom of the housing where it could be easily removed to be cleaned or replaced, and the signal amplified card, which had originally been attached to the pipe inside the housing, was mounted in the "T", so that it was more accessible in the event that repairs or adjustments were needed.

The principle of the HTM "is to heat a segment of tube wall slightly above the water temperature and then to observe its cooling rate after the heat input is removed. The cooling curve (versus time) is exponential, according to Newton's law of cooling, with a time constant which is shown to be (apart from small, calculable corrections) inversely proportional to the heat transfer coefficient, h" (3). Cooling of the segment was measured by a thermocouple. The HTM also included a Ramapo Mark V strain gauge flow

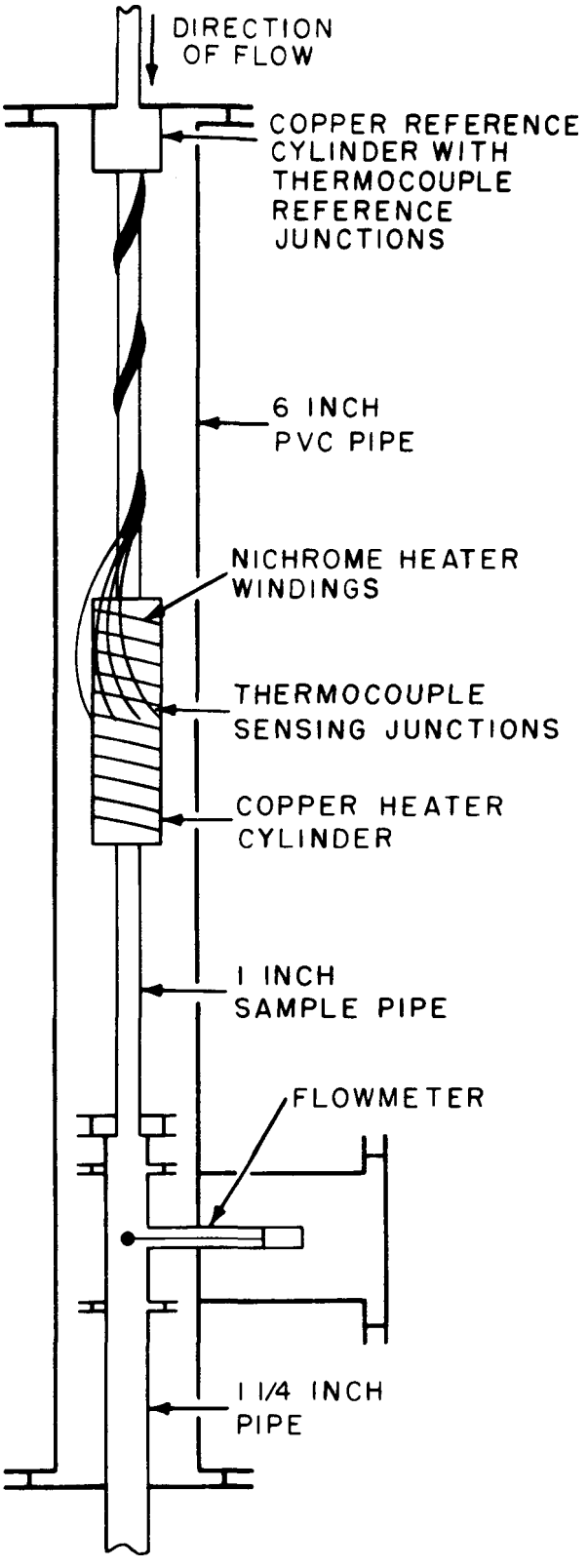

FIGURE 7 CARNEGIE-MELLON UNIVERSITY HEAT TRANSFER MONITOR (HTM)

meter to monitor flow rates and a thermistor to monitor water temperature. Signals from the thermocouple, flow meter, and thermistor were amplified within the HTM. The output from the HTM was carried by shielded cable to a control box located in the data house. The control box, designed at CMU (4), multiplexed the three signals and output them to a teletype at two second intervals. Data were stored on a purchased tape.

In the data analysis, a time constant was calculated for each cooling curve using a weighted, least-squares-fit program. The time constant along with physical parameters (flow rate, water temperature, tube dimensions, thermal conductivity, etc.) was used to calculate a normalized inverse heat transfer coefficient (1/h). The fouling resistance (R_f) was defined as 1/h minus the 1/h value calculated on the first day ($1/h_o$).

For major runs, made at seven to ten day intervals, one day's data for a unit consisted of at least ten cooling curves, of which eight were analyzed. After day 89, progress runs consisting of five cooling curves, of which four were analyzed, were frequently made between major runs.

Flow-meter and thermistor calibrations were verified whenever a major run was made. Flow meters were calibrated by measuring the fill time of a 0.038 m^3 (10 gal) bucket. Zero-flow voltage readings were taken at least twice during each run. Biofouling of the flow meter element was not a problem, but bivalves and serpulid worms did grow in the channel through which the strain gauge passed. This affected the calibration of the flow meters; however, by cleaning the channel the calibration could be returned to close to its original value.

5.2 RESULTS AND CONCLUSIONS

5.2.1 FOULING RESISTANCE (R_f). Fouling resistance, R_f, as a function of time for the two aluminum and the two titanium HTM's is presented in Figures 8 and 9. The first part of these curves (until day 80) is characterized by two distinct regions. Initially, R_f was nearly zero, and even sometimes slightly negative, then R_f increased at an approximately linear rate. The induction period for both aluminum units was one month, while for the titanium units it was only two weeks. It is believed that during the induction period the new pipe surface was being conditioned by an accumulation of a primary fouling layer. A similar induction period has been observed by previous investigators (5, 6, 7, 8 and 9) although Liebert (6) reported that the induction period for titanium was considerably longer than that for aluminum. Once this primary layer has been established our data indicates that fouling resistance increases linearly with time. This is in agreement with observations made by Fetkovich et al (5).

Biological analyses performed during the induction phase indicate that the early microbial growth occurred in patches which were observable only hours after start-up. It is possible that the added turbulance created by these patches of microorganisms may initially enhance the heat transfer coefficient. This would explain why we, and other investigators, have observed negative values of R_f during the first few days after start-up.

Between days 80 and 90, the R_f of all units decreased to a value close to zero. It is not certain whether this sudden decrease in R_f was the result of spontaneous sloughing of the biofouling layer or was caused by the additional shear force produced by an inadvertent, 50% increase in flow through the HTM's of approximately 30 minutes duration which occurred on day 86.

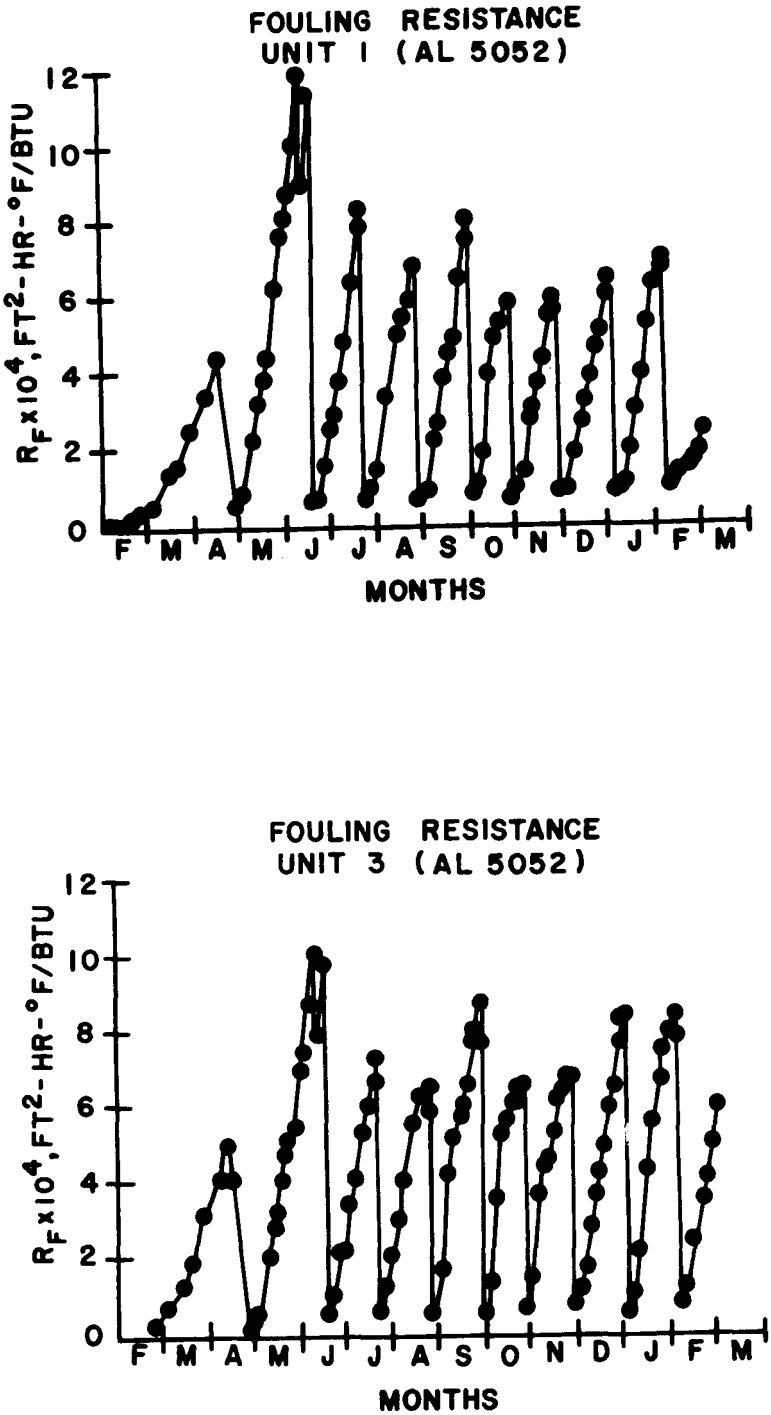

FIGURE 8 FOULING RESISTANCE OF ALUMINUM SHOWING CYCLES OF GROWTH AND CLEANING

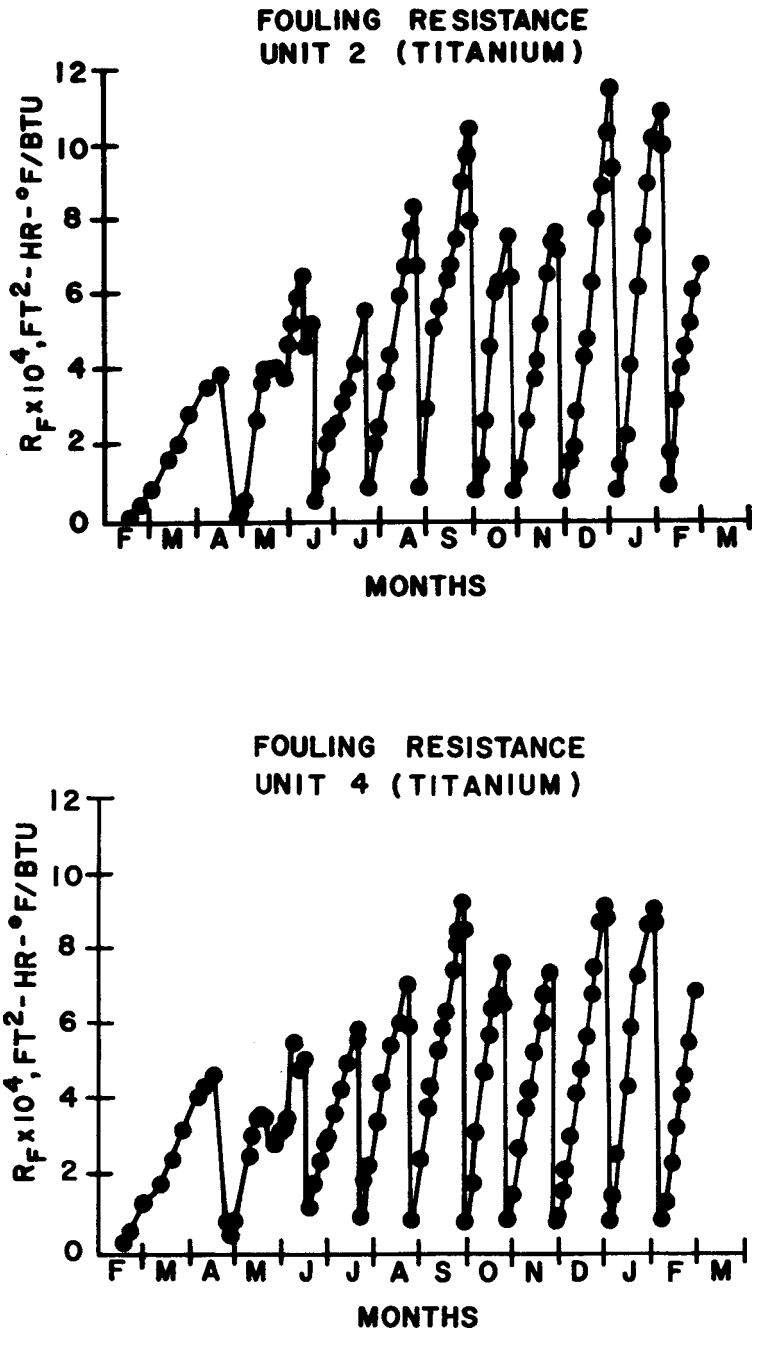

FIGURE 9 FOULING RESISTANCE OF TITANIUM SHOWING CYCLES OF GROWTH AND CLEANING

The effect of increasing flow velocity by 100% was tested before each subsequent cleaning. Results of the study indicate that some reduction in R_f occurred, but that the reduction was significantly less than that which occurred between days 80 and 90. This suggests that, at first, microorganisms adhere loosely to the surface and are easily dislodged, but that these early colonizers deposit a material to which later settlers can attach more firmly.

During May and June the tubes were allowed to foul for an extended period of time in order to determine if the film thickness would decrease spontaneously, or if it would reach an asymptotic or equilibrium value. Extensive, spontaneous film sloughing apparently occurred in both titanium units during the last two weeks in May, as is indicated by the titanium R_f plateau between 3 and 4 x 10^{-4} ft^2-hr-°F/Btu during that period. No similar occurrence was observed for the aluminum units even though the fouling resistance of both units climbed to over 10 x 10^{-4} ft^2-hr-°F/Btu, nor was there any further evidence of sloughing during the remainder of the test.

5.2.2 CLEANING. Each of the HTM's and sacrificial tubes was cleaned (vertical lines in Figures 8 and 9) by manually passing M.A.N. brushes 40 times through each tube or pipe. Results of the brush cleaning indicate that the fouling resistance was caused by two distinct biological layers. The top layer could be eliminated with several passes of a brush, while the hard, bottom layer was not removed even by 80 passes with a M.A.N. brush. Figure 10 is a graph of the fouling resistance of the aluminum and titanium tubes immediately after cleaning. After five months, thermal resistance of the hard bottom layer stabilized between 0.5 and 0.9 x 10^{-4} ft^2-hr-°F/Btu. Low initial values of the thermal resistance of the bottom layer during the first four months of the experiment correspond to the time when the biofilm

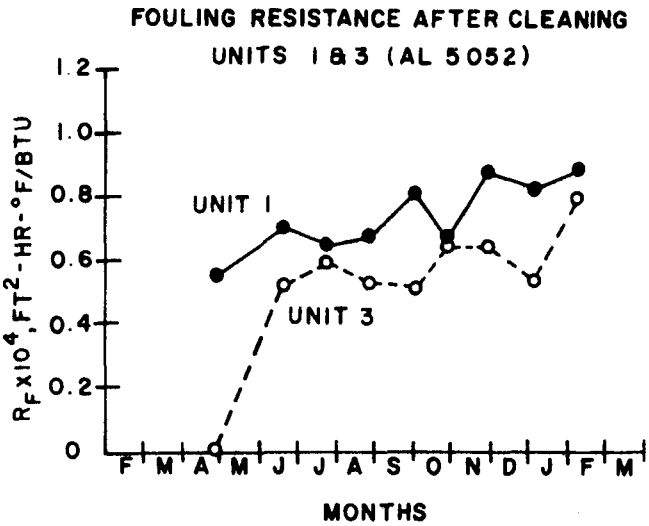

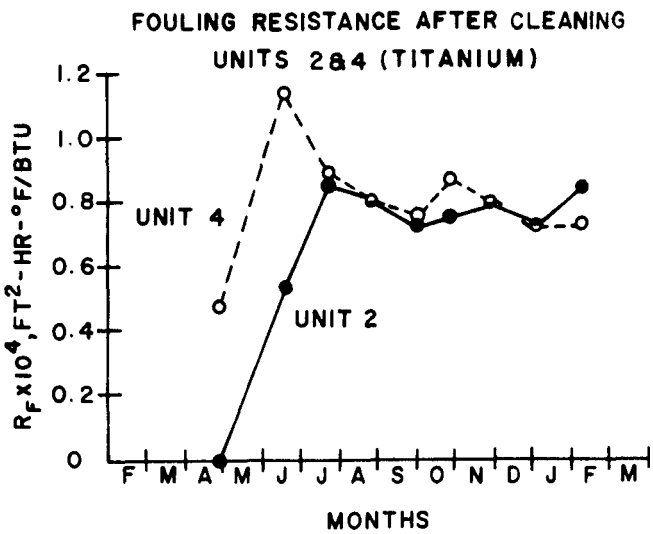

FIGURE 10 FOULING RESISTANCE OF ALUMINUM AND TITANIUM AFTER BRUSH CLEANING

was apparently only loosely attached to the metal surfaces and when the growth of biofilm was at a low rate (Figure 11)1. The higher values of post-cleaning fouling resistance correspond to the later portion of the experiment when fouling rates were higher. This supports the motion that a hard layer of extruded polysaccharides provides a necessary base for rapid biofilm growth but that this layer does not constitute a major portion of the thermal resistance of the biofouling layer.

Evidence from three Wilson Plots performed on units 2 and 3 during the course of the experiment (Table I) suggests that the non-zero value for R_f after cleaning was real and not due to inaccuracies of the experimental apparatus. The slopes and intercepts were considerably higher on the second Wilson Plots, which were taken after a brush cleaning, than for the original Wilson Plots run on new pipes. The third Wilson Plots, taken at the end of the experiment when R_f was high, demonstrate the effect of R_f on the slope and intercept. This relationship was approximately linear.

5.2.3 FOULING RATE (dR_f/dt). The initial time rates of increase in fouling resistance (fouling rate) for each unit along with subsequent post-cleaning fouling rates are shown in Figure 11 . The fouling rate of aluminum subsequent to the initital growth period was between 0.2 and 0.25×10^{-4} ft^2-hr-°F/Btu - day with the exception of the anomalous fouling rate of unit 1 during February 1981. The fouling rate of titanium generally increased during the first nine months and then stabilized between 0.25 and 0.33 (10^{-4}) ft^2-hr-°F/Btu/day.

The February decrease in the fouling rates of all units might be associated with the decrease in the ambient water temperature. Figure 12 shows the average water temperatures during each of the ten between-cleaning growth periods of the experiments and indicates a temperature low of 26.5°C

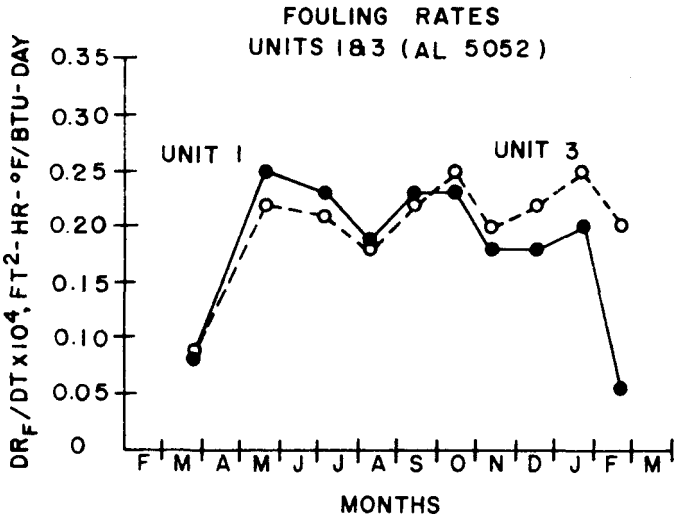

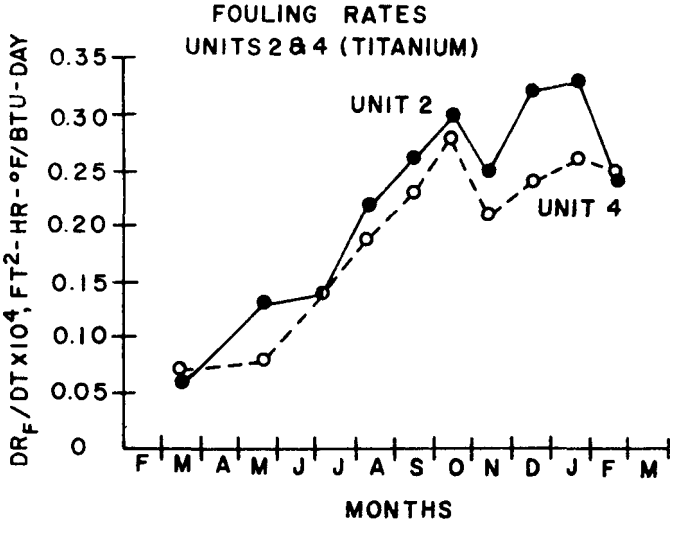

FIGURE 11 FOULING RATES (dR_f/dt) OF ALUMINUM AND TITANIUM

TABLE 1 WILSON PLOT DATA FOR UNITS 2 AND 3 MEASURED ON THREE OCCASIONS DURING THE TEST

UNIT 2

Date	Elapsed Time (days)	$^{2}R_f(x10^4)$	^{1}Slope ($x10^4$)	^{2}Intercept ($x10^4$)
18 Jan 80	0	0	36.52 ± 0.23	0.68 ± 0.07
2 Dec 80	307	0.78	38.56 ± 0.38	1.08 ± 0.11
9 Mar 81	404	7.21	48.13 ± 1.01	4.74 ± 0.27

UNIT 3

Date	Elapsed Time (days)	$^{2}R_f(x10^4)$	^{1}Slope ($x10^4$)	^{2}Intercept ($x10^4$)
18 Jan 80	0	0	36.08 ± 0.22	0.15 ± 0.06
2 Dec 80	307	0.64	39.82 ± 0.23	0.59 ± 0.06
9 Mar 81	404	6.30	49.61 ± 0.71	3.45 ± 0.19

1. (hr ft^2 °F/Btu) $(ft/sec)^{-0.8}$

2. hr ft^2 °F/Btu

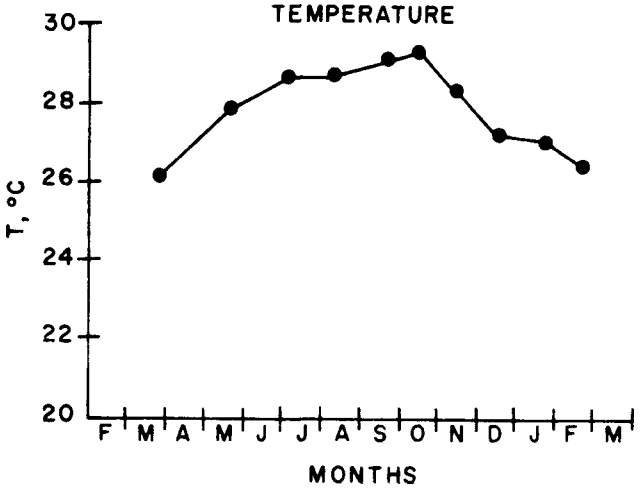

FIGURE 12 AVERAGE TEMPERATURE OF WATER DURING EACH GROWTH PERIOD

during February and March of 1981. Excluding the February data, the fouling rates of the two aluminum HTM's have a Pearson product-moment coefficient of correlation of r = 0.84, and the correlation of the fouling rates of the titanium HTM's is r= 0.94. The difference between the aluminum and Titanium units was statistically significant.

5.2.4 WET FILM THICKNESS. The fouling resistance, (R_f), and the wet film thickness, (WFT), were simultaneouly determined for both the aluminum and titanium tubes eight times during the initial three month start-up, eight times immediately proceeding each cleaning, and two additional times during the January growth period. No wet film was observed after the brush cleaning. Wet film thickness, therefore, was correlated not with the total value of R_f but rather with the difference in R_f before and after cleaning. Graphs of these simultaneously determined values of R_f and WFT for aluminum and titanium are presented in Figure 13. Close correlations exist between R_f and WFT. The R_f of the aluminum HTM's and the wet film thickness on the aluminum sacrificial tubes have a correlation of r = 0.97. The coefficient of correlation between the titanium R_f and WFT is r = 0.89, and the coefficient of correlation between all values of R_f, aluminum and titanium, and WFT is r = 0.93.

A straight line fitted by the method of least squares to R_f and WFT data gives the equation

$$R_f = 1.38\ (10^{-4}) + 2.94\ (WFT)$$

where the units of R_f are ft^2-hr-°F/Btu and WFT units are in ft. The inverse of the slope of this equation is equal to the coefficient of thermal conductivity, k. of the Wet Film. Inverting the slope yields k = 0.34 Btu/ft- hr-°F, which is almost identical to the coefficient of

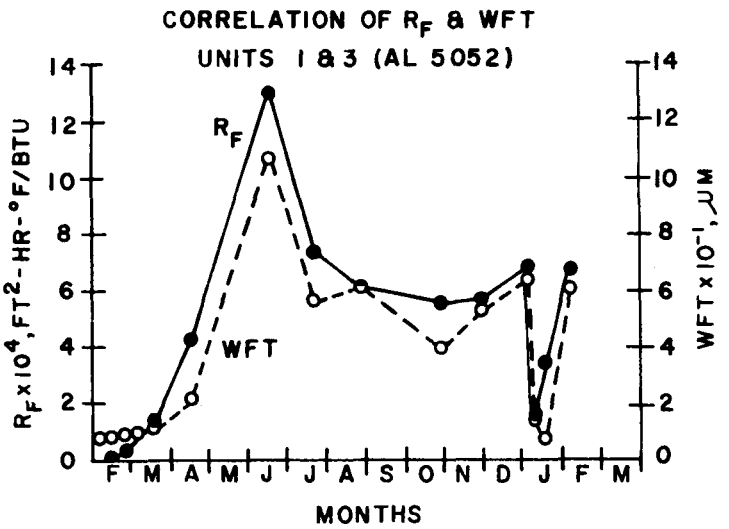

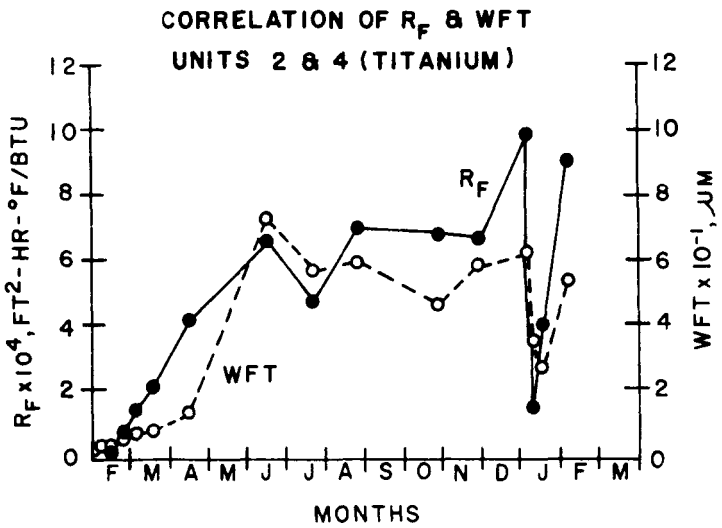

FIGURE 13 CORRELATION OF THE FOULING RESISTANCE (R_f) OF THE HTM's AND THE WET FILM THICKNESS (WFT) OF THE SACRIFICIAL TUBES

thermal conductivity, 0.35, of seawater at 28°C.

The excellent correlation between R_f and WFT and the close approximation of the coefficient of thermal conductivity of the Wet Film to that of seawater supports the hypothesis that a stagnant film of water entrapped by bacteria is largely responsible for the insulating properties of the biofilm.

5.2.5 CONCLUSIONS. During the induction period, approximately one month or less, the biofilm was only loosely attached to the metal surface. Some spontaneous sloughing occurred and much of the film could be detached by the additional shear forces produced by a 50% increase in velocity, leaving a "patchy" film on the tubes. The base layer of what appears to be exudated polysaccharides enhances the microbial adhesion and probably is necessary for rapid biofilm growth. This hard base layer has a maximum thermal resistance of less than 1×10^{-4} ft^2-°F/Btu and does not constitute the major portion of the thermal resistance of the film.

The time rate of increase of R_f was found to be best described by linear equations, aluminum and titanium generally having different rates but both experience maxima of approximately 0.3 (10^{-4}) ft^2-hr-°F/Btu-day.

Excellent correlation was found between R_f and WFT, which enabled the calculation of the coefficient of thermal conductivity of the film. This was found to be 0.34 Btu/ft-hr-°F and approximates the thermal conductivity

of seawater. It was therefore concluded that stagnant water, entrapped by microorganisms, was largely responsible for the insulating properties of the biofilm.

6. MICROBIOFOULING

6.1 SAMPLE COLLECTION AND ANALYSIS

6.1.1 COLLECTION.

During Phase I (0 - 143 days), the 12 test surfaces were sampled 11 times. This sampling schedule is outlined in Table 2 . Test surfaces were sampled 9 times during Phase II (143 - 404 days). Samples were removed before and after tubes were cleaned. The sampling schedule for Phase II appears in Table 3 . On 4 October 1980, the tubes were cleaned, but no samples were taken.

The flow of seawater through each tube was briefly stopped during the sampling process, a section was removed from the upstream end of the tube with a pipe cutter (Ridgid Tubing Cutter, Ridge Tool Co.), and flow through the tube was restored. The sample section removed was cut into small rings 0.5 in (1.27 cm) in height. Rings to be used for ATP measurement were analyzed immediately. Rings for surface residue analysis were capped on one end, filled with distilled water, capped shut and frozen immediately. The remaining samples were filled with an artificial seawater - glutaraldehyde (4%) solution, capped, and kept refrigerated (4°C) until they could be analyzed.

6.1.2 SAMPLE ANALYSIS

6.1.2.1 TOTAL SURFACE RESIDUE.

Three sample rings were cut from each tube, filled with distilled water, capped and frozen on site. Three samples were transported from the platform to the laboratory (La Parguera) on ice. Each ring contained approximately 15 ml of distilled water. In the laboratory each ring and its solution were thawed, placed in a cup sonicator (Sonic Dismembrater, Quigley-Rochester, Inc.) and sonicated at 60% full power for two minutes. This procedure was repeated three times

TABLE 2. BIOLOGICAL SAMPLE SCHEDULE FOR PHASE I

Date	Sample	Sample Interval	Mean Time	Elapsed Time (DA)
January 29	0*	8:48 PM - 9:20 PM	9:04 PM	0.00
January 30	1	8:50 AM - 2:35 PM	11:43 PM	0.61
February 3	2	4:15 PM - 8:52 PM	6:35 PM	4.93
February 8	3	12:25 PM - 3:05 PM	1:45 PM	9.71
February 15	4	10:13 AM - 1:01 PM	11:37 AM	16.63
February 26	5	9:34 AM - 12:03 PM	11:19 AM	27.62
March 7	6	11:13 AM - 1:10 PM	12:12 PM	37.65
March 20	7	9:50 AM - 12:45 PM	11:18 AM	50.62
April 18	8	11:00 AM - 12:00 PM	11:30 AM	80.63
May 3	9	9:45 AM - 1:45 PM	10:45 AM	95.59
June 20	10	9:20 AM - 1:45 PM	11:32 AM	142.60

*Experiment initiated.

TABLE 3. BIOLOGICAL SAMPLE SCHEDULE FOR PHASE II

Date	Sample	Sample Interval	Mean Time	Elapsed Time (DA)
1980				
June 20	10	9:20 AM - 1:45 PM	11:32 AM	0*
July 25	11	8:32 AM - 12:55 PM	10:44 AM	35
August 30	12	9:10 AM - 12:30 PM	10:52 AM	36
October 4	13	No Biological Samples Taken	10:00 AM	35
November 1	14	9:00 AM - 11:00 AM	10:00 AM	28
December 3	15	9:35 AM - 11:35 AM	10:35 AM	32
1981				
January 9	16	9:30 AM - 11:00 AM	10:45 AM	37
January 16	17	9:53 AM - 10:53 AM	10:23 AM	7**
January 23	18	10:17 AM - 11:17 AM	10:47 AM	14**
February 15	19	9:20 AM - 11:45 AM	10:33 AM	36

*Cleaning cycle experiment initiated.
**Experimental tubes samples, and not cleaned.

adding fresh distilled water on the final two sonications. Thus a total volume of 45 ml of sonicated suspension was obtained from each sample ring. These suspensions were freeze dried, the powdered residue material (SR) recovered and weighed (Micro Mettler Balance).

6.1.2.2 ORGANIC CARBON AND NITROGEN CONTENTS. The organic carbon and nitrogen contents of the surface residues (SR) obtained from each of the sample rings were determined by CHN analysis (Hewlett Packard). Analyses were done in duplicate.

6.1.2.3 ATP CONTENT - ADENOSINETROPHOSPHATE CONTENT. At each sampling time, two to three 0.5" rings were cut from each of the twelve sample tubes. These rings were individually placed in vials containing the membrane solubilizing agent NRB (Lumac, Inc.). The vials were chilled and agitated. The ATP contents of these extracts were determined on site employing an ATP Photometer (Luminometer M1070, Lumac, Inc.). Techniques of this type have been employed to determine microbial biomass (10,11). Each extract was tested in triplicate. These determinations were carried out on the platform during the course of the respective sampling period (approximately 2 to 4 hours).

The ATP blank reading was determined using sample rings extracted with NRB subsequently cleaned with acetone and dried. These sample rings were then re-extracted with NRB and the ATP concentration in these extracts determined as described. These blank readings were subtracted from the reading obtained for the initial NRB extract of the sample rings.

6.1.2.4 WET FILM THICKNESS (WFT) AND VOLUME (WFV). A small plaque (1 cm^2) was cut from each of four rings of test surfaces and stored in fixative for analysis. The prepared fixed plaques of the

test surfaces were mounted in petri dish chamber (100 x 15 mm). Each chamber had from one to four small plastic platforms glued to the inside bottom surface of the petri dish. The plaques were mounted (glued) on these platforms and the floor of the petri dish covered with a small quantity of distilled water against which the test surface biofilms were equilibrated. A small piece of thread was placed on each mounted plaque such that one end was in contact with the wet film on the test surface and the other immersed in the equilibration media on chamber floor. This thread provided a capillary path between the sample and the equilibrated media. Following the mounting of the test surface plaques, addition of the equilibrating media and the placing of the thread, the top of the petri dish was put in place and sealed shut with surgical grade adhesive tape. The sealed, air chamber were equilibrated for periods of from 18-24 hours at laboratory temperatures (22-24°C). The thickness of the wet films found on the test surfaces was determined with a Light Sectioning Microscope (Gaertner Scientific Co.). The techniques employed for this determination have been reported (12).

6.1.2.5 SURFACE ASSOCIATED VIABLE BACTERIA.

Quantitative enumeration of the viable aerobic heterotrophic bacteria associated with the test surfaces were determined using the standard plate count method (13, 14, 15). On site at the time of sampling, 1 cm^2 plaques were cut from both types of test surfaces and placed in vials containing 10 ml of sterile artificial seawater. The vials were agitated (vortexed) for 5 minutes and serial dilutions of the resulting suspension made. Known aliquots of each of these dilutions were mixed with 15 ml of enriched agar in sterile plastic petri dishes. The plates were wrapped in aluminum foil and transferred to the laboratory. The plates were incubated at laboratory

temperature (22-24°C) for 10 to 15 days. Following this the colonies that developed were counted and the number of viable heterotrophic bacteria per cm^2 of test surface was determined. The plates for each dilution were prepared in duplicate. Aseptic techniques were followed throughout these procedures. These experiments were carried out on samples 4, 5, 6, 7 and 9 (See Table 2).

6.1.2.6 SCANNING ELECTRON MICROSCOPY (SEM). Lengths of aluminum and titanium sacrificial tubes designated for SEM examination were cut into rings aboard ship and preserved immediately in a filtered solution of 4% glutaraldehyde in seawater. Plaques (cm^2) cut from the rings above were rinsed and dehydrated according to the following schedule:

1.	Seawater:Distilled water (1:1)	15 min.
2.	Distilled water	2 min.
3.	Distilled water	2 min.
4.	50% Ethanol	15 min.
5.	70% Ethanol	15 min.
6.	95% Ethanol	15 min.
7.	100% Ethanol	5 min.
8.	100% Ethanol	5 min.

Dehydrated plaques were air dried and then attached to SEM stubs with colloidal silver. Stubs with attached plaques were then immediately coated with gold-palladium in an ETEC vacuum coater. Observations were subsequently made with an ETEC Autoscan scanning electron microscope.

6.2 RESULTS

6.2.1 PHASE I (Day 0 to Day 143). Presented in this section are results of the microbiofouling analyses for the first portion of the experiment before brush cleaning was begun.

6.2.1.1 TOTAL SURFACE RESIDUE (SR). The surface residues associated with 388 samples were determined during the course of this study (Figure 14). In general, the accumulation of material on the aluminum was higher than that seen on the titanium surfaces. During the first ten days of the experiment, the accumulation of both test surfaces was linear with time, the aluminum surfaces gaining material at a rate of 1.6 ug/cm^2/day, the titanium at 0.4 ug/cm^2/day. Subsequent to this "film initiation" period, the amount of material associated with both surfaces decreased. Throughout the remaining period of the study, the SR increased linearly with time, at a rate of 0.6 ug/cm^2/day on aluminum and 0.1 ug/cm^2/day on titanium. During the period of approximately 15 days through 143 days of exposure to flowing seawater, the SR on aluminum increased eleven-fold; whereas on titanium, the SR increase was slightly more than double.

6.2.1.2 ORGANIC CARBON AND NITROGEN CONTENTS. Figures 15 and 16 illustrate the changes in the organic carbon contents and the carbon/nitrogen ratio of SR during this phase of the study. Following the initial period of wet film establishment, the organic carbon contents of the SR increased linearly with time at a rate of 0.7 ug/cm^2/day on aluminum and 0.3 ug/cm^2/day on the titanium surfaces. From approximately 20 through 143 days of exposure, the amount of organic carbon found on the aluminum increased nine-fold and on the titanium surfaces, approximately seven times. Thus the extent and rate at which organic carbon and total SR accumulated on the aluminum and titanium surfaces were similar.

Figure 16 shows the changes in the carbon/nitrogen ratio of the SR recovered during this phase of the study. Following an initial rise and decrease in the C/N ratio during the film initiation period, there is a

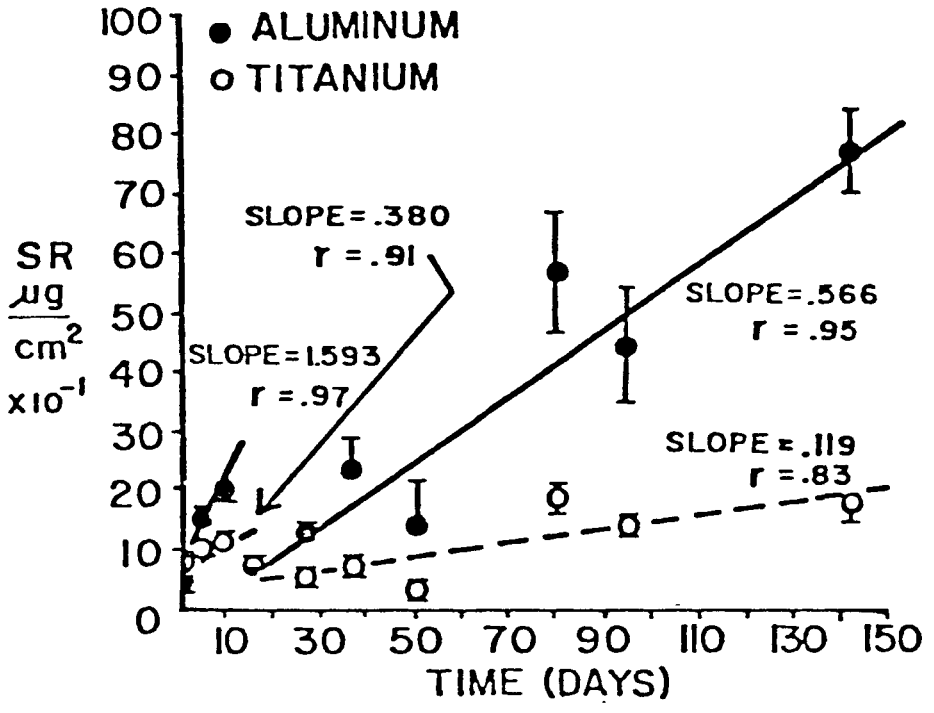

FIGURE 14 SURFACE RESIDUE DURING PHASE I

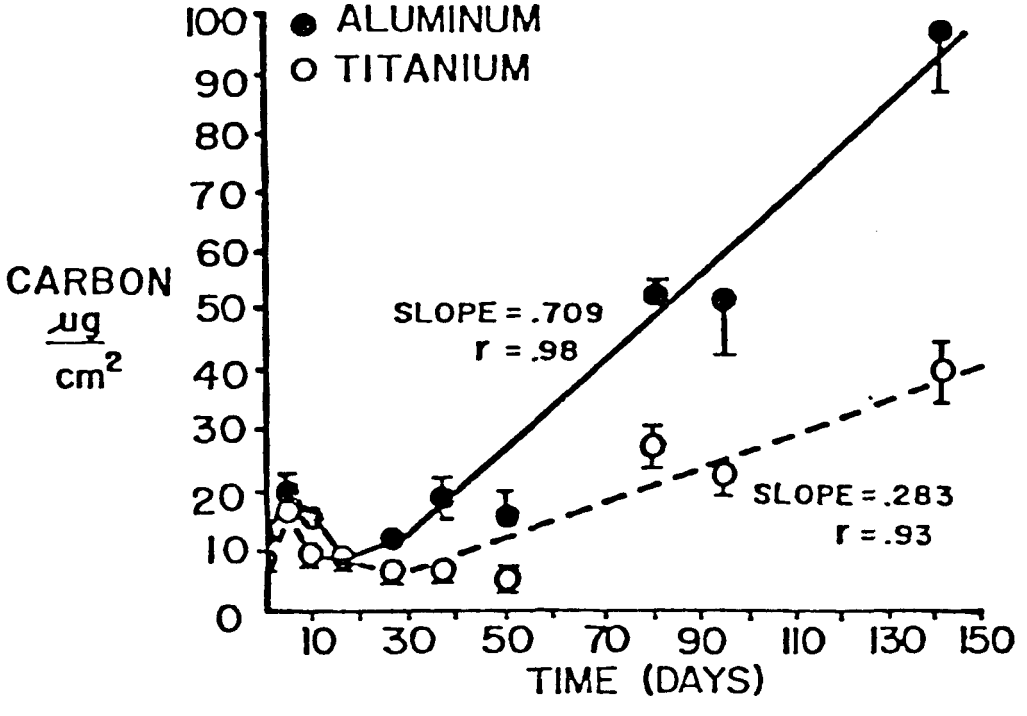

FIGURE 15 ORGANIC CARBON DURING PHASE I

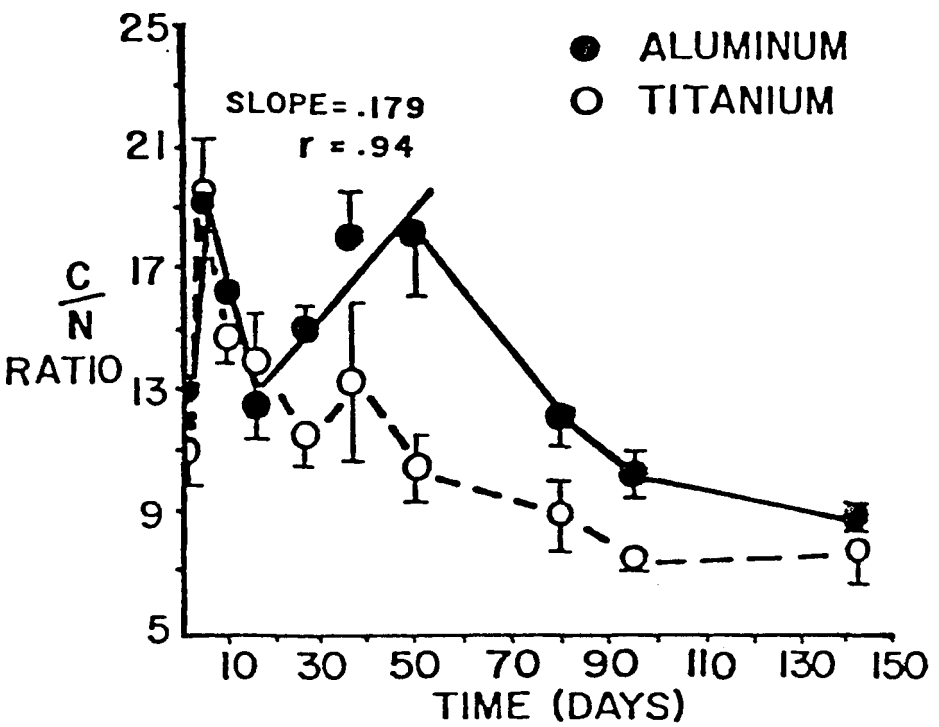

FIGURE 16 CARBON/NITROGEN RATIO

linear increase in the C/N ratio of the material found on the aluminum surfaces through 50 days of exposure. Following the initial period (0 to 10 days), the C/N ratio of the material found on the titanium surfaces decreased steadily through 143 days of exposure. On the aluminum surfaces, a similar decrease is seen after 51 days of exposure. The decreases in the C/N ratio seen on the test surfaces are exponential with time, showing similar rates.

6.2.1.3 ATP CONTENT. The ATP associated with 300 samples of the test surfaces was determined during the course of this study. The average amount of ATP associated with the test surfaces does not express the frequency with which ATP was found on those surfaces. The average frequency (the average number of rings per tube that give significant ATP readings) of ATP occurrence was higher on titanium than aluminum (Table 4). This frequency is directly related to the patchiness of the microbial biomass on these surfaces. Figure 17 shows the average quantity of ATP (pg) in terms of the area of the respective surface times the frequency (f') of ATP occurrence on that surface (log scale) as a function of time exposure.

The amount of ATP associated with the titanium surfaces increased exponentially with respect to time throughout the course of this study. On the aluminum surfaces, there was an exponential increase in ATP through 51 days of exposure. Following this, there was a sharp decrease in the ATP on the aluminum surfaces through 96 days of exposure. During the period from 96 through 143 days, there was a sharp increase in the ATP associated with the aluminum surface. The initial exponential increase in the aluminum ATP appears to be associated with increases in the C/N ratio of the material (SR) associated with these surfaces (Figure 16). During the

TABLE 4 ATP FREQUENCY (PERCENT OF SIGNIFICANT ATP READINGS PER TUBE SAMPLE)

Time (Days	Al	Ti
0.6	0*	22
4.9	22	34
9.7	17	61
16.6	23	94
27.6	42	67
37.7	17	92
50.6	33	100
80.6	33	100
95.6	94	100

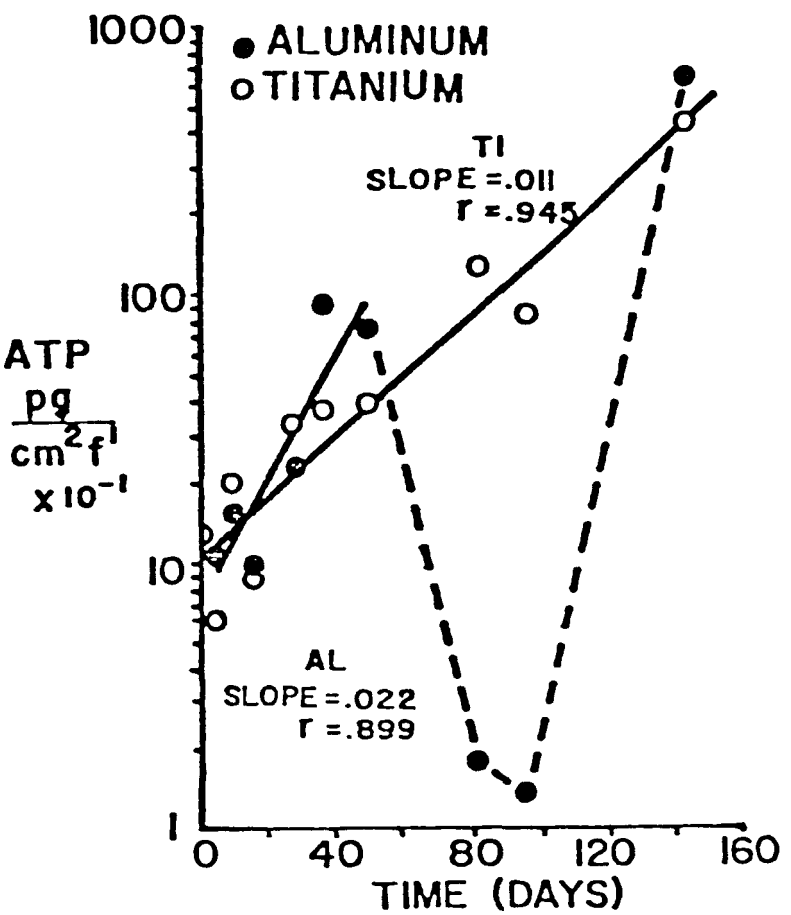

FIGURE 17 ATP CONTENT DURING PHASE I

96-143 days period, the sharp increases in biomass on the aluminum surface was not accompanied by comparable changes in the C/N ratio (Figure 16).

6.2.1.4 WET FILM THICKNESS. The films formed on the test surfaces were discontinuous and divided into areas of maximum and minimum thickness. Maximum thickness were observed immediately adjacent to a film interruption (discontinuity) and minimal thickness was seen between these "breaks" in the film. The film discontinuities appear to be due to clusters of material and/or microorganisms on the test surfaces. The thickness of the film increases in the area of these hydrated clusters and at their peak height the transparent film goes out of the plane of focus of the LSM. The minimum level thickness is taken as a minimal stable layer, possibly due only to aqueous connections between different clusters of material.

A total of 362 plaques of metallic surfaces were prepared, equilibrated and the WFT's determined. Wet films on the test surfaces were observed after 0.6 days of exposure to ambient seawater (Figure 8). These WFT's are at the limit of the resolution of the LSM technique.

There was no homogenous minimal layer and a film was observable only in the area of a discontinuity. A significant film was established after 17 days of exposure. The maximum WFT gradually increased during the 17 to 50 day period of exposure. The maximum WFT on aluminum was significantly greater than that seen on the titanium surface ($p \leq 0.1$.). There was a sharp increase in WFT from 50 through 96 days of exposure. The film appeared to grow in stages, with a pronounced bulk increase taking place in the 50 to 96 day period. The average WFT expresses the average thickness of the films that were observed, not the average frequency with which they

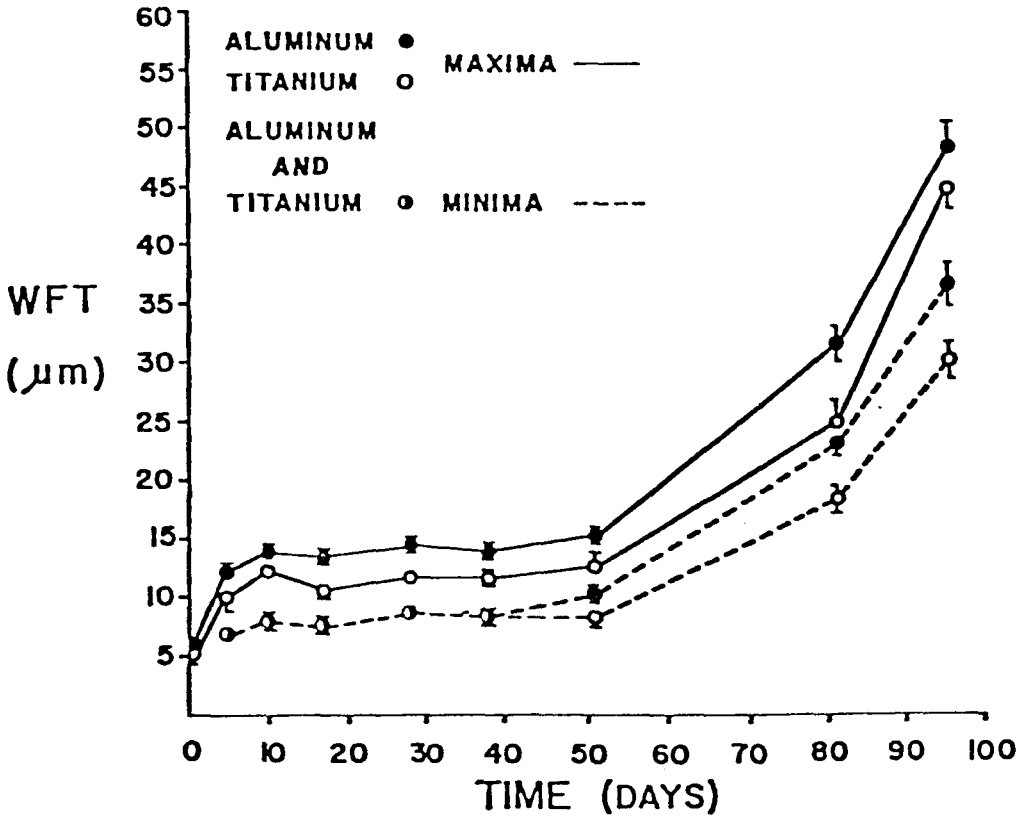

FIGURE 18 WET FILM THICKNESS (WFT) DURING PHASE I

occurred on a given material. On the average aluminum tube after 17 days of exposure 100% of the plaques examined had films. On the average titanium tube all the plaques had films only after 51 days of exposure. On aluminum the number of film discontinuities increased sharply through 10 days, subsequently decreasing through 51 days of exposure. This is followed by a sharp increase in the final stage (51 to 96 days). In the case of the titanium surfaces a similar thing is seen, however the number of discontinuities is significantly reduced from that seen on aluminum. Table 5 illustrates these changes in film frequency and discontinuities on the test surfaces.

The minimal WFT found on aluminum surfaces did not differ from that seen on titanium from 5 through 38 days of exposure. From 51 through 96 days of exposure there is a significant increase in minimum WFT. In this period the minimum WFT on aluminum is greater than that on titanium. During the final period of exposure (51 - 96 days) entire patches of material appeared to have sloughed off the test surfaces. This effect was not observed on either test surface through 51 days of exposure. The areas of these "patches" were estimated (LSM) on a series of 26 plaques selected from both types of materials on the 96 day sample. Immediately prior to taking the 96 day sample the velocity of water flow in a portion of the tubes was increased from 6 ft/sec to 9 ft/sec for a short period (1 hour). This was done to ascertain the effect of water veolcity on the sloughing of material off the test surfaces. Table 6 illustrates the results of this experiment. The relative fractional area of the patches and their frequency are higher on the titanium as compared to the aluminum surfaces. The average patch area

TABLE 5. WFT Frequencies and Film Discontinuity

	Al		Ti	
Time (Da.)	f*	B**	f	B
0.6	67 ± 8	2.5	38 ± 14	2.5
4.9	92 ± 8	7.2 ± .9	50 ± 6	3.6 ± .4
9.7	92 ± 5	6.8 ± .8	54 ± 4	2.3 ± .7
16.6	100	5.4 ± .5	75 ± 13	3.0 ± .8
27.6	100	5.8 ± .5	88 ± 7	1.5 ± .3
37.7	100	6.5 ± 1.3	92 ± 8	1.3 ± .5
50.6	100	6.3 ± 2.1	100	2.3 ± .6
80.6	100	10.5 ± 1.0	100	8.6 ± 1.4
95.6	100	8.3 ± .5	100	9.8 ± .7

* f = average frequency (%) of plaques per tube with films ± SE.

** B - average number of film discontinuities ± SE.

TABLE 6 PATCH AREAS AND RELATIVE FREQUENCIES

	Al	Al(V)	Ti	Ti(V)
Patch Area (% + SE)	0.9	3 + 3	13 + 8	10 + 6
Frequency (%)*	12.5	50	75	100
Plaques Examined	8	8	4	6

*frequency of plaques on which patches were seen.

is not significantly increased by the short period of elevated water velocity, however, the frequency of patchiness increases on both surfaces.

Three different periods of film development were observed, (a) 0 to 10 days (initiation), (b) 17 to 51 days (maturation) and (c) 51 to 96 days (bulk growth). The linear estimates of the rate of growth of the maximum and minimum WFT on the test materials during these periods are given in Table 7 . The growth rates of the maximum and minimum WFT on both types of materials are similar in the bulk growth phase of film development (0.5 to 0.7 um/day). These values are similar to those seen in the initiation phase (0.8 to 0.9 um/day). Film growth rate on aluminum does not appear too different from that seen on titanium. However, as noted before, film coverage on the aluminum surfaces is significantly greater than that on titanium until 51 days of exposure (Table 5). Film growth rate during the maturation period is approximately 1/20 that seen in the initiation period.

To calculate wet film volume (WFV), the average WFT - based on the maximal thickness of the wet film and the frequency of film discontinuities found on that surface - was multipled by the average fraction of the surface that was covered to obtain the average volume of material associated with one cm^2 of each test surface. Figures 19 and 20 summarize these results.

Following the initiation period, the WFV on the aluminum surfaces increased exponentially with time from 17 to 51 days of exposure (Figure 19). The extrapolation of this growth is indicated by the dashed line in this Figure. Following 51 days of exposure, there was an abrupt and significant increase in the rate of WFV growth on the aluminum surfaces. The WFV on the titanium surfaces increased exponentially from 17 to 51 days of exposure (Figure 20). The rate of increase in the WFV found on titanium during this

TABLE 7 FILM GROWTH RATE*

Period	Maximum WFT		Minimum WFT	
	Al	Ti	Al	Ti
Initiation	0.9 (.93)	0.8 (.97)	-	-
Maturation	0.04 (.80)	0.05 (.94)	0.03 (.70)**	
Bulk Growth	0.7 (.98)	0.7 (.95)	0.6 (.99)	0.5 (.96)

* um/day (correlation coefficient)

** Al and Ti combined, 17 to 38 days of exposure.

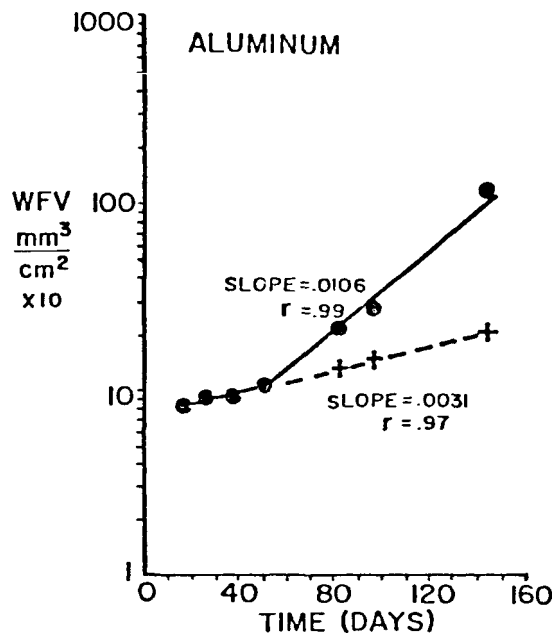

FIGURE 19 ALUMINUM WFT

FIGURE 20 TITANIUM WFT

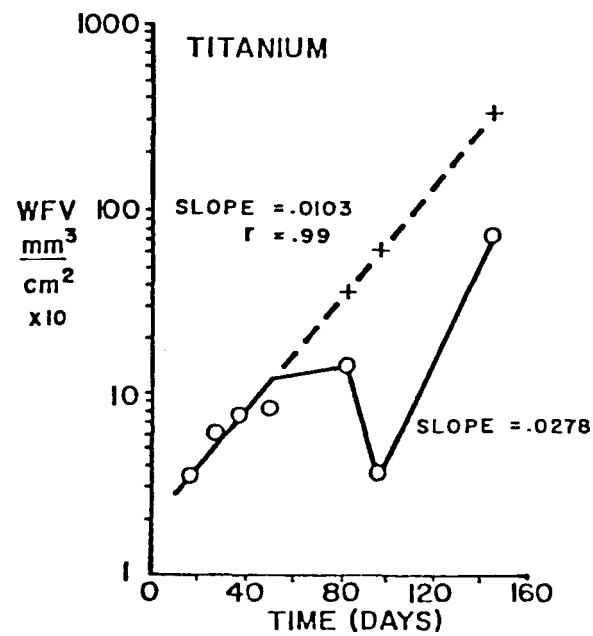

period was significantly greater than that seen on aluminum. The extrapolation of the initial WFV growth rate is indicated on Figure 20 by a dashed line. Following 51 days of exposure, the WFV on titanium did not continue to increase and in fact decreased at 96 days of exposure. This decrease was followed by a sharp increase in WFV at the termination of the study (143 days of exposure). The effects in titanium are attributed to the sloughing off that occurred during the period from 81 to 96 days of exposure. The changes in the rate of WFV growth on both the test surfaces following 51 days of exposure appear to be correlated with the sloughing off of material during the period of from 81 to 96 days. This effect was more pronounced on the titanium than on the aluminum surfaces.

On day 86, the velocity of seawater flow in all four heat transfer monitors was increased from 6 ft/sec to 10 ft/sec for a 1/2 hour period. At the time of the subsequent biological sample (96 days), one aluminum and one titanium module were exposed to a similar velocity change. There were no significant differences in SR, carbon content, C/N ratio and ATP content of the materials obtained from the tubes exposed to the velocity change. While there were differences in the frequency of sloughing off, these did not significantly affect the average WFT and WFV of the material associated with the velocity stressed tubes. The phenomenon of sloughing off had in fact been taking place since the previous sample taken after 81 days of exposure.

The changes in thermal resistance (R_f) correlate well with the average WFV of material found on the test surfaces. Figure 21 summarizes these data through 81 days of the experiment. At low values of WFV, there is little or no change in the R_f of both types of surfaces. At WFV values of between 0.4 and approximately 1.5 mm^3/cm^2, the R_f of the titanium increases linearly.

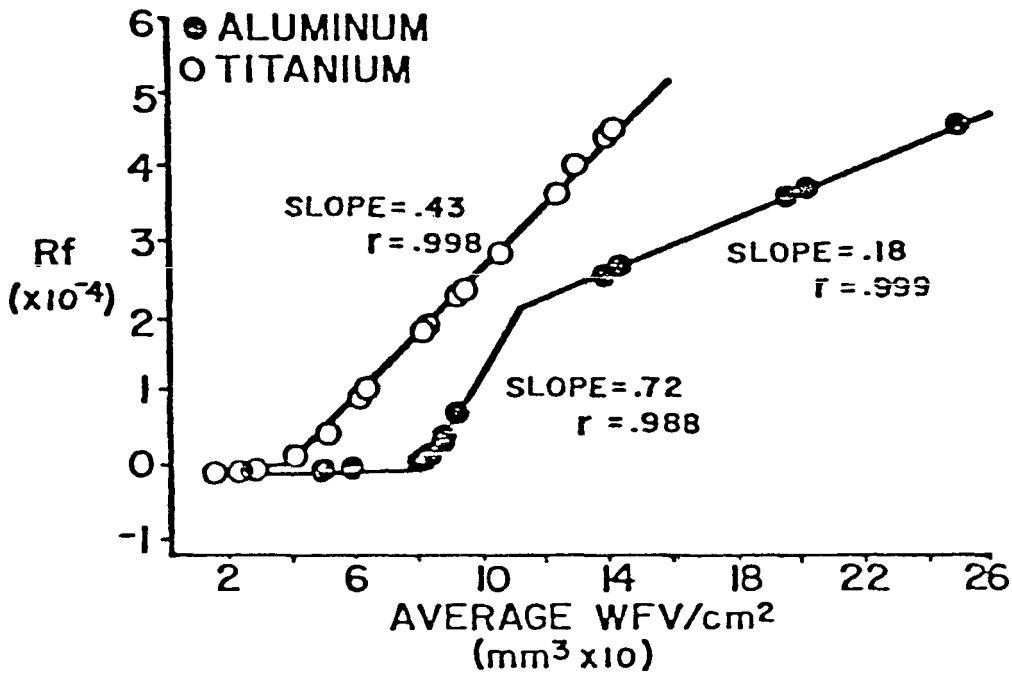

FIGURE 21 R_f AS A FUNCTION OF WFT

The aluminum surface shows a different relationship between R_f and WFV. The R_f of this material is not affected until the WFV is greater than 0.8 mm^3/cm^2, subsequently increasing linearly in two phases. These data concern that portion of the experiment prior to the time at which sloughing off became a major consideration and the point in time at which the spontaneous decrease in R_f occurred.

6.2.1.5 SURFACE ASSOCIATED VIABLE BACTERIA. The results of the quantitative enumeration of viable heterotrophic bacteria associated with the test surfaces are illustrated in Figure 22. Microbiological experiments were not conducted on sample #8 (81 days of exposure). On samples #4 through 7 (17 to 51 day period) there was a sharp increase in the number of bacteria associated with the aluminum surfaces. This affect appeared to be cyclic and is well correlated with changes in ATP and SR during this period. The increase in bacteria associated with the titanium surface were lower and correlate with changes in ATP (Figure 17) but not well with SR (Figure 14). After 96 days of exposure the bacterial populations are reduced on both these surfaces. The absence of data at 81 days of exposure does not permit a comparison to the ATP peak seen at this time on the titanium surfaces. However, on the basis of the correlation seen on the other samples, the ATP values found predict a peak in microbial biomass on titanium surfaces at this time (81 days).

The accumulation of bacteria on the titanium surface during the 17 to 51 day period does not result in a significant change in SR as seen in the aluminum surfaces. These bacteria do not appear to be contributing mass to the film on this surface. Thus in both the sequence of their occurrance and

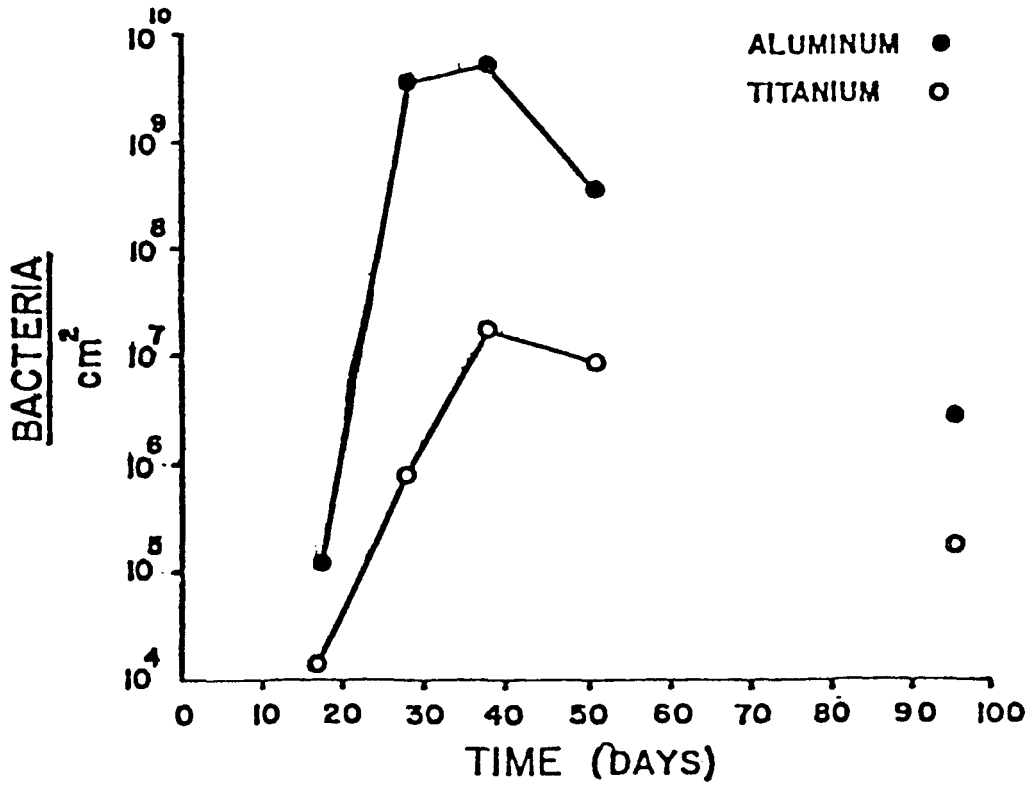

FIGURE 22 SURFACE ASSOCIATED VIABLE BACTERIA DURING PHASE I

their ability to contribute (and leave) material on the surfaces, the microbial populations associated with these two types of material appear to differ.

6.2.1.6 SCANNING ELECTRON MICROSCOPY. Three different periods of film development were observed, (a) 0 to 10 days - initiation, (b) 17 to 51 days - maturation, and (c) 51 through 142 days - bulk growth. These phases of film development on the test surfaces are illustrated in Figures 23 through 31. Figure 23 shows the presence of biomass on the aluminum surface after ten days of exposure to ambient seawater. Figure 24 shows a titanium surface exposure for the same length of time. This electron micrograph illustrates the fact that the titanium is only partially covered with material during the initiation phase of film development. Microbial clusters are evident on portions of this surface.

The condition of the surfaces during film maturation is illustrated in Figure 25, 26, 27. The aluminum surface shows the presence of a heterogeneous microbial population (Figure 25). During this period there is a peak turnover in biomass on this type of surface. The titanium surfaces (Figures 26 and 27) show less heterogeneity in their microbial populations. Some of the bacteria observed here (Figure 26) appear different from those observed on the aluminum surface. Subsequent isolation and characterization of the bacterial strains found on the two test surfaces has verified the existence of these differences (See section 6.2.2.5). The titanium surface is more completely covered than those surfaces examined during the initial phase (Figure 24).

The bulk growth period is characterized by a marked increase in the density and heterogeneity of the microbial populations found on both the test surfaces (Figures 28 and 30). The aluminum surface shows diatomaceous

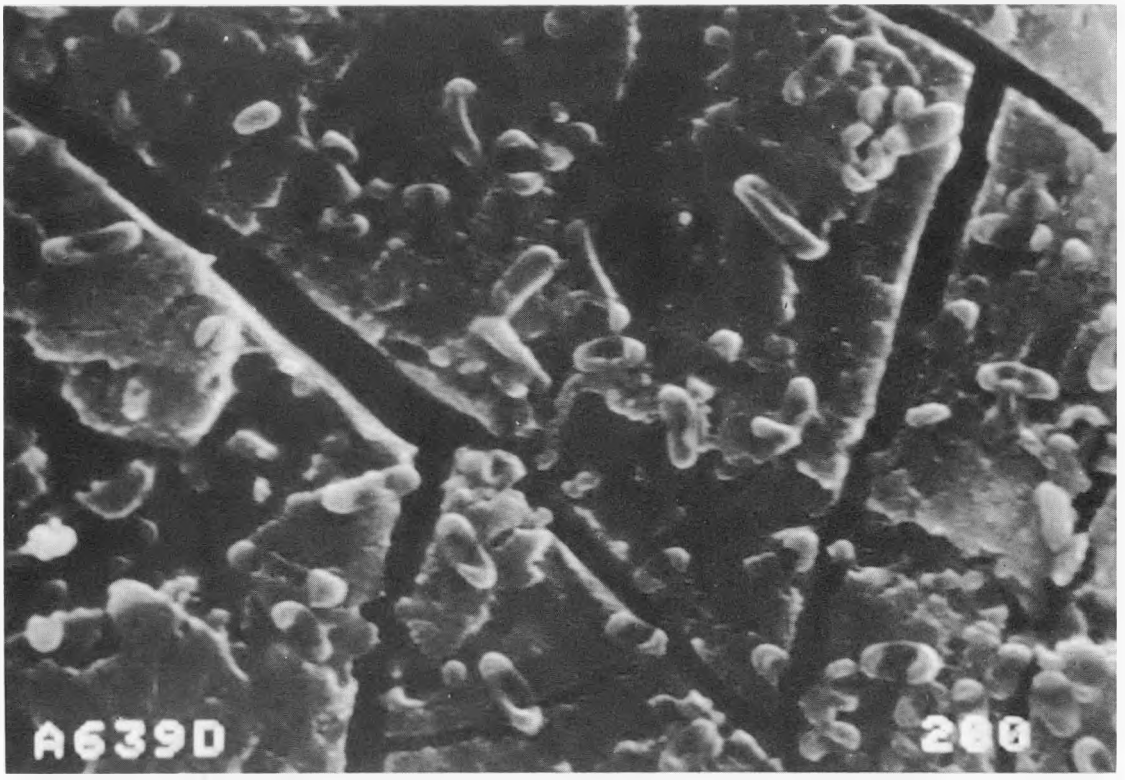

FIGURE 23 SEM VISUALIZATION OF FILM INITIATION
ON ALUMINUM SURFACE (MAG. 2700X)

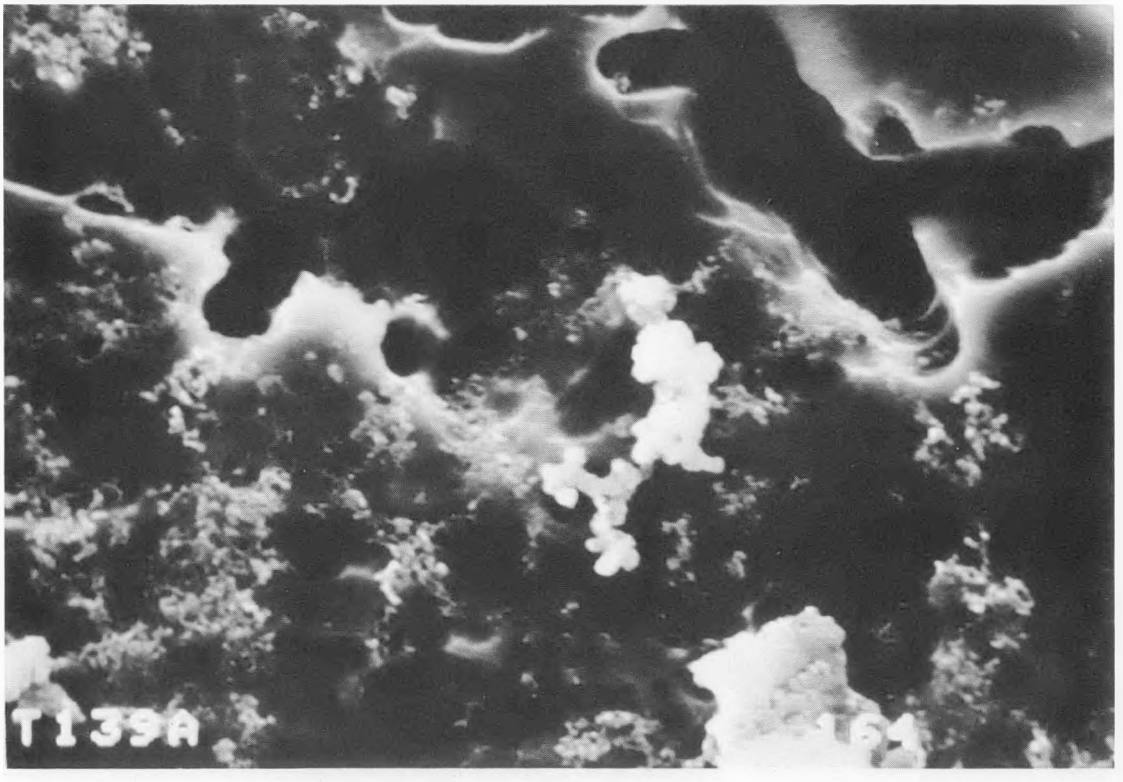

FIGURE 24 SEM VISUALIZATION OF FILM INITIATION
ON TITANIUM SURFACE (MAG. 1800X)

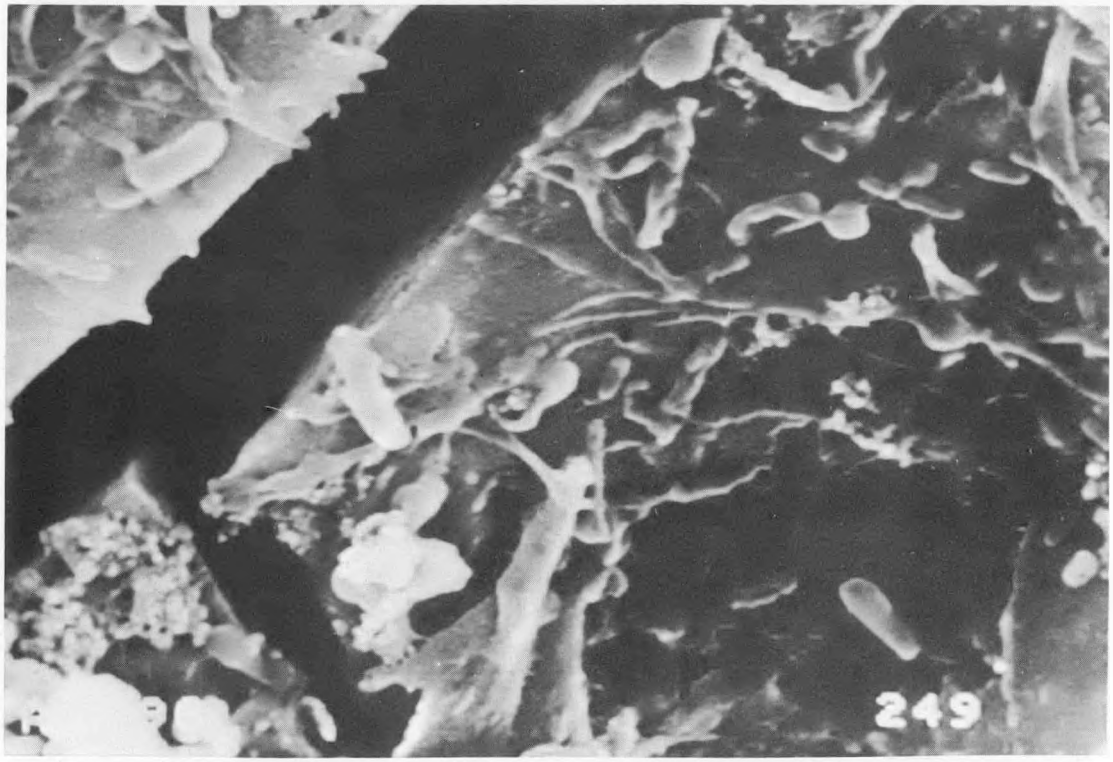

FIGURE 25 SEM VISUALIZATION OF FILM MATURATION
ON ALUMINUM SURFACE (MAG. 4500X)

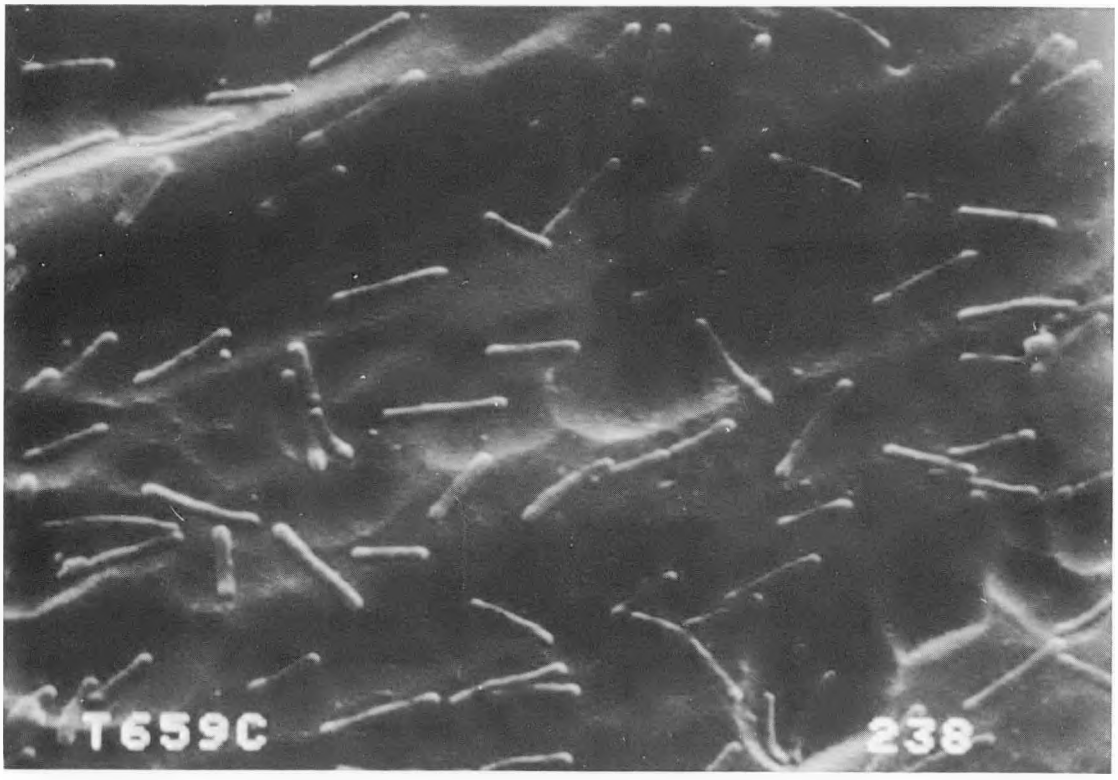

FIGURE 26 SEM VISUALIZATION OF FILM MATURATION
ON TITANIUM SURFACE (MAG. 4500X)

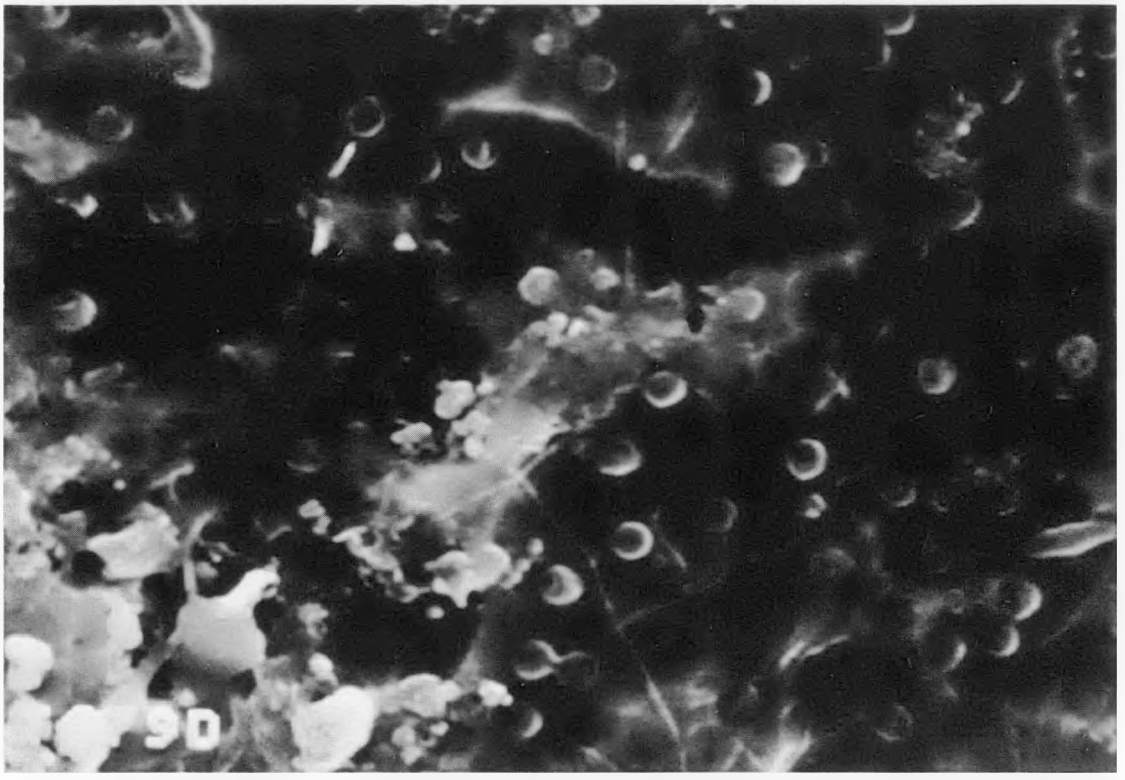

FIGURE 27 SEM VISUALIZATION OF FILM MATURATION
ON TITANIUM SURFACE (MAG. 2700X)

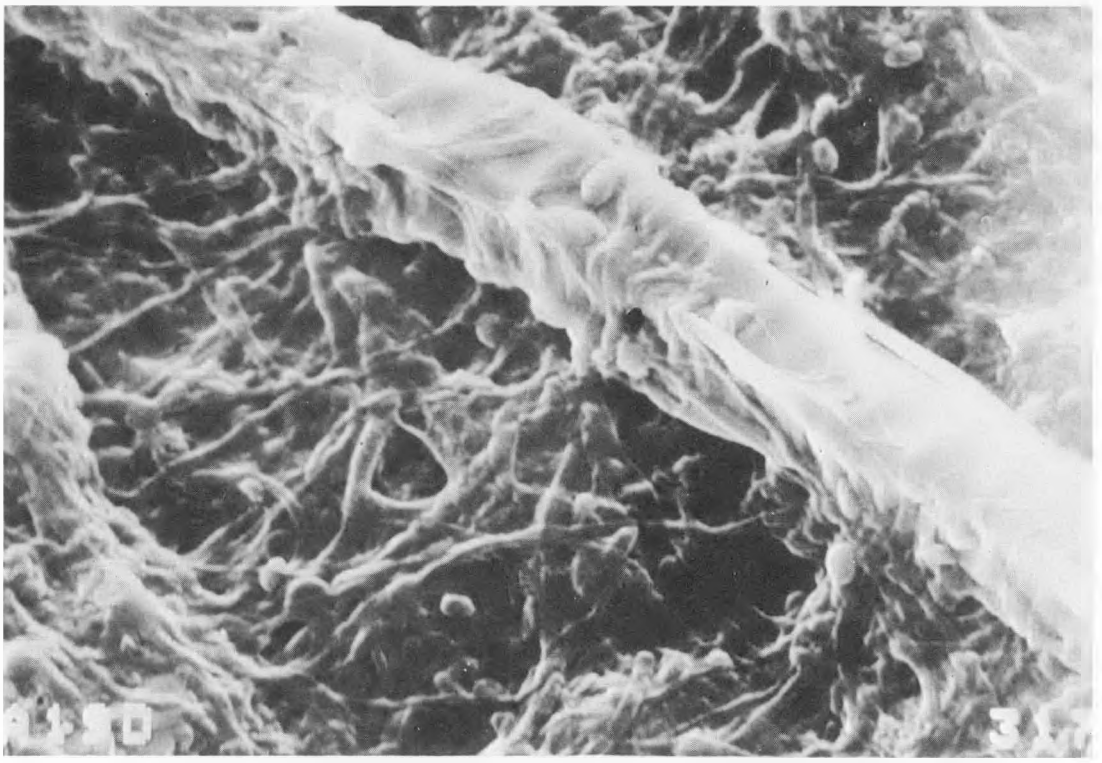

FIGURE 28 SEM VISUALIZATION OF FILM BULK GROWTH
ON ALUMINUM SURFACE (MAG. 1800X)

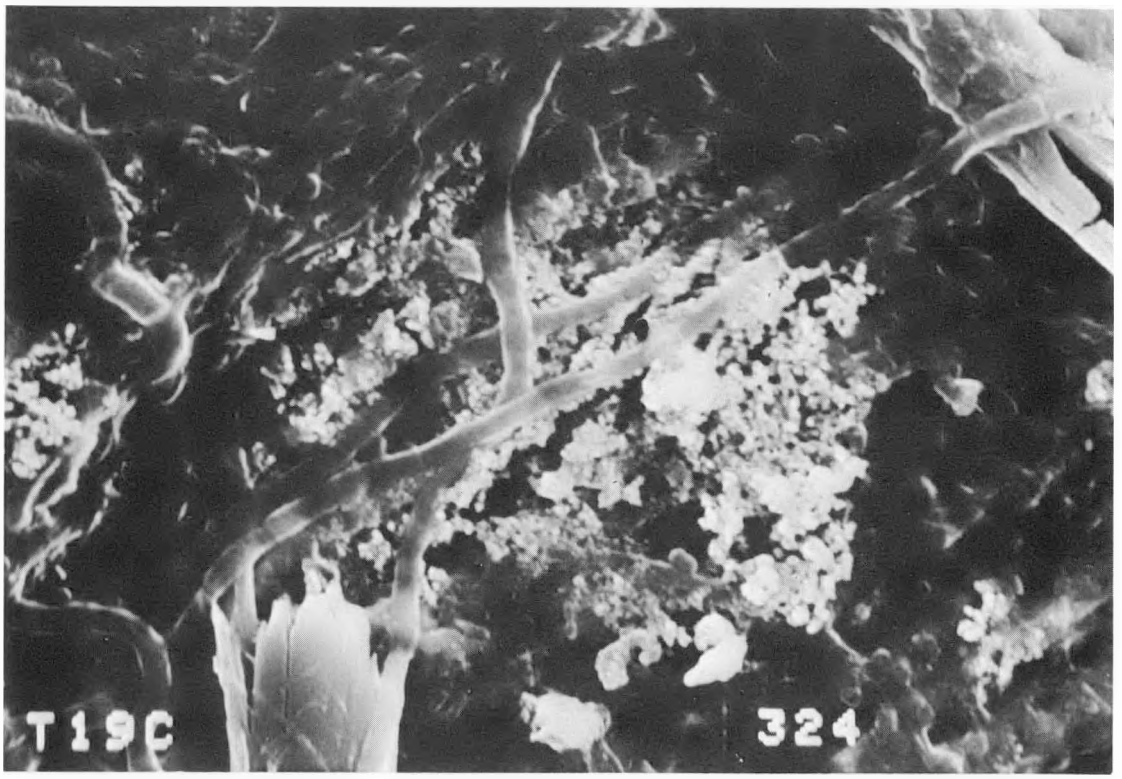

FIGURE 29 SEM VISUALIZATION OF FILM BULK GROWTH
ON TITANIUM SURFACE (MAG. 1800X)

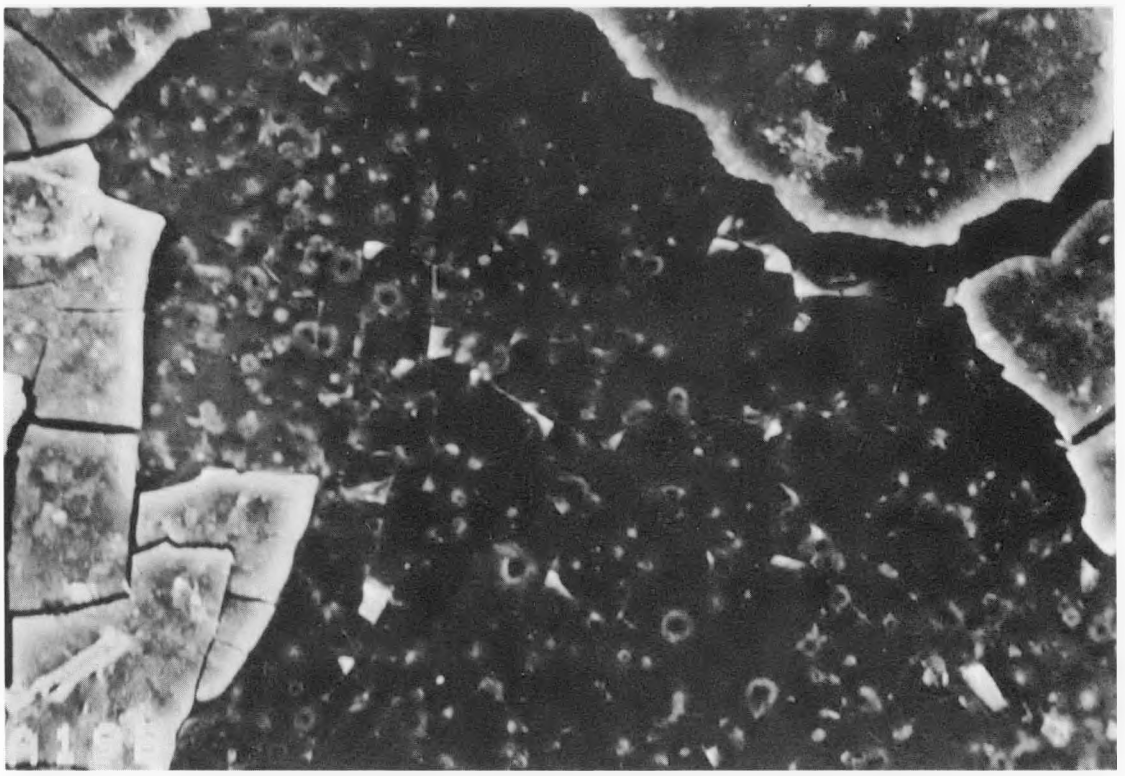

FIGURE 30 SEM VISUALIZATION OF FILM SLOUGHING
ON ALUMINUM SURFACE (MAG. 270X)

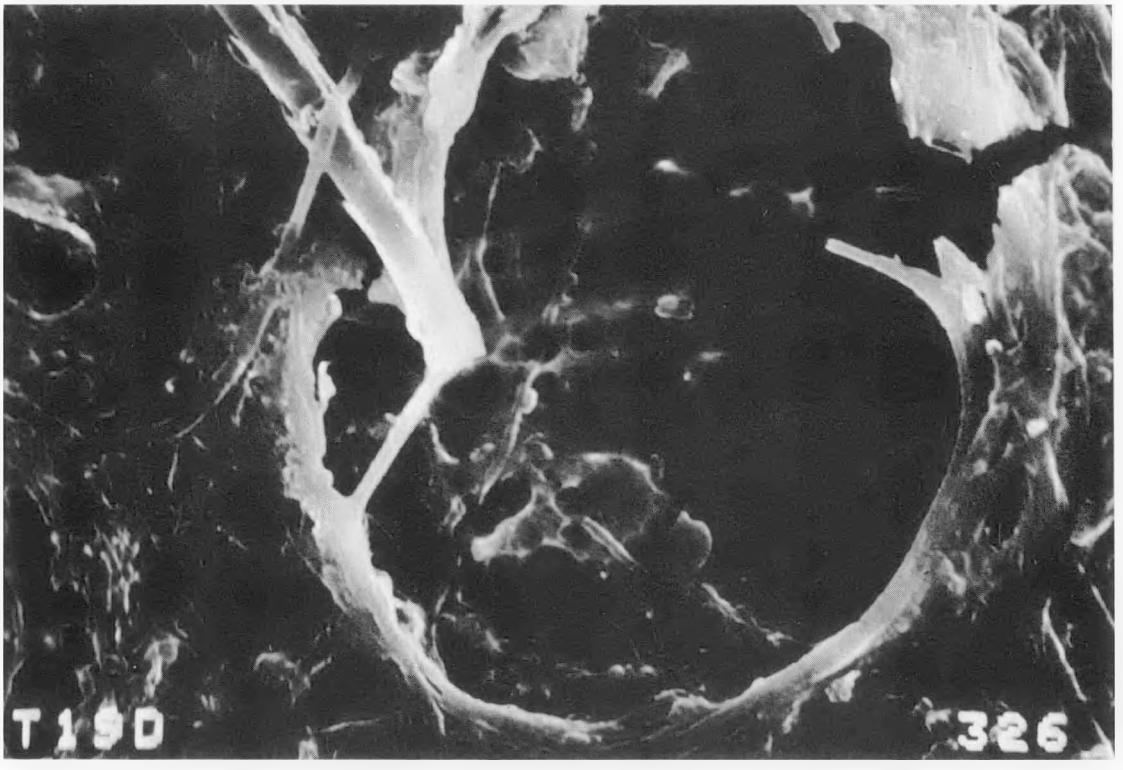

FIGURE 31 SEM VISUALIZATION OF FILM SLOUGHING
ON TITANIUM SURFACE (MAG. 1800X)

material overgrown by fibrous material most likely of microbial origin. This phase of film development is also characterized by the sloughing off of the bulk film. This effect is illustrated in Figures 30 and 33. Entire Areas have peeled off the test surfaces, essentially down to the level of the bare metal.

6.2.2 PHASE II (Days 143 - 404). This section contains results of the microfouling analyses for the second portion of the experiment which began on day 143. At this time, all tubes and HTM's were cleaned with manually operated M.A.N. brushes. During the second phase, the tubes and HTM's were cleaned a total of eight times.

6.2.2.1 SURFACE RESIDUE. The summaries of the data concerning the SR recovered during the cleaning phase of the study are presented in Appendices 3 through 15. The accumulation of SR on the test surfaces during the cleaning cycles appeared consistent (Appendix 9). Aluminum and titanium accumulated SR at an average rate of between 8 and 15 $ug/cm^2/day$. On the average "cleaning" removed significantly more material from titanium than aluminum (Appendices 10 and 11). The residue left on aluminum after cleaning had significantly more organic carbon than that seen on the "cleaned" titanium.

6.2.2.2 ORGANIC CARBON AND NITROGEN CONTENTS. A total of 382 analyses of the organic carbon and nitrogen contents of the surface associated residue were done during the course of this study. The results of these analyses on the test surfaces prior to cleaning are illustrated in Figure 32 and 33. Figure 33 shows the residual organic carbon associated with the test surfaces after cleaning on each of the respective sample dates. These data suggest considerable variability in the carbon contents of the

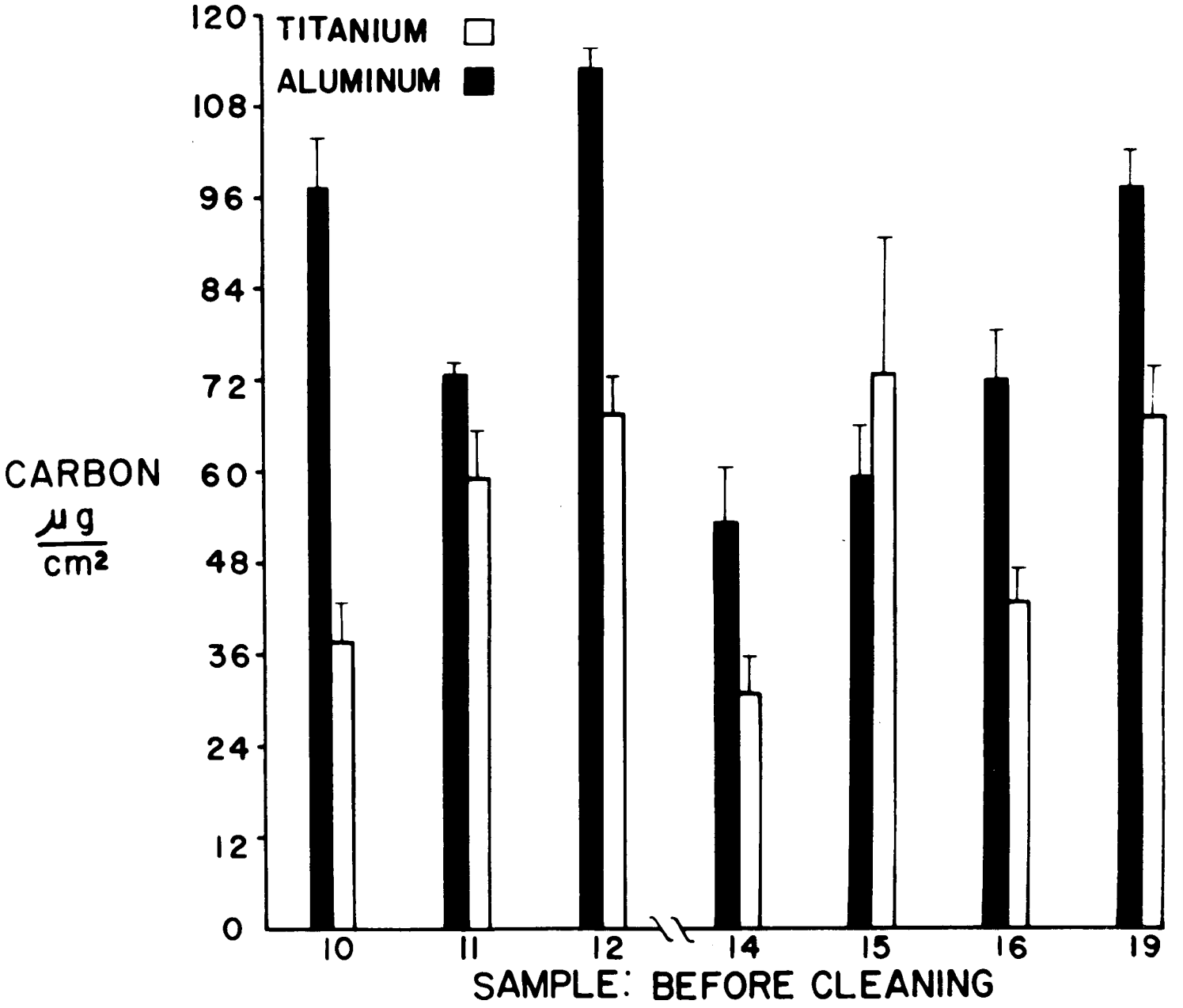

FIGURE 32 SURFACE ASSOCIATED ORGANIC CARBON BEFORE CLEANING

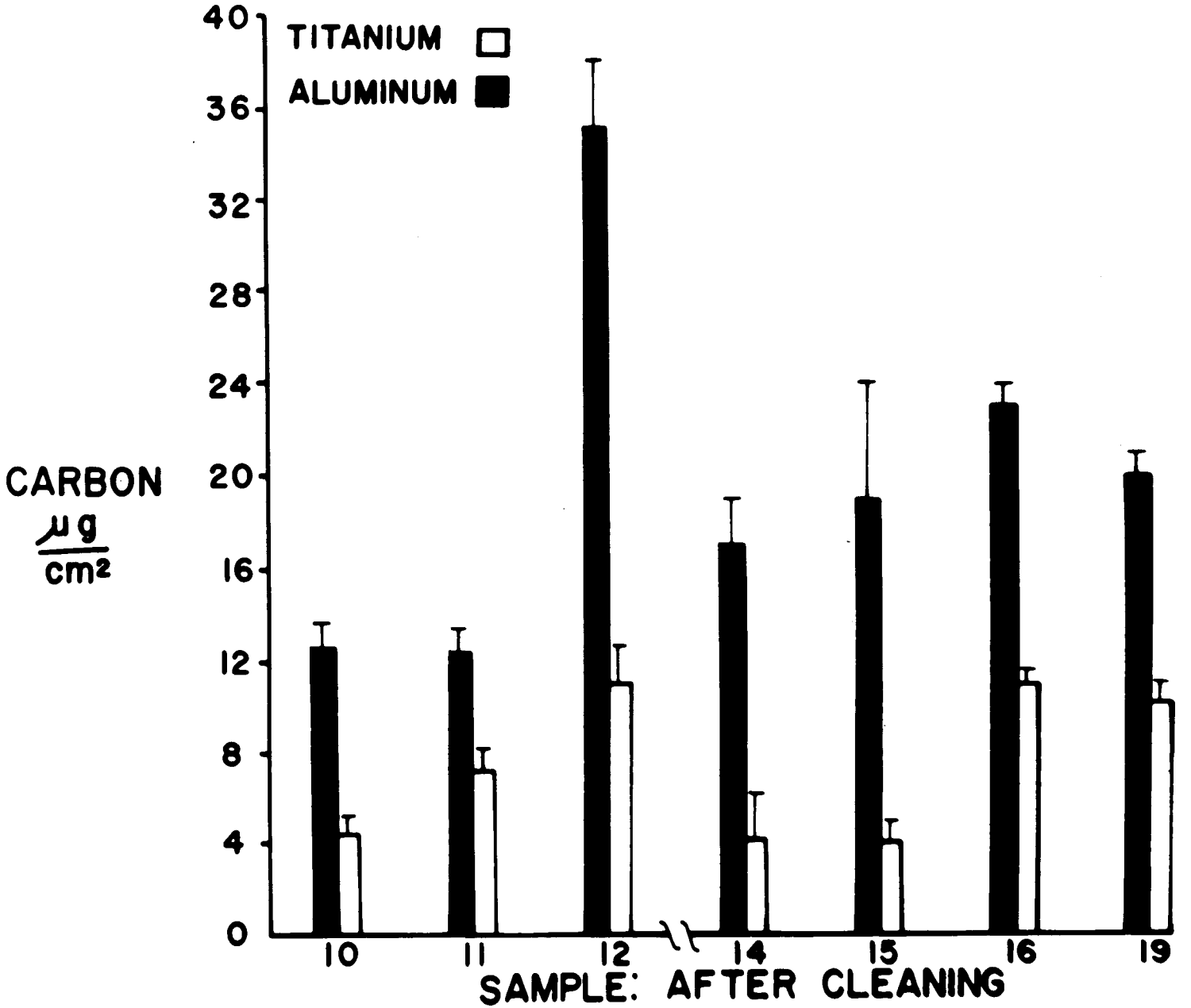

FIGURE 33 SURFACE ASSOCIATED ORGANIC CARBON AFTER CLEANING

surface associated material from sample to sample. The average interval between the samples taken in the course of this study was 34 $\pm$ 3 (SD) days. The aluminum surfaces tended to have more carbon than the titanium, both before as well as after cleaning. These results are summarized in Table 8.

The average amount of carbon associated with the aluminum surfaces prior to cleaning was significantly greater than that found on titanium. The carbon/nitrogen ratio of the material found on the aluminum surfaces prior to cleaning was significantly greater than that seen on the titanium. Similar differences exist between the test surfaces after cleaning. It is of interest to note that the C/N ratio of the material associated with the aluminum surfaces significantly increased after cleaning. The average percentage of organic carbon remaining on the clean aluminum surface was 24.7%, while that found on the titanium surfaces was 13.5%. The preponderance of carbon on the aluminum surfaces both before and after cleaning as compared to the titanium is the reverse of that seen with regard to the biomass (ATP) associated with these surfaces.

The C/N data obtained during this phase of the study is summarized in Appendices 10 and 11. The material left on aluminum after cleaning had a significantly greater C/N ratio than the material from these surfaces prior to cleaning. This effect was not seen on the titanium surfaces. The material recovered from the aluminum surfaces, either before or after cleaning had a C/N ratio significantly greater than that seen in the material recovered from titanium.

TABLE 8 ORGANIC CARBON: BEFORE CLEANING

Test Surface	Before Cleaning Organic Carbon $\mu g/cm^2$	C/N	After Cleaning Organic Carbon $\mu g/cm^2$	C/N
Aluminum	81 ± 8	9.9 + .5	20.0 ± 3.	16.2 ± 1.4
Titanium	55 ± 6	7.2 ± .3	7.4 ± 1.2	8.3 ± 0.4

6.2.2.3 ATP CONTENT. During the course of this study, the ATP contents of 360 samples of the test surfaces were determined (in duplicate). Figure 34 shows the average amount of ATP associated with the test surfaces prior to cleaning on the respective sample dates. These data suggest significant seasonal changes in the biomass associated with the test surfaces. In September and October, the surface associated biomass significantly increased. It is of interest to note that the temperature of the seawater passing through the experimental tubes reached its peak value (29.25°C) during this period of study.

After cleaning, the test surfaces revealed the presence of significant quantities of ATP on titanium on all samples (Figure 35). These results appear to roughly follow the seasonal variation seen in the biomass associated with the titanium surfaces prior to cleaning (see Figure 34 , $r = 0.843$). In the case of the aluminum surfaces, the residual ATP found after cleaning was only significant in samples 12 and 14.

6.2.2.4 WET FILM THICKNESS. The wet film thicknesses (WFT) on a total of 496 samples of the test surfaces were determined during the course of this study. Table 9 presents the results of these determinations on the test surfaces prior to cleaning. No wet films were observed on the test surfaces after cleaning. The sensitivity of the light sectioning microscope is unreliable for thicknesses below 5 um. Thus while such films may exist, they are undetectable with the technique. The average wet film thickness found on the aluminum surfaces (63.0 ± 8 (SE) um/cm^2) was not significantly different than that found on the titanium (59.3 ± 3 (SE) um/cm^2).

6.2.2.5 SURFACE ASSOCIATED VIABLE BACTERIA. The bacteria associated with the test surfaces were isolated on site at the time of sampling. Two isolation methods were employed, (a) segments of the test

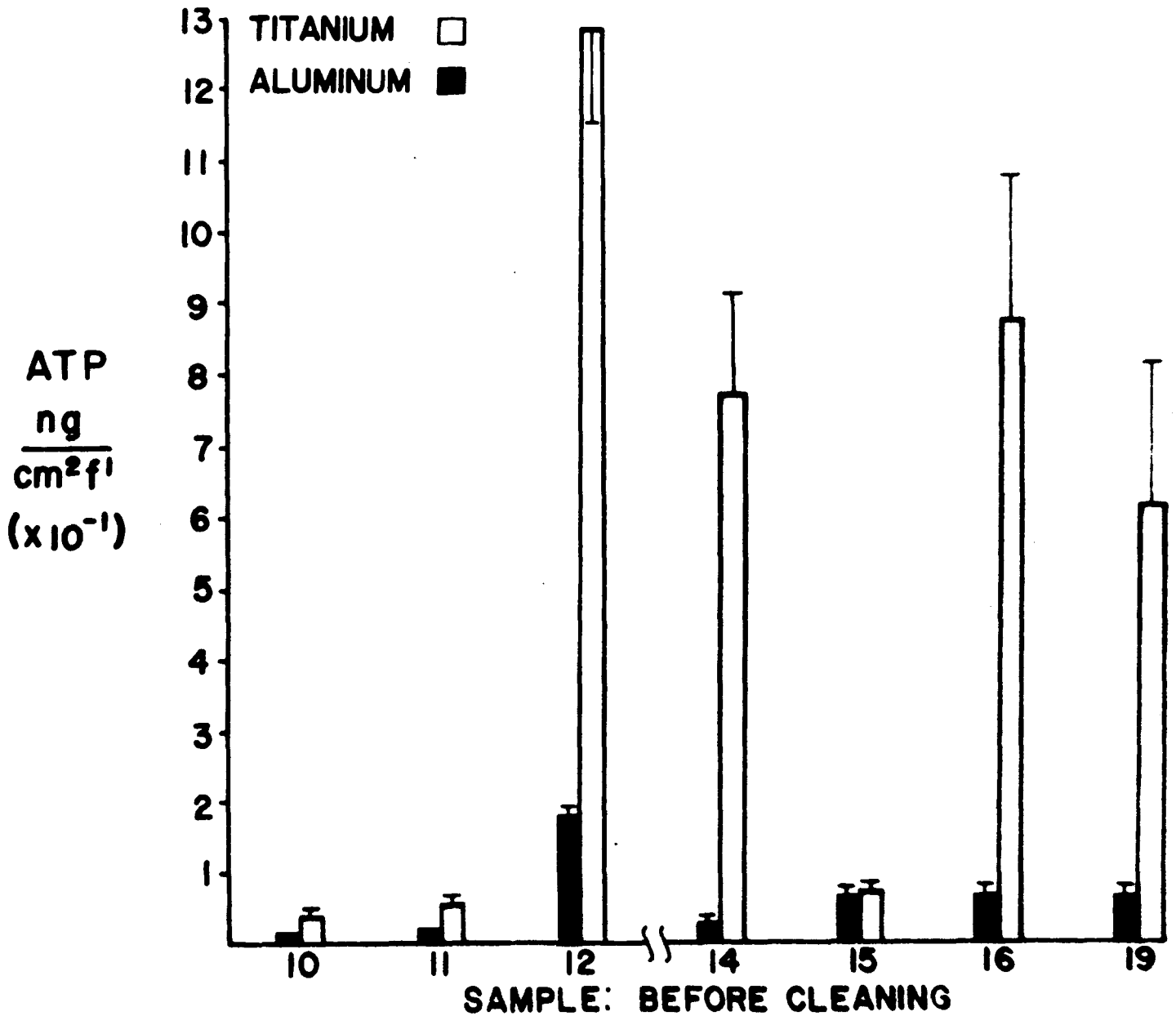

FIGURE 34 SURFACE ASSOCIATED ATP: BEFORE CLEANING

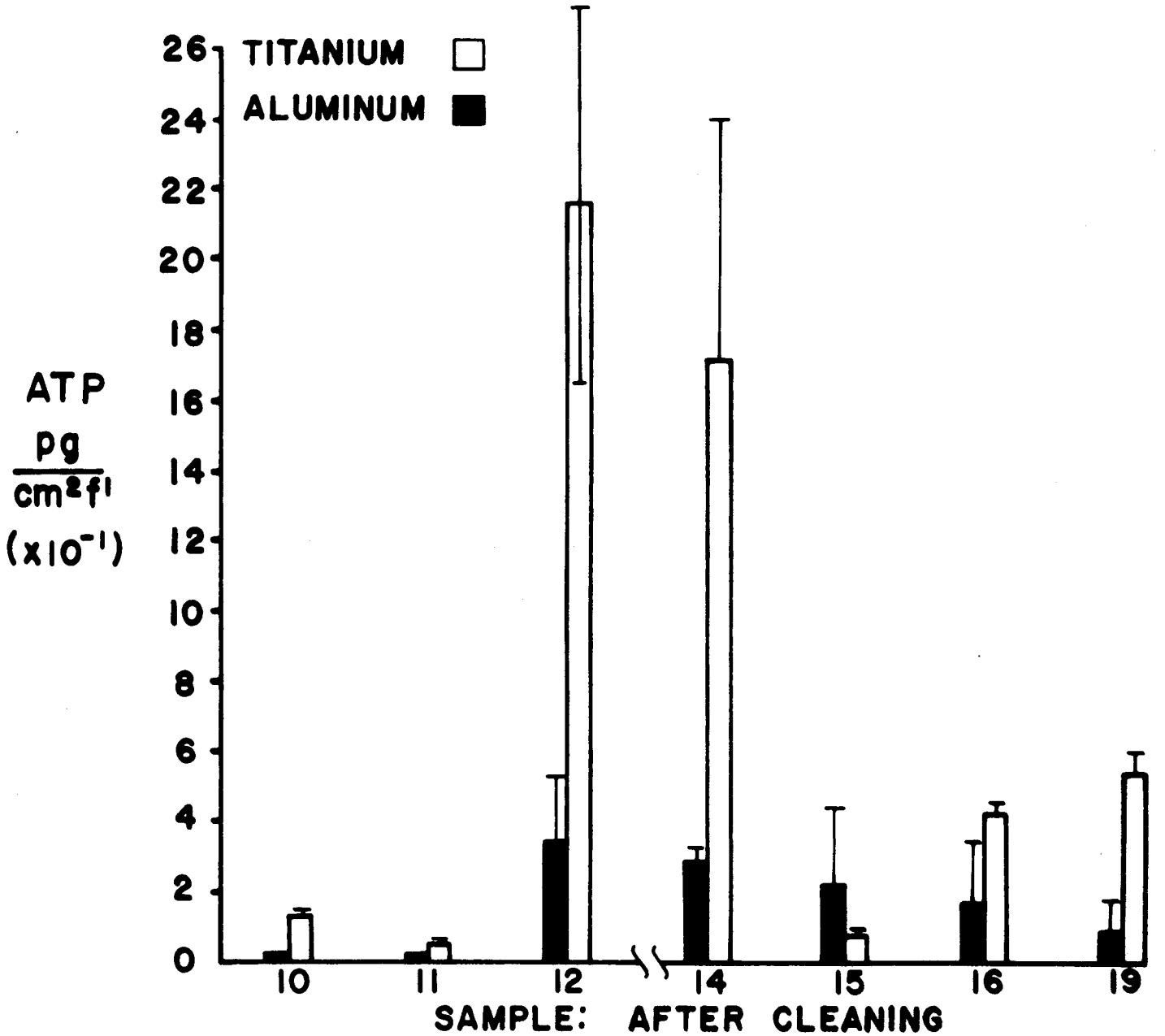

FIGURE 35 SURFACE ASSOCIATED ATP: AFTER CLEANING

TABLE 9 AVERAGE WET FILM THICKNESS: BEFORE CLEANING

Sample	Aluminum	Titanium
10	107.3 ± 4.2*	73.3 ± 4.0
11	56.1 ± 2.7	57.7 ± 3.3
12	61.7 ± 4.9	60.0 ± 6.4
13**	--	--
14	39.5 ± 2.7	47.4 ± 1.2
15	52.2 ± 3.6	58.9 ± 1.7
16	63.4 ± 9.3	63.4 ± 2.5
19	61.0 ± 3.2	54.6 ± 9.5

* values on Table $\mu m/cm^2$ ± SE

** no biological sample taken

surfaces were placed directly in a complex media broth and (b) the test surfaces were scraped with the transfer needle or loop and stabbed into complex media agar tubes. The innoculated broth and slants were transferred to the laboratory and incubated at 25°C for one week. Following this, the viable bacteria were transferred to the Zobell 2216 E Modified Media (16). The Zobell 2216 E Media was found to be the most satisfactory media. Agar plates with ZB2216E medium were streaked with samples from both the broth and agar slants and incubated. Colonies appearing on these plates of differing color, size, and shape were isolated and purified. A series of tests were employed to classify and shape these bacterial strains and to compare them in terms of numerical taxonomy (17). Twenty-six morphological, physiological and biochemical characters were employed in the numerical taxonomy study. Each test was done in duplicate and aseptic conditions were maintained throughout the study. The isolated strains were correlated using the Similarity Index (17).

A total of 14 bacterial isolates were originally obtained from the test surfaces on samples 17, 18 and 19. The Similarity Index indicated that there were five distinct strains of bacteria (84% similarity in tested characteristics). Of these five strains, three were exclusively associated with the aluminum surfaces and one was found only on the titanium. One bacterial strain was found associated with both test surfaces. Distinct from the other strains isolated, this bacterium did not form colonies when plated on agar media, but spread over the entire surface of the plate. One of the strains found only on aluminum was luminescent.

All five of the isolated bacterial strains were gram negative, oxidate positive, motile, oxidized and fermented glucose. All of the strains isolated belong to the family Vibrionaceae. The luminescent vibrie is

possibly from the genus Lucibacterium. This strain very actively produced H_2S. Most of the strains were able to grow on inorganic salts with citrate as the only source of carbon.

The distribution and sequence of appearance of these bacterial strains on the test surfaces are illustrated in Table 10. The five strains are arbitrarily designated A, B, C, D, E, with strain D being luminescent and strain E being found on both test surfaces. Bacterial samples were not taken from the titanium surfaces on sample 18. These bacterial strains found on the titanium surfaces on sample 17 were the same as seen on sample 19 at the end of the study. On the aluminum surfaces, there was a qualitative change in the composition of the bacterial population on samples 18 and 19 as compared to 17 (strain E was present on both surfaces at all sampling times). Thus the test surfaces differ in the bacteria associated with them and the aluminum surfaces show some type of succession in the appearance of these populations.

TABLE 10
BACTERIAL STRAINS ON TEST SURFACES

Sample (Time, da)	17 (7)	18 (14)	19 (36)
Ti	AE	(sample not made)	AE
Al	BCE	BDE	DE

Strain A only on Titanium

Strains B, C, D only on Aluminum

Strain E on both materials.

6.2.2.6 SCANNING ELECTRON MICROSCOPY. Visual analysis of the test surfaces with scanning electron microscopy (SEM) supported the results seen in the analysis of the biomass (ATP) associated with these surfaces. These analyses indicate a high density of microorganisms associated with the test surfaces during the period covered by samples 12 to 14 (30 August to 4 November 1980). The cleaning process removed portions of characteristic "mud flat" appearance of the aluminum surfaces; however, at higher magnification, the presence of microbial cells and thread-like material was evident on the surfaces of the remaining material.

Figures 36 through 39 illustrate the differences observed in the aluminum surfaces before and after cleaning. Figure 36 shows the typical aluminum surface at the end of a cleaning cycle (prior to being cleaned). Figures 37 through 39 illustrate several aspects of these surfaces after cleaning. The cleaning process removes a portion of the base layer (mud flat) that develops on aluminum, however, segments of this layer remain after cleaning (Figure 37). At higher magnifications, strands of fibrous material and bacterial cells are seen associated with the surfaces of the segments of material that remain on the aluminum surfaces after cleaning (Figures 38 and 39).

At the termination of the cleaning cycle the titanium surfaces are also covered with a well developed layer of biofouling (Figures 40 and 41). The cleaned titanium surface, as distinct from the aluminum, is characterized by the presence of a fairly extensive, firmly attached microbial population (Figures 42 and 43).

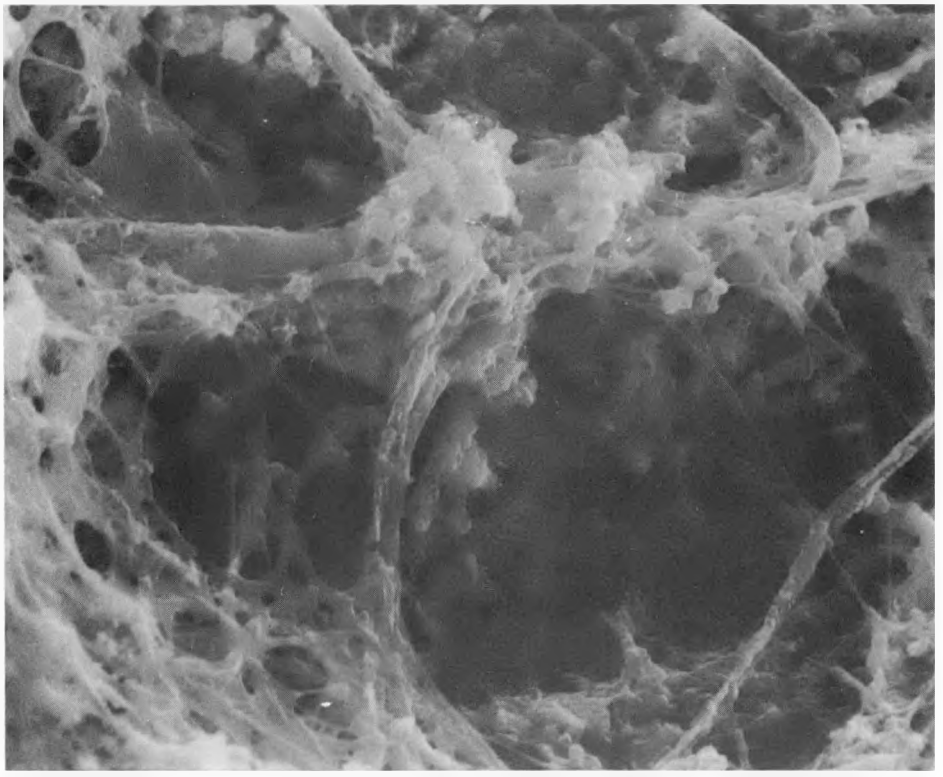

FIGURE 36 SEM VISUALIZATION OF THE ALUMINUM SURFACE AT THE END OF A CLEANING CYCLE, PRIOR TO BEING CLEANED (MAG. 1800X)

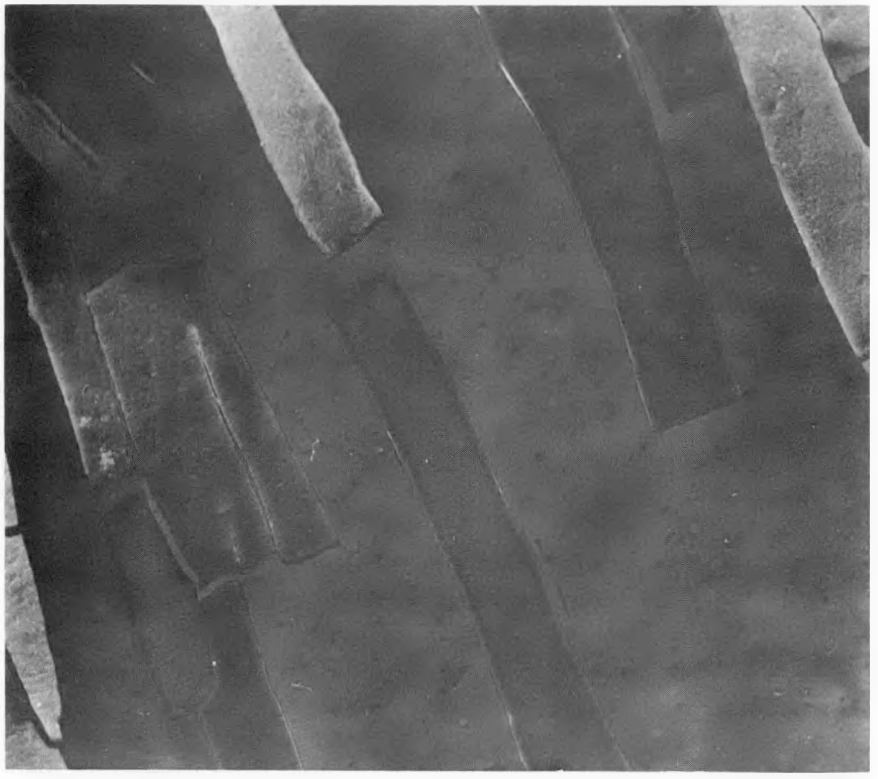

FIGURE 37 SEM VISUALIZATION OF THE CLEANED ALUMINUM SURFACES (MAG. 430X)

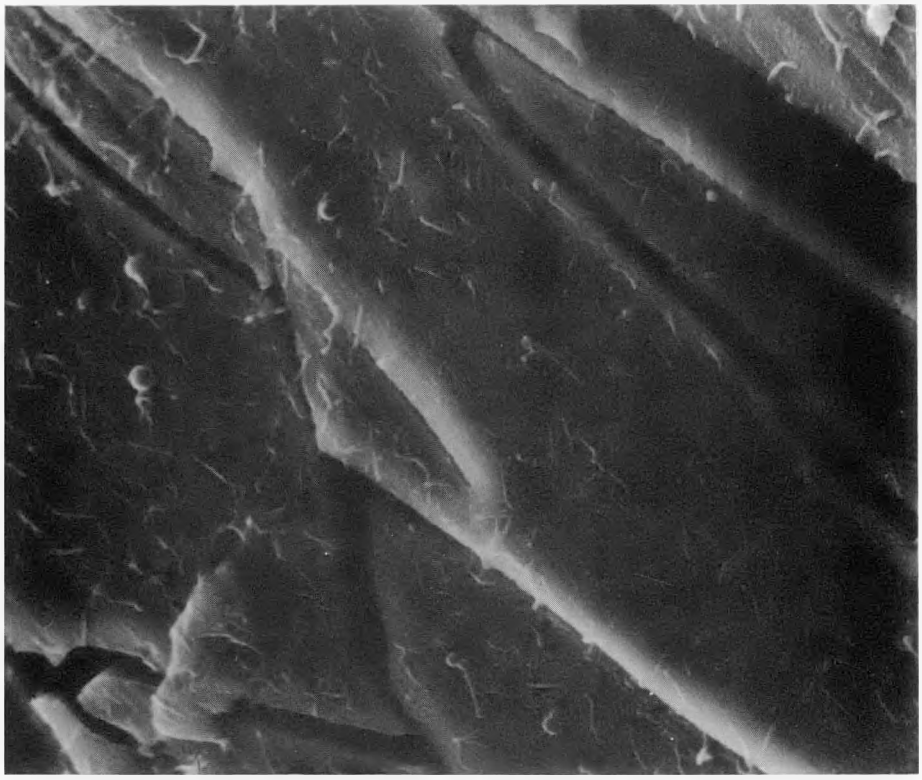

FIGURE 38 SEM VISUALIZATION OF THE CLEANED ALUMINUM SURFACE (MAG. 1700X)

FIGURE 39 SEM VISUALIZATION OF THE CLEANED ALUMINUM SURFACE (MAG. 5000X)

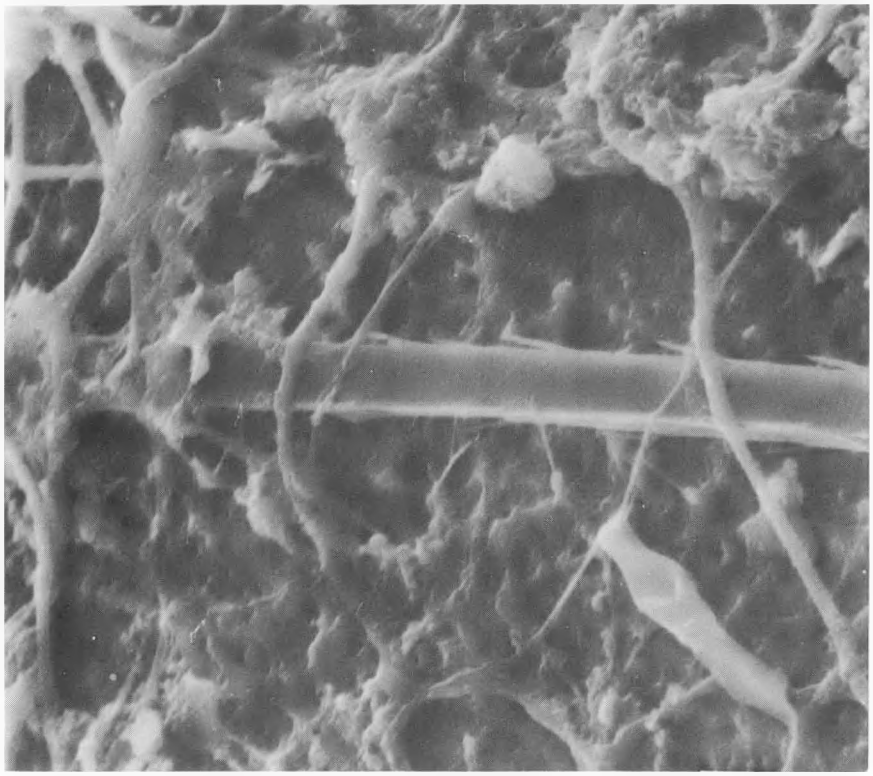

FIGURE 40 SEM VISUALIZATION OF THE TITANIUM SURFACE AT THE END OF A CLEANING CYCLE (MAG. 2600X)

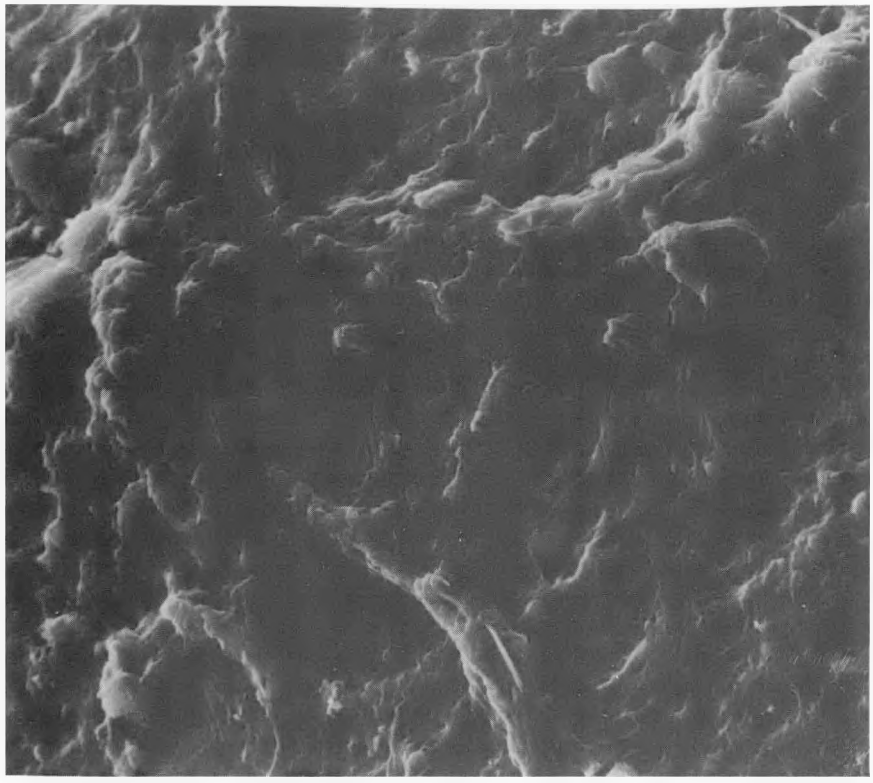

FIGURE 41 SEM VISUALIZATION OF THE TITANIUM SURFACE AT THE END OF A CLEANING CYCLE (MAG. 2000X)

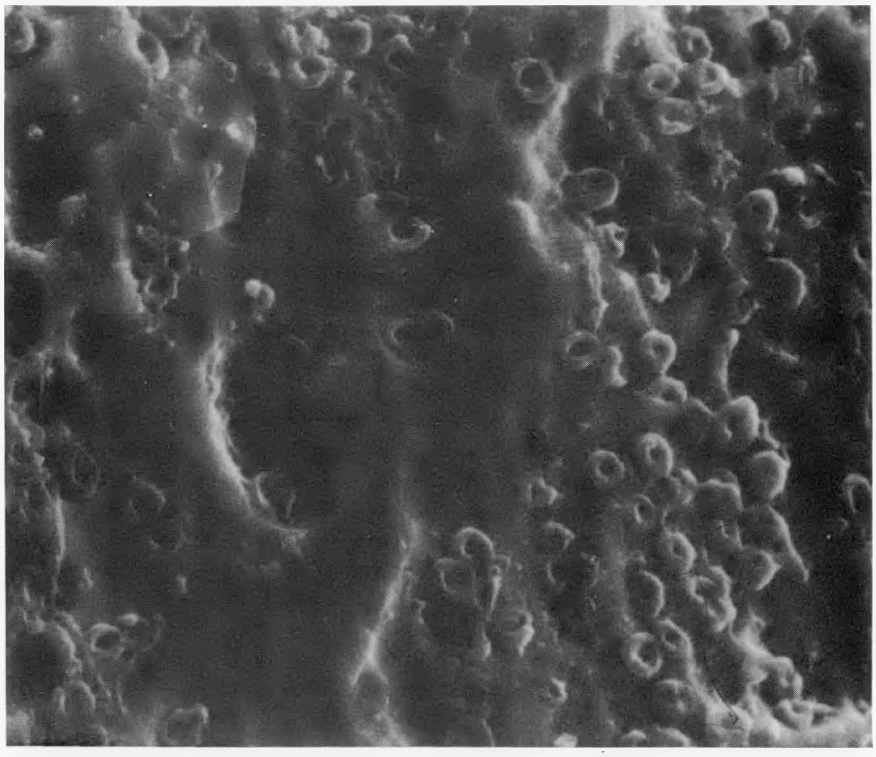

FIGURE 42 SEM VISUALIZATION OF THE CLEANED TITANIUM SURFACE (MAG. 5000X)

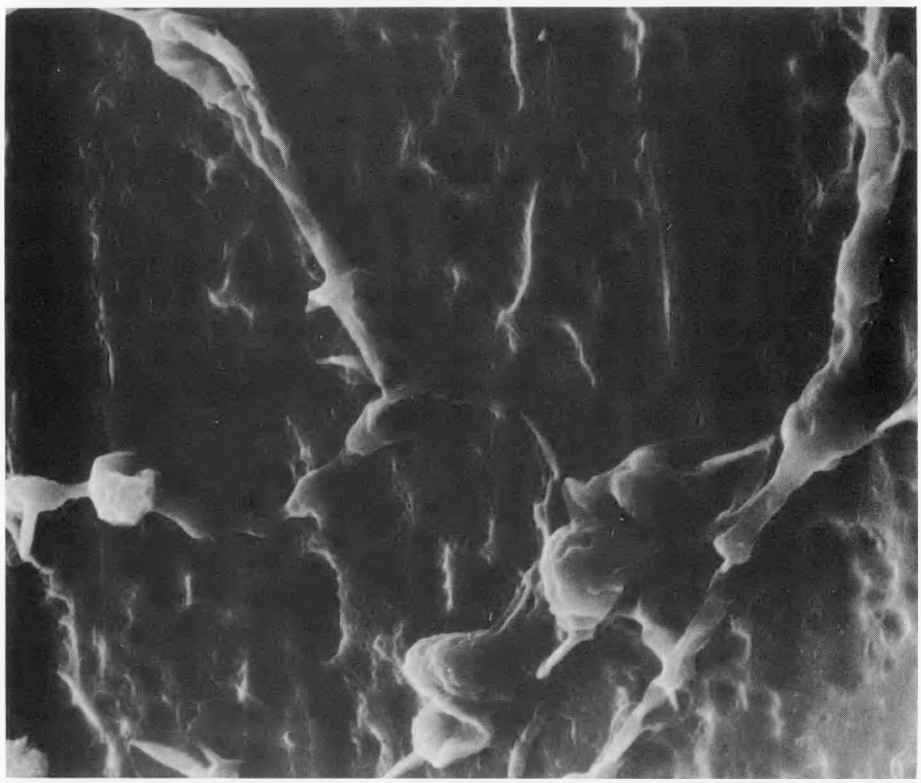

FIGURE 43 SEM VISUALIZATION OF THE CLEANED TITANIUM SURFACE (MAG. 2200X)

6.3 DISCUSSION. During the initial phase of this experiment (143 days) the thermal resistance of the test materials (R_f) increased to average values of 10.6 in the aluminum and 5.1 in the titanium monitors. The respective R_f values did not appear to systematically increase until approximately 17 days of exposure, following the initiation of wet films and the first appearance of biomass on these surfaces. The R_f on the test surfaces increased steadily from 17 through 81 days of exposure, rising to values of between 4 and 5. After 90 days of exposure, the R_f spontaneously fell to values comparable to those seen approximately 25 days after the initial of the experiment. During the subsequent 50 days, the R_f in the aluminum monitors rose to a value of 10.6 and in the titanium to a value of 5.1. Thus with respect to the increase in R_f, the experiment was composed of two phases, (a) a slow increase in R_f during the initial 81 days, this change predominantly taking 64 days (day 17 to 81) and (b) a spontaneous decay and recovery of R_f to values comparable to those seen at 81 days within an average of 38 days. At the termination of the experiment, approximately 26 days later, the R_f values exceeded those seen at 81 days of exposure. Thus the rate of increase of the R_f during period (b) was approximately twice that of period (a).

The surface residue (SR) and the carbon content of this material increased linearly following the period of film initiation, through the termination of the experiment at 143 days on both test surfaces. The WFT of the material increased exponentially with time during the first part of this period until sloughing off altered the pattern of WFT growth on both the test surfaces. At the termination of the experiment, however, the WFT on the aluminum and titanium surfaces had increased between 20 and 26 times respectively, as compared to their values after 17 days of exposure.

Thus the increase in WFT on both the test surfaces during this period was greater (roughly double) than the increases seen in SR and organic carbon on these surfaces. Considering the entire period of the experiment, the density of the WFT with respect to SR and organic carbon was decreasing as the R_f was increasing.

The cohesiveness or stability of the wet films formed on the two test surfaces appeared to differ. The phenomenon of sloughing off affected the titanium WFT much more markedly than the aluminum WFT (Figure 19 and 20). The relationship of the biomass found on these surfaces to their respective wet film volumes also appeared to differ. Following 17 days of exposure, the biomass (ATP) associated with the titanium surface increased exponentially throughout the remainder of the experiment. This increase was unaffected by the decrease in WFT seen between 81 and 96 days of exposure. The biomass on the aluminum surface increased exponentially through 51 days of exposure, decreasing between 81 and 96 and recovering to a high value at the end of the experiment (143 days). The steady increase in the aluminum WFT during this period was unaffected by the cyclic change in the quantity of biomass associated with this surface. Thus while film volume is lost from the titanium surface, the biomass remains. Conversely, on the aluminum surface while WFT steadily increases, the quantity of biomass associated with the surface goes through a cyclic change.

During this phase of the experiment the biomass on aluminum appears to be superficial to the wet film whereas on the titanium surface the film, while more loosely bound than the aluminum film, might well be the product of an underlying, firmly attached biomass.

Following the initial period of film development, the C/N ratio of the material associated with the titanium surface steadily declined. This decrease is essentially exponential throughout the remainder of the experiment. On the aluminum surface the C/N ratio of the SR increased during the period of 17 to 51 days exposure. This increase appears to be associated with an increase in biomass (ATP) during this period. The subsequent loss of biomass from the aluminum surface and its reappearance after 96 days of exposure is associated with a steady decrease in the C/N ratio of the SR. These data suggest that the microbial populations selected by the test surfaces were different at the onset of the experiment. Changes in the relationship of the biomass to film stability during this period might well have determined the increased rate of film development seen between days 96 and 143 of the experiment.

The second phase of this study revealed that the test surfaces appear to be different with respect to the relative proportions of biomass (ATP) and organic carbon associated with them both before and after cleaning. Measurable biomass is found on the clean titanium surface throughout the study period, while on aluminum, biomass is seen on the clean surface only at the end of August and early November (samples 12 and 14).

Average ratios of organic carbon/ATP in bacterial cells have been reported to be around 500 (17,18). On the basis of this, on the titanium surfaces prior to cleaning, an average of 51% of the organic carbon is microbial. This value falls to 5.2% on the clean titanium surface. These values are to be contrasted to those found on the aluminum surfaces which are 8.4% before and 0.8% after cleaning. The material remaining on both test

surfaces after cleaning does not correlate with the observed thermal resistance (R_f) of these surfaces. On the test surfaces prior to cleaning, the R_f correlates well with the WFT on the aluminum surfaces, and with the biomass (ATP) found on the titanium surfaces.

Twelve strains of bacteria have been isolated from the test surfaces during the course of this study. Those isolated from the titanium appear to be distinct from those obtained from the aluminum surfaces. The biomass remaining on the titanium surfaces may well grow during the course of the cleaning cycle. Increases in seawater temperature during the cycles in late August and October resulted in peak accumulations of biomass on these surfaces. The residual organic carbon and segments of the "mud flat" found on the clean aluminum surface may well result in the further adsorption of materials from the flowing seawater and the restructuring of the wet film associated with these surfaces during the cleaning cycle. Both of these processes, although different in nature, would result in the formation of a layer of immobilized water adjacent to the test surface, providing an "insulation" capable of increasing the thermal resistance of these surfaces.

The overall objective of this study is to determine the relationship between the accumulation of material on the test surfaces and the observed changes that occur in the thermal resistance of these material. The wet film thickness (WFT) correlated well with the changes in R_f seen during the first 51 to 81 days of exposure. The phenomenon of sloughing off seen between 81 and 96 days of exposure was enough at this juncture in the experiment to significantly reduce the R_f of both test materials. Following this cycle in both R_f and WFT the film grew at an accelerated rate. On the basis of the

complete experiment, the increase in R_f do not appear to be due to increases in the density or concentration of SR or organic carbon in the wet film volume. The sloughing off of material, coincident with the sharp decrease in R_f after 90 days of exposure suggest that the "insulator" causing the increase in the R_f of these surfaces is the unstirred layer of water trapped in the wet film structure. A more precise understanding of the microbial origin and nature of the macromolecular products that structure the wet films formed will be required to diminish or avert the thermal insulating effect of biofilm formation on these surfaces.

7. MACROFOULING

7.1 FLOW SYSTEM. The test flow system consisted of four independent modules through which water was drawn from a depth of 17m. The intake hoses were 2 in (5.1 cm) Kanaflex (an all PVC, suction hose manufactured by Totaku America, Compton, California) and each hose was equipped with a strainer at the intake end. Intake strainers were 1 m sections of 3 in (7.6 cm) PVC with numerous slits cut in them and caps on the bottom end. Water was pumped on board using Marlow chemical service pumps equipped with strainers, passes through the modules, and then back overboard. All plumbing in the modules, with the exception of the tubing sections of the metal to be tested, was of PVC plastic. A detailed description of the experimental system can be found in previous publications (15, 20). At the end of the experiment, the flow system of two modules was dismantled and examined for macrofouling organisms.

7.2 RESULTS

7.2.1 INTAKE STRAINERS. Figure 44 provides a lengthwise view

of a split intake strainer. All strainers were more than half filled with fouling organisms. Table 11 lists species, giving frequencies and wet weights, found in the strainers.

7.2.2 INTAKE HOSES. During retrieval of the intake hoses, sections of the hoses were sampled every ten feet and preserved in formaldehyde. Macrofouling was not evident. Only a thin covering of filamentous and unicellular blue-green algae, pinnate diatoms, and several species of foraminiferans were present inside the hoses.

7.2.3 PUMP STRAINERS. The pump strainers were periodically checked throughout the experiment, and it was not unusual to find small clams, shrimp, crabs, brittle starts and sea urchins growing in the strainers. Some of these organisms could have been carried by the flowing water from the intake strainers but most probably settled on the intake manifold and were consequently sucked into the pump strainers when pumps were rotated.

7.2.4 EXPERIMENTAL MODULES. In areas of the modules where flow was maintained, there was little macrofouling. Only an occasional barnacle was found attached to a PVC surface. However, in areas where flow was reduced, such as in by-pass loops and in "T's" where on pathway was entirely plugged, macrofouling organisms thrived. The macrofouling species found in the experimental modules, their frequencies and wet weights, are given in Table 11.

7.3 DISCUSSION. A total of 61 species of benthic invertebrates representing ten phyla were found growing in the flow system. One can safetly expect that wherever an OTEC plant is located, the potential for a macrofouling problem will exist. In the tropics, about 85% of all species of benthic invertebrates have planktonic larval stages which

FIGURE 44 PHOTOGRAPH OF AN INTAKE STRAINER SPLIT LENGTHWISE TO EXPOSE THE ORGANISMS LIVING INSIDE

TABLE 11 IDENTIFICATION, FREQUENCY, AND WET WEIGHT OF ORGANISMS FOUND IN THE INTAKE STRAINERS AND EXPERIMENTAL MODULES AFTER THIRTEEN MONTHS OF CONTINUOUS FLOW

Species	Intake Strainer Number	Intake Strainer Wet Weight (g)	Experimental Module Number	Experimental Module Wet Weight (g)	Feeding habit
Phylum Porifera (sponge)					
Scypha sp.	*	-	*		suspension
Phylum Cnidaria					
Class Hydrozoa (hydroid)					
Plumularia sp.	*	-	*		suspension
Class Anthozoa					
Order Actiniaria (sea anemone)					
Aiptasiogeton sp.	8	Trace	5	Trace	suspension
Phylum Platyhelminthes (flat worm)					
unidentified sp.	4	Trace	3	Trace	browser-grazer
Phylum Annelida					
Class Polychaeta					
Subclass Errantia					
Eunice sp. a	3	1	1	Trace	browser-grazer
Eunice sp. b	3	3			" "
Eunice sp. c	1	30			" "
Eurythoe complanata					
Hermodice carunculata (Pallas)	8	50			" "
Nereis sp.	4	Trace			" "
unidentified phyllodocid	1	Trace			" "
unidentified syllid	18	1			" "
Subclass Sedentaria					
Branchiomma sp.	1	Trace			suspension
Chaetopterus sp.			1	3	"
Hydroides sp. a	*	-	*	-	"
Hydroides sp. b	Few	-			"
Vermiliopsis sp.	*	-	*	-	"
Phylum Sipunculida (acorn worm)					
Golfingia (Golfingia) sp.	14	3	5	1	deposit
Phylum Mollusca					
Class Gastropoda (snail)					
Cymatium labiosum Wood	1	1			browser-grazer
Cymatium pileare Linné	1	22			" "
Epitonium echinaticostum Orbigny			1	Trace	" "
Lucapinella limatula Reeve			1	Trace	" "
Thais haemastroma floridana Conrad			1	1	" "
Class Pelecypoda (clam)					
Aequipecten muscosus Wood	1	1			suspension
Anadara notabilis Roding	1	4			"
Anomia simplex Orbigny	7	2	4	1	"
Chama macerophylla Gmelin	12	9	10	7	"
Chlamys imbricata Gmelin	1	4	1	2	"
Chlamys ornata Lamarch	1	4			"
Isognomon bicolor Adams	1	Trace			"
Leptopecten bavayi Dautzenberg	7	1			"
Lima lima Linné	2	1	3	2	"
Lima pellucida Adams	7	5	4	7	"
Lima scabra Born	3	7	4	22	"
Lopha frons (Linné)	6	15			"
Lyropecten antillarum Récluz	6	7	3	1	"

TABLE 11 (continued)

Species	Intake Strainer Number	Intake Strainer Wet Weight (g)	Experimental Module Number	Experimental Module Wet Weight (g)	Feeding habit
Musculus lateralis Say	8	Trace	8	Trace	suspension
Ostrea equestris Say	14	36	14	10	"
Pinctada imbricata Roding	12	21	10	30	"
Pinna rudis (Linné)	65	213	22	83	"
Pteria columbus Roding	2	24			"
Phylum Arthropoda					
Class Crustacea					
Subclass Cirripedia (barnacle)					
Balanus amphitrite Darwin	5	1	2	1	suspension
Chthamalus stellatus (Poli)			4	Trace	"
Tetraclita squamosa (Bruguiere)			3	1	"
Subclass Malacostra					
Order Amphipoda					
unidentified caprellid			*		predator
Elasmopus pocillimanus (Bate)	*		*		browser-grazer
Stenothoe crenulata (Chevreax)	*		*		" "
Order Decapoda					
Suborder Natantia (shrimp)					
Brachycarpus biunguiculatus (Lucas)	1	1			predator
Synalpheus sp.	1	1			predator
Suborder Reptantia (lobsters and crabs)					
Panopeus sp.	1	Trace			predator
Phylum Bryozoa					
Bugula sp.	*		*		suspension
Phylum Echinodermata					
Class Echinoidea (sea urchin)					
Diadema antillarum (Philippi)	1	1			browser-grazer
Eucidaris tribuloides (Lamarck)	10	11	3	2	" "
Class Ophiuroidea (brittle star)					
Ophiocoma echinata (Lamarck)	10	15	3	4	deposit
Ophiocoma riisei Lufken	18	23	4	4	"
Ophiotelx angulata Lufken	1	Trace	1	Trace	"
Class Holothuroidea (sea cucumber)					
Holothuria impatiens Forskal			3	1	deposit
Phylum Chordata					
Subphylum Urochordata					
Class Ascideacea (sea squirt)					
Ascidia sydneiensis Stimpson	5	28	4	20	suspension
Botryllus planus (Van Name)	1 colony	Trace			"
Herdmania momus (Savigny)	1	1			
Styella plicata (Lesueur)	58	365	3	4	"

*These are colonial organisms or small organisms too numerous to count.

drift passively with ocean currents. These species generally broadcast large numbers of larvae into the ocean (21) so that at least a few will find a suitable habitat and survive to adulthood. Duration of the larval stage varies with the species, but can be several months long. In addition, many larvae are capable of postponing metamorphosis until they find a suitable habitat (22).

Most macrofouling occurred inside the intake strainers, where the flow velocity was less than 0.1 fps, and in portions of the modules where there was a low rate of water exchange. In the remainder of the flow system, where the flow rate exceeded 3 fps, little macrofouling occurred. This was probably because the macrofouling organisms could not withstand the shear forces of the rapidly flowing water. It must be remembered, though, that PVC has a smooth, slippery surface to which many organisms may have trouble adhering. On the outside of the intake hoses, the dominants were algae, calcareous tube worms, and the sea anemoe Aiptasiogeton. Barnacles, clams, and sea squirts were noticeably absent from the outer surface. Within the flow system, many of the sessile organisms were attached to the large pen shells, Pinna rudis, rather than to the PVC itself. If a material other than PVC were used, one to which macrofouling organisms could attach more readily, fouling in the flow stream itself could be a problem.

Since the modules simulated heat exchangers, the experiment dramatically illustrated the need to consider macrofouling in the design of OTEC heat exchangers. Restriction of flow was not evident during the experiment, but fouling organisms would probably have begun obstructing

flow both in the intake strainers and the experimental modules if the experiment had continued. Flow stoppages of a few hours in duration may amplify the problem by allowing organisms such as barnacles and clams to settle in areas which normally experience high flow rates. This problem has been encountered by Fetkovich's group in Hawaii (5).

Trophic organization may provide clues as to the kind of macrofouling community to expect within a flow system. Table 11 gives each species classified according to its feeding habits. For our purposes, suspension feeders are defined as those organisms which feed on material (living or non-living) suspended in the water column. Deposit feeders are those which feed on non-living adhering to the substrate. Browser-grazers feed on sessile organisms, while the term predator applies here only to raptorial predators which actively seek and capture their prey.

The suspension feeders were probably the first to become established in the flow system by attaching to the substrate. The presence of a few suspension feeders probably created a suitable environment for other organisms, including more suspension feeders, the raptorial predators, and the browser-grazers, many of which preyed on the suspension feeders. Finally the developing community provided material on which the deposit feeders could feed. Many of the organisms growing in the flow system are not usually found together. The pen shell, Pinna, by far the most prevalent organisms in this collection, generally occurs in shallow water growing buried in a sandy substrate . The polychaete Chaetopterus is usually found in shallow, muddy bottoms, while the sea anemone Aiptasiogeton sp. is an, as yet, undescribed species found only in deeper water (20 m) on a coral bottom. Several of these species such

as Scypha, Plumularia, Branchiomma, Hydroides, several of the clams, Balanus, Cthamalus, and the sea squirts are members of the so-called "shallow-water fouling community" which grow on pilings, mangrove roots, and any other available hard substrate (23, 24). Some such as Eurythoe, Hermodice, the scallop and file shells, Eucidaris, the brittle stars, and Holotharia, are commonly associated with coral reefs, while others such as Nereis, Anadara, and Diadema are commonly associated with seagrass communities (24).

Among the clams, a common character was shared. All are capable of forming a strong attachment to a substrate either by means of a byssus (a bundle of tough, thread-like fibers secreted by the animal to anchor it to a surface) or by cementing their shells directly to a substrate.

7.4 CONCLUSIONS

1. A large number and diversity of benthic invertebrates was found in the flow system of an experiment which tested biofouling in simulated OTEC evaporators at a potential OTEC site in Puerto Rico.

2. The organisms were concentrated in portions of the flow system where there was a low rate of water exchange.

3. In the absence of flow stoppages, there was little macrofouling in areas of the flow system where flow was maintained in excess of 3 fps.

4. The lack of macrofouling in areas of high flow was probably because organisms could not withstand the shear forces of rapidly flowing water. A contributing factor may have been that most of the pumping of the flow system had a smooth surface to which macrofouling

organisms had trouble attaching.

5. Regardless of where an Ocean Thermal Energy Conversion (OTEC) plant is sited, the potential for obstruction of the flow system by macrofouling organisms probably exists.

6. To minimize macrofouling in an OTEC flow system, areas of low flow must be avoided. If unavoidable, these areas should be readily accessible so they can be cleaned regularly.

8. REFERENCES

1. Atwood, O. K., Duncan, P. "Ocean Thermal Energy Conversion: Resource Assessment and Environment Impact for Proposed Puerto Rico Site" Final Report NSF Grant No. AER 75-00145, 1976.

2. Goldman, G., Hernández Avila, M. L., González, Juan G., and Pesante, D. "Results of Measurements Relatable to an OTEC Installation at Punta Tuna, Puerto Rico", CEER-0-57, 1979, 588 pp.

3. Fetkovich, J. G., A System for Measuring the Effect of Fouling and Corrosion on Heat Transfer under Simulated OTEC Conditions, Design Report COO-4041-10, 1976, 294 pp.

4. R. W. Finley and D. L. Meier, Design Report for PS-105 Data Acquisition System for Biofouling Studies of Heat Exchangers in Sea Water. U.S. Department of Energy COO-4041-6, 1977, 36 pp.

5. Fetkovich, J. G., Grannemann, G. N., Mahalingam, L. M., and Meier, D. L., "Measurements of Biofouling in OTEC Heat Exchangers," Proceedings of the Fifth Ocean Thermal Energy Conversion, edited by A. Lavi and T. N. Veziroglu, 1978, pp VIII-7 to VIII-21.

6. Liebert, B. E., Berger, L. R., White, H. J., Moore, J., McCoy, Wm., Berger, J. A. and Larsen-Basse, J., "The Effects of Biofouling and Corrosion on Heat Transfer Measurements," Proceedings of the Sixth Ocean Thermal Energy Conversion (OTEC) Conference Vol. 2 edited by G. L. Dugger, 1979, pp 12.7-1 to 12.7-10.

7. Hirshman, J., Meier, D. L., Munier, R.S.C., and Taylor, B. F., "Introduction of the St. Croix Biofouling and Corrosion Study," Proceedings of the Ocean Thermal Energy Conversion (OTEC) Biofouling, and Corrosion Symposium, edited by R. H. Gray, 1978, pp 381-390.

8. Little, B., Lavoie, D., "Gulf of Mexico Ocean Thermal Energy Conversion (OTEC) Biofouling and Corrosion Experiments," Proceedings of the Ocean Thermal Energy Conversion (OTEC) Biofouling, Corrosion, and Materials Workshop, 1979, pp 60-100.

9. Little, B., Morse, J., Loeb, G., and Spiehler, F., "A Biofouling and Corrosion Study of Ocean Thermal Energy Conversion (OTEC) Heat Exchanger Candidate Metals," Proceedings of the Sixth Ocean Thermal Energy Conversion (OTEC) Conference. Vol. 2 edited by G. L. Dugger, 1979, pp 12.13-1 to 12.13.9.

10. Holm-Hansen, O. and C. R. Booth, "The Measurement of Adenosine Triphosphate in the Ocean and its Significance" Limnoli Oceanog. Vol. 11, pp 510-519.

11. Seely, H. W., Jr. and Paul J. Van Denmark. Microbes in Action: A Laboratory Manual of Microbiology. W. H. Freeman & Co., San Francisco, 1972.

12. Loeb, George, I., "Measurements of Marine Fouling Films by Light Sectioning Microscopy." J. Mar. Tech. Soc. (in press 1980).

13. Pelczer, M. J. Jr. Laboratory Exercise in Microbiology. McGraw-Hill, New York, 1965.

14. Collins, C. H. and P. M. Lyne (eds.) Microbiological Methods. University Park Presss, Baltimore, 1970.

15. Sasscer, D. S., T. R. Tosteson, K. B. Pedersen, F. Rosa, and F. L. Benítez, "Design and Construction Phase of a Biofouling Corrosion and Materials Study from a Moored Platform at Punta Tuna, Puerto Rico," Proceedings of the Sixth Ocean Thermal Energy Conference. Edited by G.L. Dugger, (Wash., D.C.).

16. Zobell, C. E. and H. C. Upham. A list of Marine Bacteria Including Description of Sixty New Species. Bull. Scripps Inst. Oceanogr. 5:239-292, 1944.

17. Botler, M. Numerical Taxonomy and Character Analysis of Saphrophytic Bacteria Isolated from Kiel Fjord and the Kiel Bight, In: Microbial Ecology of a Brackish Water Environment. ed. G. Rheinheimer, Springer Verlag, Berlin, New York, 1977.

18. Karl, D. M., J. A. Haugsness, L. Campbell and O. Holm-Hansen. Adenine Nucleotide Extraction from Multicellular Organisms and Beach Sand: ATP Recovery, Energy Charge Ratios and Determination of Carbon/ATP Ratios. J. Exp. Mar. Biol. Ecol., 34:163-181, 1978.

19. Karl, D. M. Adenosine Triphosphate and Guanosine Triphosphate Determinations in Intertidal Sediments. In: Methodology for Biomass Determinations and Microbial Activities in Sediments, ed. C.D. Litchfield and P.L. Seyfried, pp 5-20, ASTM STP 673, American Society for Testing and Materials, Philadelphia, PA, 1979.

20. Sasscer, D. S., Morgan, T., Tosteson, T. R., and Grannemann, G. N., "In Situ Biofouling of Ocean Thermal Energy Conversion (OTEC) Evaporator Tubes" Journal of Solar Energy Engineering, Vol. 103 (1981), pp. 121-125.

21. Thorson, G., "Reproductive and larval ecology of marine bottom invertebrates" Biol. Rev., Vol. 25 (1950), pp 1-45.

22. Thorson, G., "Length of pelagic larval life in marine bottom invertebrates as related to larval transport by ocean currents" In Oceanography Amer. Ass. Adv. Sci. Publ. No. 67 (1961), pp 455-474.

23. T. N. Veziroglu, 1978, pp VIII-7 to VIII-21. Puerto Rico

Water Resources Authority report number WRA E.S.-8F, Aguirre Power Plant Complex Final Environmental Impact Statement, December, 1972.

24. Kolehmainen, S., Morgan, T., Castro, R., "Mangrove-root communities in a thermally altered area in Guayanilla Bay, Puerto Rico" In Thermal Ecology, Proceedings of Thermal Ecology Symposium (May, 1973), Ed. J. W. Gibbons and R. R. Sharitz, U.S. AEC Conf-730505, pp 371-390.

APPENDIX 1

WILSON PLOT DATA

APPENDIX 1

WILSON PLOT DATA

	UNIT 1		UNIT 2		UNIT 3		UNIT 4	
	Slope[1]	Intercept[2]	Slope[1]	Intercept[2]	Slope[1]	Intercept[2]	Slope[1]	Intercept[2]
1/28/80	36.27 ± .21	.36 ± .06	36.52 ± .23	.68 ± .07	36.08 ± .22	.15 ± .06	35.90 ± .21	.80 ± .06
12/2/80	36.25 ± .27	1.16 ± .07	38.56 ± .38	1.08 ± .11	39.82 ± .23	.59 ± .06	37.12 ± .40	1.11 ± .11
3/8/81	--	--	48.13 ± 1.01	4.74 ± .27	49.61 ± .71	3.44 ± .19	--	--

Footnotes

1. $(hr\ ft^2\ °F/Btu)(ft/sec)^{-0.8} \times 10^4$

2. $hr\ ft^2\ °F/Btu \times 10^4$

APPENDIX 2

2 R_f DATA

2 A - UNIT 1

2 B - UNIT 3

2 C - UNIT 2

2 D - UNIT 4

Progress Runs are indicated by a "P" after the date. Standard Error of R is given. Numbers with no standard error are from days when not all the runs were analyzed.

UNIT 1

Date	Day	R_f
1/31/80	1	0
2/5/80	6	0.06 ± .02
2/12/80	13	0.07 ± .03
2/18/80	19	0.23 ± .03
2/25/80	26	0.37 ± .04
3/4/80	34	0.51 ± .03
3/15/80	45	1.36 ± .04
3/22/80	52	1.52 ± .04
3/30/80	60	2.54 ± .08
4/10/80	71	3.35 ± .04
4/19/80	80	4.40 ± .04
4/29/80	90	0.55 ± .05
5/1/80-P	92	0.48 ± .04
5/4/80	95	0.83 ± .03
5/12/80	103	2.25 ± .04
5/16/80-P	107	3.25 ± .04
5/19/80	110	3.83 ± .04
5/21/80-P	112	4.45 ± .04
5/28/80	119	6.26 ± .04
5/31/80-P	122	7.58
6/4/80	126	8.07
6/6/80-P	128	8.68
6/9/80	131	10.03
6/13/80	135	11.87
6/15/80	137	8.95
6/19/80	141	11.31 ± .08
6/20/80	142	0.70 ± .04
6/25/80-P	147	0.65 ± .03
6/28/80	150	1.56
7/2/80-P	154	2.49
7/5/80	157	2.92
7/9/80-P	161-P	3.74
7/13/80	165	4.82
7/18/80-P	170-P	6.40
7/23/80	175	8.28
7/24/80-P	176-P	7.82
7/26/80	178-S	0.65
7/30/80-P	181	0.97 ± .08
8/3/80	186	1.46
8/10/80	193	3.40
8/17/80	200	4.99
8/20/80	203	5.45
8/24/80-P	207	5.96
8/27/80	210	6.62
8/28/80-P	211	6.82
8/29/80	212	0.67
9/4/80	218	0.90
9/9/80	223	2.15

Date	Day	R_f
9/12/80-P	226	2.66
9/16/80	230	3.82
9/20/80-P	234	4.49 ± .02
9/23/80	237	4.89 ± .02
9/27/80-P	241	6.48 ± .02
9/30/80-P	244	7.55 ± .02
10/2/80	246	7.97 ± .04
10/3/80-P	247	7.46 ± .05
10/5/80	249	0.81 ± .01
10/8/80-P	252	1.08
10/12/80	256	1.85
10/16/80-P	260	3.92
10/20/80	264	4.91
10/22/80-P	266	4.92 ± .04
10/25/80-P	269	5.26 ± .02
10/30/80	274	5.86 ± .02
10/30/80-P	274	5.58 ± .09
10/31/80	275	0.67 ± .05
11/4/80-P	279	0.98 ± .03
11/8/80	283	1.42 ± .02
11/13/80-P	288	2.75 ± .06
11/16/80	290	3.09 ± .02
11/19/80-P	294	3.71 ± .02
11/22/80	297	4.36 ± .05
11/27/80-P	302	5.44 ± .05
11/30/80	305	5.92 ± .05
12/1/80-P	306	5.60 ± .04
12/2/80	307	0.87 ± .03
12/7/80-P	312	0.90 ± .04
12/10/80	315	1.08 ± .02
12/13/80-P	318	1.86 ± .07
12/18/80	323	2.69 ± .03
12/20/80-P	325	3.20 ± .10
12/23/80	328	3.86 ± .07
12/28/80-P	333	4.58 ± .03
12/31/80	336	5.08 ± .03
1/3/81-P	339	6.02 ± .09
1/6/81	342	6.50 ± .05
1/7/81-P	343	6.33 ± .01
6/8/81	344	0.82 ± .02
1/11/81-P	347	0.82 ± .04
1/14/81	350	1.08 ± .01
1/19/81	355	1.94 ± .03
1/23/81-P	359	2.98 ± .07
1/28/81	364	3.91 ± .04
2/1/81-P	368	5.18 ± .04
2/5/81	372	6.27 ± .04
2/10/81-P	377	6.96 ± .03
2/10/81-P	377	6.72 ± .04
2/11/81	378	0.88 ± .03

Date	Day	R_f	
2/14/81-P	381	0.97	.02
2/18/81	385	1.30	.02
2/23/81-P	390	1.88	
2/25/81	392	1.48	.04
2/28/81-P	395	1.61	.01
3/4/81	399	1.90	.03
3/8/81	403	2.41	.01

Appendix 2 B

UNIT 3

Date	Day	R_f
1/31/80-3	1	0
2/5/80-3	6	-0.12 ± .04
2/12/80-3	13	-0.03 ± .05
2/17/80-2	18	-0.01 ± .04
2/24/80-3	25	0.20 ± .04
3/4/80-1	34	0.69 ± .04
3/15/80-2	45	1.24 ± .04
3/22/80-2	52	1.85 ± .04
3/29/80-3	59	3.12 ± .04
4/9/80-3	70	4.13 ± .04
4/14/80-P	75	4.99 ± .04
4/19/80	80	4.08 ± .04
4/29/80	90	-0.07 ± .04
5/1/80-P	92	0.18 ± .06
5/4/80	95	0.54 ± .06
5/13/80	104	2.05 ± .04
5/16/80-P	107	2.85 ± .08
5/18/80	109	3.23 ± .04
5/21/80-P	112	4.07 ± .07
5/24/80-P	115	4.73
5/26/80	117	5.14 ± .03
5/31/80-P	122	5.45
6/4/80	126	6.99
6/6/80-P	128	7.45
6/9/80	131	8.67
6/13/80	135	10.07
6/15/80	137	7.90
6/19/80	141	9.77 ± .04
6/21/80	143	0.52 ± .05
6/25/80	147	1.02 ± .03
6/28/80	150	2.22
7/2/80-P	154	2.15
7/5/80	157	3.39
7/9/80-P	161	4.11
7/14/80	166	5.27
7/18/80-P	170	5.98
7/23/80	175	7.31
7/24/80-P	176	6.64
7/26/80	178	0.59
7/30/80-P	181	1.27
8/3/80	186	2.00
8/7/80-P	190	3.01
8/10/80	193	4.01
8/17/80-P	200	5.53
8/21/80	204	6.24
8/25/80-P	208	6.37
8/29/80	212	6.49
8/29/80-P	212	5.85
8/29/80	212	0.53
9/4/80	218	1.62

Date	Day	R_f
9/9/80	223	4.15
9/12/80-P	226	5.14
9/17/80	231	5.66
9/20/80-P	234	5.97 ± .05
9/23/80	237	6.59
9/28/80-P	242	7.65 ± .05
9/30/80-P	244	7.95 ± .05
10/3/80	247	8.67 ± .03
10/3/80-P	247	7.66 ± .01
10/4/80	248	0.51 ± .05
10/9/80-P	253	1.33
10/12/80	256	3.56
10/16/80-P	260	5.21
10/20/80	264	5.64
10/23/80-P	267	6.04
10/26/80-P	270	6.04
10/29/80	273	6.41 ± .02
10/30/80-P	274	6.53 ± .07
10/31/80	275	0.64 ± .03
11/4/80-P	279	1.45 ± .02
11/8/80	283	3.59 ± .04
11/13/80-P	288	4.38 ± .06
11/16/80	291	4.60 ± .03
11/20/80-P	295	5.31 ± .06
11/24/80	299	6.05 ± .02
11/27/80-P	302	6.43 ± .03
11/30/80	305	6.82 ± .04
12/1/80-P	306	6.71 ± .01
12/2/80	307	0.64 ± .03
12/4/80-P	309	0.67 ± .06
12/7/80-P	312	1.12 ± .06
12/10/80	315	1.74 ± .02
12/14/80-P	319	2.78 ± .01
12/18/80	323	3.65 ± .04
12/20/80-P	325	4.18 ± .03
12/24/80	329	4.92 ± .05
12/28/80-P	333	5.96 ± .02
12/31/80	336	6.50 ± .03
1/4/81-P	340	7.67 ± .02
1/6/81	342	8.31 ± .02
1/7/81-P	343	8.35 ± .02
1/8/81	344	0.54 ± .03
1/11/81-P	347	1.01 ± .02
1/14/81	350	2.10 ± .02
1/20/81	356	4.27 ± .02
1/24/81-P	366	5.56 ± .01
1/29/81	365	6.61 ± .05
2/1/81-P	368	7.45 ± .04
2/6/81	373	7.81 ± .04
2/10/81-P	377	8.27 ± .03
2/10/81-P	377	7.71 ± .02
2/11/81	378	0.79 ± .01
2/14/81-P	381	1.19 ± .03
2/19/81	386	2.34 ± .03

Date	Day	R_f
2/26/81	393	3.49 $\pm$ .03
2/28/81-P	395	3.98 $\pm$ .04
3/4/81	399	4.94 $\pm$ .02
3/8/81	403	5.93 $\pm$ .04

UNIT 2

Date	Day	R_f
1/31/80-2	1	0
2/5/80-2	6	-0.08 ± .04
2/12/80-1	13	-0.11 ± .04
2/16/80-1	17	0.15 ± .04
2/24/80-1	25	0.44 ± .06
3/2/80-1	32	0.87 ± .04
3/14/80-1	44	1.62 ± .08
3/21/80-1	51	2.05 ± .04
3/29/80-1	59	2.85 ± .05
4/9/80-2	70	3.55 ± .04
4/19/80-1	80	3.89 ± .04
4/29/80	90	-0.06 ± .04
5/1/80-P	92	0.15 ± .05
5/4/80	95	0.49 ± .04
5/13/80	104	2.70 ± .04
5/16/80-P	107	3.59 ± .05
5/18/80	109	3.98 ± .03
5/21/80-P	112	4.00 ± .05
5/24/80-P	115	3.98
5/26/80	117	4.03 ± .03
5/31/80-P	122	3.79
6/4/80	126	4.64
6/6/80-P	128	5.18
6/9/80	131	5.91
6/13/80	135	6.45
6/15/80	137	4.56
6/19/80	141	5.18 ± .08
6/20/80	142	0.53 ± .04
6/25/80-P	147	1.14 ± .04
6/28/80	150	1.93
7/2/80-P	154	2.32
7/15/80	157	2.47
7/19/80-P	161	3.06
7/13/80	165	3.49
7/18/80-P	170	4.11
7/23/80	175	5.45
7/24/80-P	176	5.57
7/26/80	178	0.85
7/30/80-P	181	1.91
8/2/80	185	2.42
8/7/80-P	190	3.59 ± .06
8/10/80	193	4.37
8/17/80-P	200	5.93
8/21/80	204	6.69
8/24/80-P	207	7.63
8/27/80	210	8.30
8/28/80-P	211	6.75
8/29/80	212	0.80
9/3/80	217	2.92

Date	Day	R_f
9/9/80	223	5.07
9/12/80-P	226	5.62
9/17/80	231	6.35
9/20/80-P	234	6.74 ± .04
9/23/80	237	7.44 ± .03
9/27/80-P	241	8.69 ± .02
9/30/80-P	244	9.67 ± .03
10/2/80	246	10.40 ± .02
10/3/80	247	7.93 ± .04
10/5/80	249	0.72 ± .02
10/8/80-P	252	1.38 ±
10/12/80	256	2.57
10/16/80-P	260	4.85
10/19/80	263	6.03
10/22/80-P	266	6.34
10/26/80-P	270	6.97
10/29/80	273	7.49 ± .02
10/30/80-P	274	6.37 ± .04
10/31/80	275	0.75 ± .03
11/4/80-P	279	1.35 ± .05
11/8/80	283	2.55 ± .02
11/13/80-P	288	3.67 ± .03
11/16/80	291	4.16 ± .08
11/19/80-P	294	5.11 ± .04
11/23/80	298	6.49 ± .03
11/27/80-P	302	7.32 ± .05
11/30/80	305	7.58 ± .06
12/1/80-P	306	7.09 ± .11
12/2/80	307	0.78 ± .04
12/7/80-P	312	1.46 ± .04
12/10/80	315	1.86 ± .04
12/13/80-P	318	2.79 ± .04
12/18/80	323	4.23 ± .03
12/20/80-P	325	4.76 ± .06
12/24/80	329	6.27 ± .02
12/28/80-P	333	7.92 ± .08
12/31/80	336	8.78 ± .03
1/3/81-P	339	10.25 ± .02
1/6/81	342	11.43 ± .03
1/7/81-P	343	9.25 ± .03
1/8/81	344	0.73 ± .03
1/11/81-P	347	1.43 ± .02
1/14/81	350	2.15 ± .03
1/19/81	355	4.04 ± .02
1/24/81-P	360	6.11 ± .06
1/28/81	364	7.45 ± .04
2/1/81-P	368	8.85 ± .09
2/5/81	372	10.07 ± .04
2/10/81-P	377	10.73 ± .03
2/10/81-P	377	9.91 ± .06
2/11/81	378	0.84 ± .04
2/14/81-P	381	1.69 ± .07
2/18/81	385	3.05 ± .03

Date	Day	R_f
2/22/81-P	389	3.95 ± .03
2/25/81	392	4.47 ± .05
2/28/81-P	395	5.11 ± .04
3/3/81	398	5.97 ± .04
3/8/81	403	6.68 ± .02

Appendix 2 D

UNIT 4

Date	Day	R_f
2/1/80-1	1	0
2/6/80-1	6	-0.01 ± .05
2/12/80-2	12	-0.09 ± .05
2/17/80-1	17	0.19 ± .04
2/24/80-2	24	0.53 ± .06
3/3/80-2	32	1.34 ± .06
3/15/80-1	44	1.80 ± .04
3/22/80-1	51	2.44 ± .04
3/29/80-2	58	3.21 ± .04
4/9/80-1	69	4.09 ± .04
4/14/80-P	74	4.35
4/20/80	80	4.63 ± .04
4/29/80	89	.82 ± .04
5/1/80-P	91	.47 ± .04
5/4/80	94	.84 ± .04
5/13/80	103	2.51 ± .05
5/16/80-P	106	3.06 ± .06
5/18/80	108	3.46 ± .05
5/21/80-P	111	3.60 ± .07
5/24/80-P	114	3.49
5/27/80-P	117	3.03 ± .04
5/30/80-P	120	2.85
6/3/80	124	3.18
6/6/80-P	127	3.25
6/8/80	129	3.51
6/13/80	134	5.49
6/15/80	136	4.73
6/19/80	140	5.08 ± .04
6/21/80	142	1.13 ± .06
6/25/80-P	146	1.82 ± .04
6/28/80	149	2.33
7/2/80-P	153	2.79
7/5/80	156	2.97
7/9/80-P	160	3.62
7/14/80	165	4.24
7/18/80-P	169	4.85
7/24/80	175	5.83
7/24/80	175	5.55
7/26/80	177	0.89
7/30/80-P	180	1.83
8/2/80	184	2.25
8/7/80-P	189	3.40
8/11/80	193	4.43
8/17/80-P	199	5.35
8/21/80	203	6.01
8/25/80-P	207	6.25
8/27/80	209	7.07
8/28/80-P	210	5.91
8/30/80	212	0.80 ± .03

Date	Day	R_f
9/4/80	217	2.41
9/9/80	222	3.77
9/12/80-P	225	4.34
9/17/80	230	5.31
9/20/80-P	233	5.81 ± .03
9/23/80	236	6.33 ± .05
9/27/80-P	240	7.35 ± .02
9/30/80-P	243	8.08 ± .11
10/3/80	246	9.17 ± .03
10/3/80	246	8.43 ± .05
10/4/80	247	0.75 ± .03
10/9/80-P	252	1.79
10/12/80	256	3.17
10/16/80-P	259	4.73
10/20/80	263	5.65
10/23/80-P	266	6.35
10/26/80-P	269	6.76
10/29/80	272	7.61 ± .02
10/30/80-P	273	6.49 ± .04
10/31/80	274	0.87 ± .03
11/4/80-P	278	1.47 ± .04
11/8/80	282	2.68 ± .02
11/13/80-P	387	3.79 ± .03
11/16/80	290	4.28 ± .08
11/19/80-P	293	5.23 ± .04
11/25/80	299	6.01 ± .04
11/27/80-P	301	6.75 ± .03
12/1/80	305	7.21 ± .05
12/1/80-P	305	7.36 ± .05
12/2/80	306	0.79 ± .05
12/4/80-P	308	0.93 ± .04
12/7/80-P	311	1.54 ± .04
12/10/80	314	2.07 ± .03
12/14/80-P	318	2.97 ± .07
12/18/80	322	4.10 ± .02
12/21/80-P	325	4.80 ± .06
12/24/80	328	5.59 ± .01
12/28/80-P	332	6.75 ± .03
12/31/80	335	7.45 ± .03
1/4/81-P	339	8.66 ± .01
1/6/81	341	9.06 ± .03
1/7/81-P	342	8.75 ± .02
1/8/81	343	0.72 ± .03
1/11/81-P	346	1.42 ± .08
1/14/81	349	2.48 ± .04
1/20/81	355	4.33 ± .02
1/24/81-P	359	5.85 ± .02
1/29/81	364	7.23 ± .04
2/6/81	372	8.53 ± .06

Date	Day	R_f
2/10/81-P	376	9.05 ± .06
2/10/81-P	376	8.62 ± .05
2/11/81	377	0.73 ± .03
2/14/81-P	380	1.23 ± .05
2/19/81	385	2.23 ± .04
2/22/81-P	388	3.25 ± .05
2/26/81	392	4.06 ± .03
2/28/81-P	394	4.55 ± .03
3/3/81	397	5.47 ± .04
3/8/81	402	6.80 ± .02

APPENDIX 3

SUMMARY OF SURFACE RESIDUE, CARBON AND C/N RATIO OF THE TOTAL RECOVERABLE MATERIAL FROM EXPERIMENTAL SURFACE

ALUMINUM

Sample Number	$\overline{SR}$ (ug/cm^2)	$\overline{C}$ (ug/cm^2)	$\overline{C/N}$	$\overline{C/SR} \times 10^2$
1	55.0 ± 16	12.4 ± 4.0	13.0 ± 0.4	22.0 ± 4.0
2	157.0 ± 26	20.0 ± 3.4	19.0 ± 2.5	13.0 ± 1.1
3	202.0 ± 14	15.3 ± 1.3	16.3 ± 1.0	7.7 ± 0.7
4	69.0 ± 15	9.3 ± 0.6	12.5 ± 1.0	19.0 ± 6.1
5	127.0 ± 12	12.5 ± 1.1	15.1 ± 0.6	10.0 ± 0.6
6	241.0 ± 58	19.5 ± 3.2	18.1 ± 1.5	9.5 ± 1.3
7	144.0 ± 72	16.0 ± 4.2	18.3 ± 2.1	18.3 ± 3.7
8	573.0 ± 98	53.0 ± 2.0	12.2 ± 0.7	10.0 ± 1.3
9	492.7 ± 92	57.0 ± 9.3	10.4 ± 0.7	12.0 ± 1.0
9 V	396.0 ± 11	46.0 ± 0.9	10.2 ± 0.3	12.0 ± 0.3
9 combined		51.7 ± 5.0	10.3 ± 0.3	

TITANIUM

Sample Number	$\overline{SR}$ (ug/cm^2)	$\overline{C}$ (ug/cm^2)	$\overline{C/N}$	$\overline{C/SR} \times 10^2$
1	79 ± 11.0	8.7 ± 1.3	11.0 ± 1.3	11.0 ± 0.8
2	109 ± 3.9	16.0 ± 1.4	20.0 ± 1.7	15.0 ± 1.4
3	114 ± 12.0	9.7 ± 1.3	15.0 ± 0.9	8.3 ± 1.2
4	67 ± 7.0	8.2 ± 0.9	14.0 ± 1.4	13.2 ± 2.0
5	57 ± 12.0	6.9 ± 0.7	12.0 ± 0.8	15.0 ± 3.0
6	75 ± 3.5	6.8 ± 1.2	13.4 ± 2.6	9.2 ± 1.9
7	40 ± 15.0	5.4 ± 1.3	10.5 ± 1.3	16.0 ± 2.0
8	195 ± 19.0	28.0 ± 3.0	9.0 ± 1.1	14.0 ± 0.7
9	120 ± 3.0	17.2 ± 3.3	8.0 ± 0.4	14.0 ± 2.3
9 V	173 ± 17.0	28.0 ± 1.2	7.0 ± 0.07	16.0 ± 1.3
9 combined		22.8 ± 3.0	7.5 ± 0.5	

APPENDIX 4

CONCENTRATION OF CARBON IN MATERIAL ASSOCIATED WITH EXPERIMENTAL SURFACES

ALUMINUM

Time	(Day)		$\bar{C}$ ($\mu g/cm^2$)	$\overline{C/N}$	Avg. Vol. (mm^3/cm^2)	C($\mu g/mm^3$)
1	0.61		12.4 ± 3.8	13.0 ± 0.4	0.004	3100
2	4.93		19.8 ± 3.4	19.2 ± 2.5	0.74	27
3	9.71		15.3 ± 1.3	16.3 ± 1.0	0.78	20
4	16.63		9.3 ± 0.6	12.5 ± 1.0	0.82	11
5	27.62		12.5 ± 1.1	15.1 ± 0.6	0.92	14
6	37.65		19.5 ± 3.2	18.1 ± 1.5	0.93	21
7	50.62		16.1 ± 4.2	18.3 ± 2.1	1.07	15
8	80.60		52.6 ± 1.5	12.2 ± 0.7	2.15	24
9	95.60	1-2	57.3 ± 9.3	10.4 ± 0.7		
		3-4	46.2 ± 0.9	10.2 ± 0.3		
	combined 9		51.7	10.3	2.8	18
10	142.60		97.5	8.7	10.7	9

TITANIUM

Time	(Day)		$\bar{C}$ ($\mu g/cm^2$)	$\overline{C/N}$	Avg. Vol. (mm^3/cm^2)	C($\mu g/mm^3$)
1	0.61		8.7 ± 1.3	11.1 ± 1.3	0.002	4350
2	4.93		16.0 ± 1.4	19.6 ± 1.7	0.31	52
3	9.71		9.7 ± 1.3	14.8 ± 0.9	0.38	26
4	16.63		8.2 ± 0.9	14.0 ± 1.4	0.36	23
5	27.62		6.9 ± 0.7	11.5 ± 0.8	0.60	12
6	37.65		6.8 ± 1.2	10.6 ± 0.9	0.75	9
7	50.62		5.4 ± 1.3	10.5 ± 1.3	0.82	7
8	80.60		28.2 ± 3.0	9.0 ± 1.1	1.45	19
9	95.60	1-2	17.2 ± 3.3	7.7 ± 0.4		
		3-4	28.4 ± 1.2	7.3 ± 0.07		
	combined 9		22.8	7.5	0.4	57
10	142.6		39.8	7.7	7.3	5

APPENDIX 5

TOTAL DENSITY OF RECOVERED MATERIAL ON EXPERIMENTAL SURFACE DURING PHASE I

ALUMINUM

Time	Wet Film Volume (um/cm^2)	Surface Residue ug/cm^2	Surface Residue $ug/um^3 \times 10^8$	Surface Residue ug/mm^3
0.61	0.040	55.5	1388.0	13875
4.93	7.4	156.8	21.2	212
9.71	7.8	202.0	25.9	259
16.63	8.2	68.6	8.4	84
27.62	9.2	126.8	2.9	29
37.65	9.3	240.9	25.9	259
50.62	10.7	143.7	13.4	134
80.60	21.5	572.8	26.6	266
95.60	28.4	444.5	15.7	157
142.60	107.3	776.0	7.2	72

TITANIUM

Time	Wet Film Volume (um/cm^2)	Surface Residue ug/cm^2	Surface Residue $ug/um^3 \times 10^8$	Surface Residue ug/mm^3
0.61	0.020	78.5	3925.0	39250
4.93	3.1	109.1	35.2	352
9.71	3.8	113.8	29.9	299
16.63	3.6	67.1	18.6	186
27.62	6.0	56.6	9.4	94
37.65	7.5	74.7	10.0	100
50.62	8.2	40.2	4.9	49
80.60	14.5	194.5	13.4	134
95.60	3.6	146.4	40.7	407
142.60	73.3	184.0	2.5	25

APPENDIX 6

ATP CONTENT OF MATERIAL ADHERING TO EXPERIMENTAL SURFACE

ALUMINUM

Sample	Pipe 1	Pipe 2	Pipe 3	Pipe 4	Pipe 5	Pipe 6	f'	$\bar{x}$ (pg/cm^2)	S	S/$\bar{x}$ (%)	SE	N	ATP x $\frac{1}{f'}$
1	0	0	0	0	0	0	.000	0	0	0	0	0	0
2	0.754	1.199	0	0	0	0	.223	24.75	8.629	35	6.102	2	111
3	0	1.552	1.132	0.526	0	0	.167	27.189	12.276	45	7.087	3	163
4	0	2.051	0.754	0.549	0	0	.277	28.265	19.59	69	11.310	3	102
5	0	4.288	0.934	2.233	1.658	0	.416	97.579	31.654	32	15.82	4	235
6	0	3.090	2.164	0	0	0	.167	156.18	37.128	24	26.25	2	935
7	1.395	0	0.974	0	1.515	12.835	.333	257.4	359.54	140	179.8	4	773
8	1.634	3.346	2.279	-	-	-	.833	145.5	52.5	36	30.3	3	175
9	7.374	4.490	1.391	2.154	2.906	1.415	.945	126.3	42.9	34	17.5	6	134

TITANIUM

Sample	Pipe 1	Pipe 2	Pipe 3	Pipe 4	Pipe 5	Pipe 6	f'	$\bar{x}$ (pg/cm^2)	S	S/$\bar{x}$ (%)	SE	N	ATP x $\frac{1}{f'}$
1	0	0.821	0	1.417	1.329	0	.222	30.76	9.07	29	5.236	3	139
2	0.723	1.264	0	0	0.477	0	.335	21.051	10.261	49	5.924	3	63
3	0	8.143	1.697	1.722	1.986	10.053	.610	126.99	112.24	88	50.196	5	208
4	11.190	1.086	1.456	3.425	1.833	1.297	.945	88.297	95.26	108	38.89	6	93
5	0	0	4.772	3.221	2.704	4.522	.667	230.646	60.499	26	30.249	4	346
6	7.041	6.349	4.825	5.248	7.275	3.590	.917	350.9	83.878	24	34.243	6	383
7	12.766	10.640	4.903	4.405	3.859	2.874	1.000	398.8	236.6	59	96.6	6	399
8	21.981	30.906	12.307	-	-	-	1.000	1301.5	552.2	42	318.8	3	130
9	23.263	16.271	15.895	25.056	19.083	12.769	1.000	879.3	389.2	44	159.2	6	879

APPENDIX 7

WET FILM THICKNESS AND VOLUME OF FILM ASSOCIATED WITH THE EXPERIMENTAL SURFACE DURING PHASE I

ALUMINUM

Time (Days)	f'	f_{max}	f_{min}	(um) f^B(max)	(um) f^B(min)	(um) WFT	(mm^3/cm^2) WFV
0.61	0.67	0.01	0.99	0.059	-	0.059	0.040
4.93	0.917	0.08	0.92	0.984	7.084	8.068	7.398
9.71	0.917	0.08	0.92	1.104	7.452	8.556	7.846
16.63	1.0	0.07	0.93	0.945	7.254	8.199	8.199
27.62	1.0	0.08	0.92	1.152	8.004	9.156	9.156
37.65	1.0	0.08	0.92	1.104	8.188	9.292	9.292
50.62	1.0	0.09	0.91	1.368	9.282	10.65	10.65
80.6	0.84	0.30	0.70	9.552	16.002	25.554	21.465
95.6	0.69	0.37	0.63	18.038	23.140	41.178	28.41
142.6	1.0	0.98	0.02	106.3	0.964	107.26	107.26

TITANIUM

Time (Days)	f'	f_{max}	f_{min}	(um) f^B(max)	(um) f^B(min)	(um) $\overline{WFT}$	(mm^3/cm^2) WFV
0.61	0.375	0.01	0.99	0.053	-	0.053	0.020
4.93	0.46	0.03	0.97	0.300	6.402	6.702	3.083
9.71	0.48	0.03	0.97	0.366	7.469	7.835	3.761
16.63	0.50	0.03	0.97	0.318	6.887	7.205	3.603
27.62	0.688	0.02	0.98	0.232	8.526	7.938	6.026
37.65	0.959	0.01	0.99	0.115	7.722	7.837	7.516
50.62	1.00	0.03	0.97	0.375	7.857	8.214	8.214
80.6	0.75	0.19	0.81	4.731	14.596	19.327	14.495
95.6	0.10	0.40	0.60	18.028	18.132	36.135	3.635
142.6	1.0	0.87	0.13	69.774	3.562	73.336	73.336

Footnotes

1. f' is frequency of samples showing measurable wet film thickness.
2. f_{max} estimated fraction of area (1 cm^2) covered by film of maximum thickness.
3. f_{min} estimated fraction of area (1 cm^2) covered by film of minimal thickness.
4. $f^B_{max} = f' [WFT_{max} \times f_{max}]$
5. $f^B_{min} = [WFT_{min} \times f_{min}]$
6. $\overline{WFT}$ = average thickness of film on 1 cm^2
7. $WFV = WFT/cm^2$

APPENDIX 8

SURFACE RESIDUE, CARBON, AND C/N RATIO OF THE SURFACE ASSOCIATED RESIDUE ON THE EXPERIMENTAL SURFACE BEFORE AND AFTER EACH CLEANING CYCLE DURING THE SECOND PHASE

ALUMINUM

Before

Sample	$\overline{SR}$ (ug/cm^2)	$\overline{C}$ (ug/cm^2)	$\overline{C/N}$	$\overline{\%}$ Inorganic
10	776 ± 44	98 ± 7.1	8.7 ± 0.5	82 ± 0.68
11	435 ± 22.9	73 ± 3.5	8.2 ± 0.3	76 ± 1.3
12	647 ± 25	113 ± 3.9	10.0 ± 0.4	76 ± 0.9
14	531 ± 89	53 ± 8.0	10.4 ± 0.5	56 ± 14.0
15	424 ± 89	59 ± 7.2	9.3 ± 1.03	59 ± 9.2
16	568 ± 62	72 ± 5.7	10.5 ± 1.05	83 ± 0.58
19	736 ± 40	98 ± 3.3	12.2 ± 0.15	81 ± 0.67

After

10	127 ± 27	12.5 ± 1.3	14.1 ± 0.76	66 ± 9.2
11	90 ± 17	12.3 ± 1.3	18.0 ± 1.9	68 ± 7.9
12	219 ± 23	35 ± 2.8	15.8 ± 0.4	78 ± 0.9
14	183 ± 38	17 ± 2.2	23.4 ± 6.0	65 ± 9.5
15	86 ± 41	19 ± 5.4	12.0 ± 1.8	50 ± 22
16	164 ± 30	23 ± 0.88	15.4 ± 0.26	78 ± 2.2
19	91 ± 16	20 ± 1.33	14.9 ± 0.94	60 ± 5.04

TITANIUM

Before

Sample	$\overline{SR}$ (ug/cm^2)	$\overline{C}$ (ug/cm^2)	$\overline{C/N}$	$\overline{\%}$ Inorganic
10	184 ± 16	40 ± 3.2	7.8 ± 0.58	74 ± 0.98
11	274 ± 46	57 ± 8	6.5 ± 0.09	69 ± 2
12	326 ± 48	70 ± 2.9	7.1 ± 0.2	76 ± 0.9
14	126 ± 28	32 ± 2.9	7.3 ± 0.18	28 ± 12
15	493 ± 178	75 ± 17	6.3 ± 0.26	48 ± 8.2
16	305 ± 27	44 ± 2.6	6.9 ± 0.07	79 ± 1.2
19	351 ± 29	69 ± 5	8.4 ± 0.61	74 ± 0.88

After

10	15 ± 4.6	4.2 ± 0.98	6.9 ± 0.64	68 ± 4.9
11	53 ± 14	7.1 ± 0.9	7.6 ± 0.5	48 ± 12
12	62 ± 10	11 ± 1.7	8.2 ± 0.6	57 ± 3
14	8 ± 5	4.2 ± 2	32.3 ± 4.9	16 ± 5
15	50 ± 22	4.0 ± 0.97	9.5 ± 0.58	39 ± 20
16	71 ± 17	11 ± 0.53	7.8 ± 2	49 ± 15
19	43 ± 5	10 ± 0.98	9.7 ± 0.56	28 ± 6.4

APPENDIX 9

RATE OF CHANGE IN SURFACE RESIDUE AND CARBON CONTENT DURING EACH CLEANING CYCLE OF THE SECOND PHASE

ALUMINUM

Sample	Cycle Time (Days)	ug/cm^2 ΔSR	ΔSR/day	ug/cm^2 ΔC	ΔC/Day
10-11	35	308	8.80	60.5	1.73
11-12	36	557	15.47	100.7	2.80
14-15	32	241	7.53	72	2.25
15-16	37	482	13.03	43	1.16
16-19	36	572	15.89	17	0.47

TITANIUM

Sample	Cycle Time (Days)	ug/cm^2 ΔSR	ΔSR/day	ug/cm^2 ΔC	ΔC/Day
10-11	35	259	7.40	52.8	1.51
11-12	36	273	7.58	62.9	1.75
14-15	32	485	15.16	70.8	2.21
15-16	37	255	6.89	40.0	1.08
16-19	36	280	7.78	58.0	1.61

APPENDIX 10

SUMMARY OF SURFACE RESIDUE, CARBON, C/N RATIO, AND PERCENT INORGANIC BEFORE AND AFTER EACH CLEANING DURING THE SECOND PHASE

ALUMINUM

	$\overline{SR}$ (ug/cm^2)	$\overline{C}$ (ug/cm^2)	C/N	% Inorganic
Before				
$\bar{x}$	588	81	9.9	73
SE	52	8	.50	4
$(SE)^2$	2731	72	.25	18
$S/\bar{x}$	.24	.28	.13	.15
After				
$\bar{x}$	137	20	16.2	66
SE	20	3	1.4	3.7
$(SE)^2$	395	9	1.9	14
$S/\bar{x}$	.38	.39	.22	.15

TITANIUM

	$\overline{SR}$ (ug/cm^2)	$\overline{C}$ (ug/cm^2)	C/N	% Inorganic
Before				
$\bar{x}$	294	55	7.2	54
SE	45	6	.28	11
$(SE)^2$	2017	40	.08	111
$S/\bar{x}$	.40	.30	.10	.52
After				
$\bar{x}$	43	7.4	8.3	44
SE	9	1.2	.42	7
$(SE)^2$	79	1.5	.17	44
$S/\bar{x}$	.54	.45	.13	.40

APPENDIX 11

TIME SERIES OF THE CHANGES IN SURFACE RESIDUE, CARBON, AND C/N RATIO DURING THE FINAL CYCLE. NUMBER IN PARENTHESIS IS SE^2

ALUMINUM

Sample	$\bar{SR}$ (ug/cm^2)	$\bar{C}$ (ug/cm^2)	C/N	$\bar{\%}$ Inorganic
16	164 (907)	23 (0.78)	15.4 (0.07)	78 (4.8)
17	129 (111)	25 (5.3)	19.0 (1.08)	70 (30)
18	280 (664)	37 (17)	14.8 (0.46)	75 (50)
19	736 (1611)	98 (11.1)	12.2 (0.02)	81 (44)

TITANIUM

Sample	$\bar{SR}$ (ug/cm^2)	$\bar{C}$ (ug/cm^2)	C/N	$\bar{\%}$ Inorganic
16	71 (305)	11 (0.28)	7.2 (2.1)	46 (217)
17	52 (59)	14 (7)	10.8 (0.97)	44 (129)
18	83 (492)	16 (2.11)	7.1 (0.08)	54 (175)
19	351 (821)	69 (25)	8.4 (0.37)	74 (0.78)

APPENDIX 12

SUMMARY OF ATP CONTENT OF THE FILM BEFORE AND AFTER EACH CLEANING DURING THE SECOND PHASE

ALUMINUM

Sample	Before		After	
	(pg/cm^2)	$pg/(cm^2.f')$	pg/cm^2	$pg/(cm^2.f')$
9	126 ± 18	134 ± 18	---	---
10	788 ± 41	788 ± 41	5.7 ± 3.6	22.8 ± 14
11	1,330 ± 195	1,330 ± 195	12.8 ± 5.9	22.0 ± 10
12	18,897 ± 2049	18,897 ± 2049	387 ± 105	464 ± 126
13	no sample	no sample	no sample	no sample
14	2,575 ± 342	2,575 ± 342	307 ± 49	307 ± 49
15	6,489 ± 1025	6,489 ± 1025	217 ± 112	434 ± 134
16	6,951 ± 1143	6,951 ± 1143	177 ± 177	531 ± 177
19	6,472 ± 874	6,472 ± 874	82 ± 82	246 ± 246

TITANIUM

Sample	Before		After	
	(pg/cm^2)	$pg/(cm^2.f')$	pg/cm^2	$pg/(cm^2.f')$
9	879 ± 159	879 ± 159	---	---
10	4,468 ± 594	4,468 ± 594	77 ± 9.7	77
11	5,458 ± 282	5,458 ± 282	36 ± 11	48
12	129,709 ± 12,539	129,709 ± 12,539	2,158 ± 525	2,158 ± 525
13	no sample	no sample	no sample	no sample
14	77,866 ± 12,687	77,866 ± 12,687	1,703 ± 700	1,703 ± 700
15	7,180 ± 1590	7,180 ± 1590	72 ± 11	72 ± 11
16	89,377 ± 19,035	89,377 ± 19,035	426 ± 33	426 ± 33
19	62,683 ± 22,611	62,683 ± 22,611	522 ± 78	522 ± 78

APPENDIX 13

TIME SERIES OF THE INCREASE IN ATP CONTENT OF THE FILM DURING THE FINAL CLEANING CYCLE (SAMPLES 16,17,18 and 19)

ALUMINUM

Sample	ATP Pg/cm^2	ATP $Pg/(cm^2.f')$
16	177 ± 177	532 ± 265
17	10,725 ± 2,632	16,079 ± 3,946
18	3,043 ± 217	4,562 ± 325
19	6,472 ± 874	6,472 ± 874

TITANIUM

Sample	ATP Pg/cm^2	ATP $Pg/(cm^2.f')$
16	426 ± 33	426 ± 33
17	30,337 ± 6,425	30,337 ± 6,425
18	34,285 ± 5,950	34,285 ± 5,950
19	62,683 ± 22,611	62,683 ± 22,611

APPENDIX 14

SUMMARY OF WET FILM THICKNESS DATA DURING THE SECOND PHASE.

B IS THE AVERAGE NUMBER OF BREAKS PER CM ON THE PLAQUE SURFACES

ALUMINUM

Sample	Maximum Wet Film Thickness	Maximum $(SE)^2$	Maximum $\bar{B}\ (SE)^2$	Minimum Wet Film Thickness
10	108.5 ± 4.0	17.1	10.0 ± 1.70	48.2 ± 5.0
11	78.9 ± 3.1	9.9		42.1 ± 2.4
12	91.9 ± 1.4	2.0		37.9 ± 6.5
14	70.5 ± 1.8	3.2	3.3 ± 0.11	31.3 ± 2.9
15	87.3 ± 4.3	18.8	4.0 ± 0.33	36.5 ± 3.1
16	94.3 ± 14	19.8	4.3 ± 0.11	46.0 ± 4.8
19	93.3 ± 4.6	21.3	5.0 ± 0.3	37.6 ± 1.4

TITANIUM

Sample	Maximum Wet Film Thickness	Maximum $(SE)^2$	Maximum $\bar{B}\ (SE)^2$	Minimum Wet Film Thickness
10	80.2 ± 4.2	18	12.0 ± 1.3	27.4 ± 1.6
11	78.8 ± 3.3	11		42.5 ± 2.7
12	97.6 ± 6.4	40.8		20.7 ± 6.4
14	94.5 ± 1.9	3.5	3.0 ± 0.11	30.8 ± 0.9
15	89.03 ± 0.8	0.67	4.7 ± 0.11	40.4 ± 2.1
16	102.8 ± 3.0	8.7	4.3 ± 0.11	37.2 ± 2.2
19	84.4 ± 14	197	5.3 ± 0.8	34.8 ± 4.4

APPENDIX 15

TIME SERIES OF THE INCREASE IN WET FILM THICKNESS DURING THE FINAL CLEANING CYCLE (SAMPLES 16,17,18 and 19)

ALUMINUM

Time Days)	Max (SE)	$(SE)^2$	B $(SE)^2$	f'	Min (SE)	$(SE)^2$	f'
0	0	0	0	0	0	0	0
7	55.97 ± 4.3	18.7	2.7 (0.57)	.50	36.0 ± 0.3	.09	.333
14	0	0	0	0	30.7	-	.167
36	93.30 ± 4.6	21.3	5 (0.3)	1.0	37.6 ± 1.4	1.9	1.0

TITANIUM

Time Days)	Max (SE)	$(SE)^2$	B $(SE)^2$	f'	Min (SE)	$(SE)^2$	f'
0	0	0	0	0	0	0	0
7	54.97 ± 4.3	18.7	3.3 (0.78)	.833	32.6 ± 1.6	2.5	1.0
14	59.38 ± 3.1	9.6	4.3 (1.4)	.5	31.9 ± 1.4	2.04	0.83
36	84.40 ± 14.1	197	5.3 (0.8)	1.0	34.8 ± 4.4	19.9	1.0